STRUCTURE AND DYNAMICS OF THE NEOCORTICAL MICROCIRCUIT CONNECTIVITY

THÈSE N^{O} 3802 (2007)

PRÉSENTÉE LE 23 JUILLET 2007

À LA FACULTÉ DES SCIENCES DE LA VIE

Laboratoire des neuroscience des microcircuits

PROGRAMME DOCTORAL EN NEUROSCIENCES

ÉCOLE POLYTECHNIQUE FÉDÉRALE DE LAUSANNE

POUR L'OBTENTION DU GRADE DE DOCTEUR ÈS SCIENCES

PAR

Jean-Vincent LE BÉ

ingénieur physicien diplômé EPF
et de nationalité française

acceptée sur proposition du jury:

Prof. R. Schneggenburger, président du jury
Prof. H. Markram, directeur de thèse
Prof. A. Lüthi, rapporteur
Prof. C. Petersen, rapporteur
Prof. A. Thomson, rapporteur

ÉCOLE POLYTECHNIQUE
FÉDÉRALE DE LAUSANNE

Suisse
2007

Abstract

The neocortex is the most computationally advanced portion of the brain. It is currently assumed to be composed of a large number of "cortical columns" – intricate arrangements of cortical neurons approximately 300-500μm in diameter and 2-5 mm in height in humans – that might serve as the elementary computational unit of the neocortex. Understanding the computation performed by this microcircuit is one of the keys to our comprehension of the brain. The so-called cortical column is not a static entity, however, and it evolves throughout a lifetime and continually adapts to the information from its cortical environment. Despite the differences between cortical columns across the cortex, a number of common features have been identified: a laminar structure, the dynamics of connections between identified neurons or the mechanisms for these connections to be modified (that give its specificity to each microcircuit). This thesis presents the description of the differential connectivity and synaptic dynamics across cell populations and the long term neuronal rewiring in a particular neuronal population within the cortical column.

Somatic whole cell recordings have been performed to probe the connectivity, synaptic dynamics and plasticity of the connections in the rat neocortex. Two populations of layer V pyramidal neurons were studied in particular: cortico-callosally projecting pyramidal cells (CCPs) and thick tufted pyramidal cells (TTCs).

The first major results from this work revealed the degree of connectivity and the linear dynamics of the CCPs population when compared to the TTCs. CCPs have nearly 4 times fewer interconnections and subsequent post-synaptic potentials were less decreasing in amplitude along a pre-synaptic series of action potentials.

Long term configuration of TTC networks was explored. These experiments show for the first time the emergence of new functional synaptic connections between TTCs within hours. Activation of the slice by glutamate greatly increases their rate of emergence and this work demonstrated that metabotropic glutamate receptor 5 (mGluR5) activation and action potential firing are required for new connections to be formed in this experimental protocol. Newly formed connections respond in a more linear fashion and have weaker post-synaptic influence than already existing connections. Pre-existing connections are also modified after stimulation, requiring mGluR5, action potentials as well as α-amino-3-hydroxy-5-methyl-4-isoxazole-propionic acid (AMPA) and N-methyl-D-aspartic acid (NMDA) receptors activation. The activation of group III metabotropic glutamate receptors (mGluRs) however results in a decrease in the strength of connections.

Finally, the influence of inhibitory interneurons on the activity and connectivity between TTCs was also investigated. The results of this study show that firing of inhibitory interneurons can be triggered by the input of only one pyramidal cell. They further show that stimulation of a single TTC can result in an hyperpolarization of the post-synaptic TTC mediated by an interneurone. When the pre-synaptic neuron is also directly connected to the post-synaptic neuron with an excitatory synapse, the indirect inhibitory connection serves to curtail the excitatory response.

This work has provided a new insight into the dynamic nature of the cortical microcircuitry, showing that it evolves rapidly and can adapt, reconfigure and rewire itself in remarkably short time-spans. It also describes the variety of dynamics exhibited by the different types of pyramidal cells, due to either the projecting site specificity or to the action of an intermediate interneuron.

Key words: Pyramidal cells, synaptic connections, corpus callosum, cortico-callosal cells, plasticity, memory, cortical column, neuron connections dynamics, metabotropic glutamate receptors, mGluR5, long-term potentiation, patch-clamp, *in vitro* electrophysiological recordings.

Résumé

Le néocortex est la principale structure cérébrale responsable de l'intégration de l'information. Il est composé de "colonnes corticales" – arrangements de neurones intriqués d'environ 300-500µm de diamètre sur 2-5 mm de haut chez l'humain – qui servent d'unité de calcul de base au néocortex. Etudier l'intégration de l'information réalisée par ces microcircuits est cruciale pour la compréhension du fonctionnement du cerveau. La colonne corticale n'est cependant pas une entité statique et évolue au long de la vie en s'adaptant continuellement aux informations reçues des structures adjacentes. Malgré les différences d'une colonne corticale à l'autre, un certain nombre de caractéristiques communes ont été identifiées : la structure laminaire, la dynamique de connexion entre deux neurones particuliers ou les mécanismes modifiant ces connections (donnant sa spécificité à la colonne). Cette thèse présente les différences de connectivité et de dynamique de connexion entre deux populations de neurones ainsi que la reconfiguration de connectivité au sein d'une population de neurones de la colonne corticale.

La technique du "patch clamp" a été utilisée pour mesurer la connectivité, la dynamique synaptique et la plasticité des connexions dans le néocortex de rats. Deux populations de neurones pyramidaux de la couche V du néocortex ont été étudiées : les neurones cortico-callosaux (CCPs, de l'anglais "Cortico-Callosally Projecting cells") et les larges neurones pyramidaux (TTCs, de l'anglais "Thick Tufted pyramidal Cells").

Le premier résultat majeur de ce travail montre le degré de connectivité ainsi que la linéarité de la dynamique au sein de la population des CCPs lorsqu'ils sont comparés aux TTCs. Les CCPs sont environ 4 fois moins interconnectés et les potentiels post-synaptiques décroissent moins en amplitude au cours d'une série de potentiels d'action pré-synaptiques.

La configuration des réseaux de TTCs à long terme a été explorée. Ces expériences montrent pour la première fois l'émergence de nouvelles connexions synaptiques fonctionnelles entre TTCs en l'espace de quelques heures. L'activation de la tranche par du glutamate augmente considérablement la proportion de nouvelles connections et cette étude a démontré que l'activation de récepteurs métabotropiques au glutamate 5 (mGluR5) ainsi que la décharge de potentiels d'action sont requises pour que de nouvelles connexions apparaissent avec ce paradigme. Les nouvelles connexions répondent de manière plus linéaire et sont de moins grande amplitude que les connexions déjà existantes au début de l'expérience. Ces dernières sont aussi modifiées par la stimulation, modification qui requiert mGluR5, la décharge de potentiels d'action ainsi que l'activation de récepteurs de l'acide α-amino-3-hydroxy-5-methyl-4-isoxazole-propionique (AMPA) et de l'acide N-methyl-D-aspartique (NMDA). L'activation de récepteurs métabotropiques au glutamate (mGluRs) du groupe III induit une diminution de la force des connexions.

Finalement, L'influence d'interneurones inhibiteurs sur l'activité et la connectivité des TTCs a aussi été étudiée. Les résultats de cette étude montrent que la décharge de neurones inhibiteurs peut être déclenchée par un seul neurone pyramidal. De plus ils montrent que la stimulation d'un seul TTC peut résulter en une hyperpolarisation du TTC post-synaptique. Lorsque le neurone pré-synaptique est aussi directement connecté au TTC post-synaptique, la connexion indirecte inhibitrice permet de modifier la réponse excitatrice.

Ce travail a apporté une nouvelle perspective dans la manière d'appréhender la nature dynamique des microcircuits néocorticaux. Il montre que ces derniers peuvent évoluer rapidement, s'adapter, se reconfigurer et se reconnecter en un temps remarquablement court. Il décrit aussi la variété de la dynamique propre aux différents types de neurones pyramidaux,

variété qui dépend de la cible d'une population de neurones ou de l'action d'un interneurone intermédiaire.

Mots Clés: Neurones pyramidaux, connexions synaptiques, corps calleux, neurones cortico-callosaux, mémoire, colonne corticale, dynamique des connexions de neurones, récepteurs métabotropiques au glutamate, mGluR5, potentiation à long terme, patch clamp, enregistrements électrophysiologiques *in vitro*.

1 General introduction

1.1 Neocortical columns

The brain is composed of various structures that appeared successively throughout evolution. The most recent is the neocortex, a sheet of cells organized in 6 basic layers situated just below the pia. The neocortex itself is found in various shapes in different mammals. The more complex the species, the more convoluted the neocortex is. The human neocortex is larger and has many more convolutions than the rat neocortex (Figure 1). However, despite these differences, the underlying neuronal and local circuit architecture of rat and human bears many similarities (DeFelipe *et al.* 2002).

The neocortex is the locus of the highest cognitive functions. The primary sensory areas of the neocortex receive direct inputs from the thalamic nuclei (relays of the sensory apparatus, see Guillery and Harting 2003) and propagate a processed signal to higher sensory areas that in turn innervate associative areas. Most of the primary sensory areas in the neocortex are well identified and the structure of the sensors is reflected on the cortical surface for example in retinotopic or somatotopic maps for visual and somatosensory processing respectively (see Mountcastle 1997; Flanders 2005; Horton 2006). Characteristic features of vision processing such as motion, orientation and colour are integrated within the cortical area corresponding to the activated retinal portion. Similarly, adjacent fingers activate adjacent areas in the somatosensory cortex (see Pons *et al.* 1985; Mountcastle 1997). These maps have however been observed only for a part of sensory integration and are not always continuous (see Flanders 2005). Moreover, they have been shown to vary with experience. The underlying cellular mechanisms remain unclear but synaptic plasticity might be at the origin of these reorganizations (see Buonomano and Merzenich 1998). More advanced areas integrate the information from these primary maps and the interactions between these various areas generate the perception of the outside world and the body position. The frontal cortex is currently supposed to be the locus of the most computationally advanced processing subserving the highest forms of cognition. It is the most developed in humans compared to other species and is believed to have a central role in planning and executing complex behaviour.

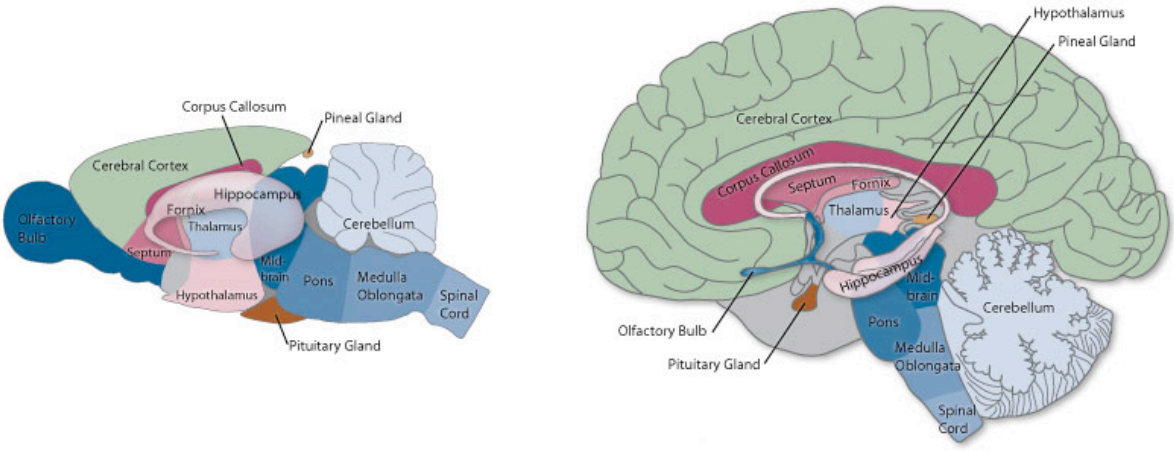

Figure 1 Comparison of the rat brain with the human brain. The neocortex is labelled "cerebral cortex" on the figure. Pictures from the University of Utah.

The cortical column. The neocortex is composed of 6 basic neuronal layers and can be divided into small functional modules of about 300µm in diameter referred to as *cortical columns* (Lorente de Nó 1938; Mountcastle 1957; DeFelipe *et al.* 2002 and see Mountcastle 1997). The cortical column is believed to be the fundamental computing unit of the neocortex. The concept of the neocortex as an assemblage of such cortical columns originates from the observation of basic functional units where neurons share similar properties and respond to similar sensory stimulations, in somatosensory (Mountcastle 1957), visual (Hubel and Wiesel 1962) or motor cortex (Keller 1991) in the cat or the primate.

Such functionally identifiable columns have not been reported in rodents except for the barrel field. Indeed, some recent experiments showed that the rat visual cortex neurons responding to the same visual stimulus are not grouped within a volume that correspond to a cortical column unlike the neurons recorded in the cat (Ohki *et al.* 2005). Nevertheless, we refer by analogy to *cortical column* as the microcircuit of neurons contained in a cylinder of 300-500µm in diameter which is approximately the mean spread of the horizontal dendrites of layer V principal neurons (see DeFelipe *et al.* 2002; Silberberg *et al.* 2002).

The region equivalent to a cortical column contains roughly 7-10'000 neurons and is between 1 and 2 mm in height in rodents (DeFelipe *et al.* 2002). In humans, the cortical column height varies between 2 and 4 mm (DeFelipe *et al.* 2002). Neurons contained in these neocortical columns can be divided into two main classes according to their functional roles: the principal excitatory neurons that project to distant brain regions and the inhibitory interneurons that arborize mostly locally or spread within the neocortical sheet to innervate neighbouring cortical columns.

Local excitation in neocortical microcircuits. Excitatory neurons have diverse morphologies but are divided into three major groups: (1) Pyramidal cells (PC), also called principal neurons, mostly with a triangular shaped cell body and an apical dendrite extending towards the pia, (2) star pyramids found mostly in layer IV that appear like normal pyramidal neurons but with a less obvious apical dendrite and (3) spiny stellate cells (SSC), primarily found in layer IV of primary sensory cortices (LeVay 1973; Lund 1973). The cell body is typically round with a symmetrical dendritic arborisation around the soma and a high density of spines (hence the name "spiny" stellate). These excitatory neocortical neurons release glutamate to activate ionotropic or metabotropic receptors. Inverted pyramidal cells and bipolar pyramidal cells can also be found in layer VI of the neocortex.

Ionotropic receptors are ligand-gated ion channels (see Hosli *et al.* 1973; Salt and Eaton 1996) and the three main types of excitatory ionotropic receptors activated by glutamate are the α-amino-3-hydroxy-5-methyl-4-isoxazolepropionic acid (AMPA), the Kainate and the N-methyl-D-aspartic acid (NMDA) receptors named after their specific responsiveness to AMPA, Kainate and NMDA respectively. AMPA and Kainate receptors channels are mostly permeable to Na^+ and K^+ and AMPA receptor channels lacking GluR2 subunit are also permeable to Ca^{2+}, although this latter type is rare in the neocortex (Jonas *et al.* 1994; Buldakova *et al.* 1999). NMDA receptor channels are permeable to Na^+, K^+ and Ca^{2+}; they require glycine binding and are gated by a Mg^{2+} ion that unblocks the channel when the membrane is sufficiently depolarized (Mayer *et al.* 1984; Nowak *et al.* 1984; Thomson *et al.* 1985; Ascher and Nowak 1988). AMPA and Kainate receptors open faster and their activation increases the efficiency of NMDA receptors. However, as NMDA receptors are permeable to Ca^{2+}, they participate to signalling cascades in the post-synaptic cell whereas the majority of AMPA and Kainate receptors in the neocortex do not.

Metabotropic receptors (mGluRs) are linked to a G-protein and then trigger a biochemical pathway in the cell (see Salt and Eaton 1996). mGluRs are classified into three groups according to their common agonists. Group I contains the mGluRs 1 and 5, group II

contains mGluRs 2 and 3 and group III contains mGluRs 4,6,7 and 8. The receptors are further sub-classified according to their various specific agonists and their genetic specificities.

Local inhibition in neocortical microcircuits. The second major class of neurons are the inhibitory interneurons. They are also referred to as GABAergic neurons after their neurotransmitter γ-amino-butyric acid (GABA). Post-synaptic GABA receptors are classified in three groups: $GABA_A$, $GABA_B$ and $GABA_C$ receptors. Type A and C are ionotropic receptors permeable to Cl^- whereas the type B is a metabotropic receptor. $GABA_A$ receptors open faster than the two other types.

Various approaches have been used to classify interneurons. Immunocytochemical and histochemical approaches lead to a classification according to the differential neuropeptides and calcium binding proteins expressions across GABAergic interneurons (DeFelipe 1993). Intrinsic electrophysiological properties were early used to differentiate GABAergic interneurons from excitatory cells (McCormick *et al.* 1985; Chagnac-Amitai and Connors 1989). Later, more detailed classifications of GABAergic interneurons were proposed according to their more detailed firing patterns (see Toledo-Rodriguez *et al.* 2002; Markram *et al.* 2004 and Petilla convention in 2005). Some morphological classification can end up in about eleven different types of GABAergic interneurons (see Toledo-Rodriguez *et al.* 2002; Gupta *et al.* 2004; Markram *et al.* 2004). The primary method for morphological classification of GABAergic interneurons is according to their axonal morphology (see Toledo-Rodriguez *et al.* 2002; Gupta *et al.* 2004). Additionally, neurons in each class target specifically the axon, soma or dendrite of the post-synaptic PC (see Somogyi *et al.* 1998 and Figure 2*A*). Morphological classes are then grouped according to the target on the post-synaptic cell. This classification makes sense also in terms of neuronal function. Inhibiting the postsynaptic cell at different domains of a neuron can have a differential effect. In a simple sense, inhibition at the initial axon segment controls the output of the target neuron whereas inhibition in the dendrites controls the input (axon in black and dendrites in blue for the pyramidal neuron schematized on Figure 2*A*). Somatic, peri-somatic and axonal inhibitions have received much attention, especially inhibition from basket cells and chandelier cells (Martin *et al.* 1983; DeFelipe *et al.* 1986; Li *et al.* 1992; Halasy *et al.* 1996; Ali *et al.* 1998; Tamas *et al.* 1998; Wang *et al.* 2002; Somogyi *et al.* 2004). Dendritic inhibition, on the other hand, is less described but is now studied increasingly (Williams and Stuart 2000; Pouille and Scanziani 2004; Perez-Garci *et al.* 2006; Silberberg and Markram 2007). Dendrites integrate the input signals locally and in a nonlinear fashion (Polsky *et al.* 2004). These observations imply that the presence of an inhibitory signal at the site of local integration controls the processing and the transmission of incoming information. Peri-somatic targeting interneurons were at first given more importance than the dendrite targeting cells (and even less importance was attributed to small or distal dendrites). However it is now clear that distal dendrite targeting neurons influence the local integration significantly and are important in dendritic integration. An aspect of the importance of dendritic and tuft inhibition in shaping the neuronal dynamics is presented in the chapter 4 of this thesis.

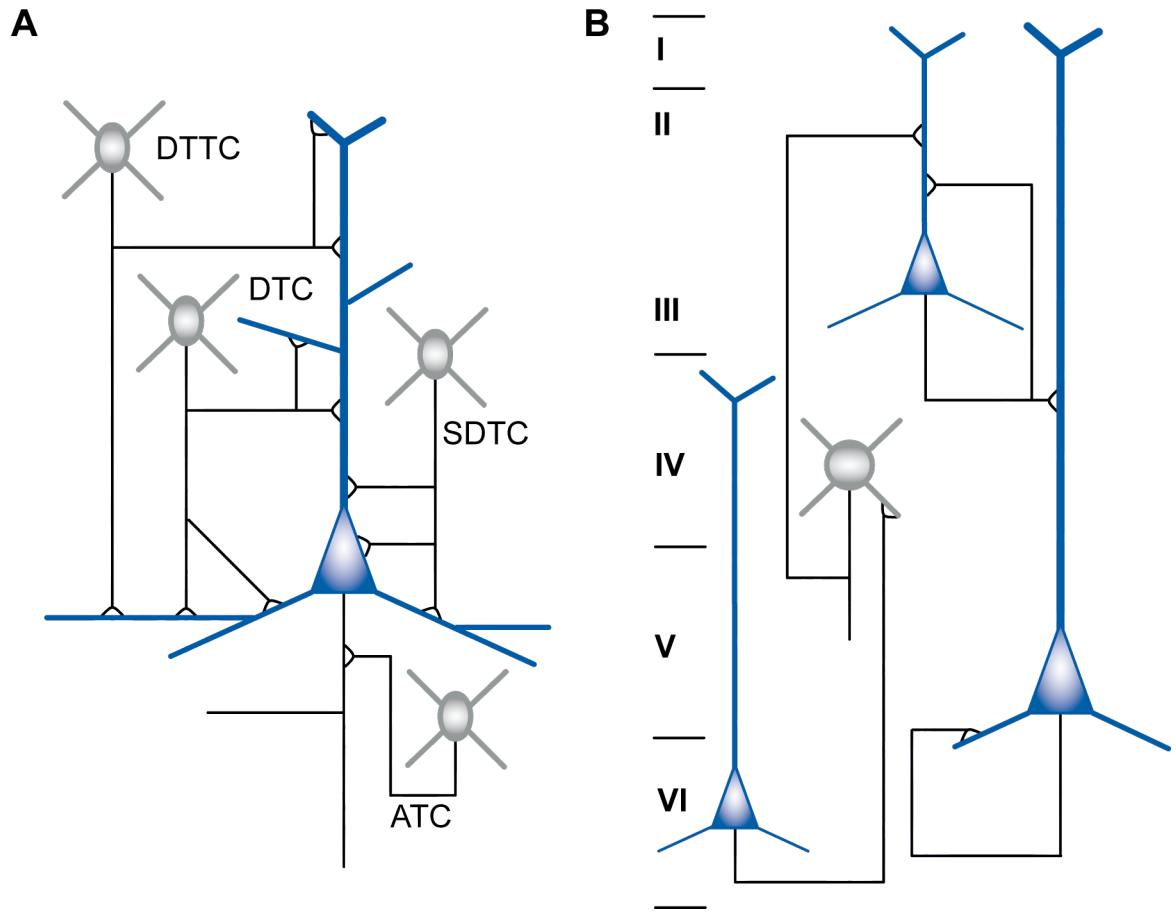

Figure 2 Morphological principles of connectivity between neocortical neurons
A − Schematic representation of target-domain specific innervations of PCs by different types of inhibitory neurons. Inhibitory neurons may be functionally divided into distal dendritic- and tuft-targeting cells (DTTC), dendritic-targeting cells (DTC), soma- and proximal dendritic-targeting cells (SDTC) and axon-targeting cells (ATC) according to their preferential innervations of specific postsynaptic compartments.
B − Schematic representation of the main excitatory pathway in the cortical column. All cells represent a population of neurons. Round cells represent spiny stellate cells. A cell showing a connection onto itself represents an interconnected population. Axons are shown in black, the layers of the cortex are numbered on the left.

1.2 Cortical column connectivity

Synaptic connectivity within the cortex has been extensively studied in the past decade highlighting some anatomical principles of connectivity. Firstly, *reciprocity* and *asymmetry* are present in the way layers and columns are connected to each other (see Thomson and Bannister 2003). There are feedback loops (reciprocity) but also forward synaptic pathways (layer four to layer five-six via layer two three, asymmetry). Secondly, *specificity* and *precision* underlie the accuracy with which neurons target their post-synaptic cells and domains (see Somogyi *et al.* 1998). Finally, *divergence* and *convergence* emerge when considering many neurons that project onto a single one and when this neuron in turn projects to many others. These principles are also present at the circuitry level.

Inputs and outputs of the cortical column. The main projecting type of neuron in the neocortex is the PC. Briefly, the main pathways that connect the cortical column to other regions of the brain are as follow (for a complete review, see Thomson and Bannister 2003 and Lund 1988).

The *inputs* to the cortical column from the thalamus mainly target layer IV and to a lesser extent lower layer III and upper layer VI. There is also a vast majority of afferents that originate from within the neocortex. These axons innervate the cortical column mainly through layers I, II-III and VI. It is worth noting that the innervations in a specific layer do not imply that the direct input is restricted to the cells present in this layer. For instance the thick-tufted layer V pyramidal cells (TTCs) that have an apical dendrite extending across all superficial layers with ramifications in layer I are likely to receive direct input from almost all of the areas projecting to the cortical column.

The *output* of the cortical column is also layer dependent for most of the projections. Layer V TTCs project to the superior colliculus and the thalamus (Kasper *et al.* 1994a; Bourassa *et al.* 1995), a portion of layer VI PCs project to the thalamus and other PCs of the same layer project to the ipsilateral neocortex. Layer II-III PCs as well as some layer IV SSCs (but at shorter distances) project to the adjacent cortical columns and to other parts of the ipsilateral neocortex. The projections via the corpus callosum, on the contrary to other targets, originate from all layers of the cortical column although some layers contain more callosally projecting cells than others (layers III and V in rodents, see Innocenti 1986).

Main excitatory pathway in the cortical column. Within the cortical column, excitatory cells form two to eight synapses per connection to their homologues, mostly on spines (80%) (see White 1989), the rest on dendritic shafts and rarely on somata. There seem to be a variation in the number of synapses formed on average as well as in the distribution of synaptic locations across layers (see Feldmeyer and Sakmann 2000). The major trans-laminar pathway is as follows (see Figure 2*B*). Layer VI PCs (projecting also in a feedback manner to the thalamus) innervate layer IV SSCs (Ahmed *et al.* 1994). Then SSCs innervate layer II-III PCs (Staiger *et al.* 2000; Feldmeyer *et al.* 2002; Thomson *et al.* 2002) that in turn form synapses onto layer V PCs (Staiger *et al.* 2000; Thomson *et al.* 2002). Layer II-III excitatory neurons are more interconnected than cells from any other layers (Thomson *et al.* 2002; Mercer *et al.* 2005; West *et al.* 2006). This suggests that the layer II-III is an important integration centre of the neocortex.

1.3 Connection dynamics

Electro-encephalogram frequency bands. An important neuronal microcircuits feature is the connection dynamics, i.e. the way a cell transmits the signal during a train of action potentials (APs). *In vivo*, the spiking activity depends on the state of wakefulness. The various states were first characterized according to the frequency of electro-encephalogram (EEG) recordings. The electrical signal recorded at the surface of the skull is, in humans, between 1 Hz and 60 Hz. This frequency range is traditionally divided into five bands which precise boundary values are differentially defined according to various authors. An average cutting of the frequency range would be as follow: alpha (8-13 Hz), beta (13-30 Hz), gamma (30-60Hz), delta (0.5-4 Hz) and theta (4-7 Hz) (Schlosser *et al.* 1998; Ferri *et al.* 2001; McLin Iii *et al.* 2003). The alpha band is characteristic of relaxed wakefulness whereas the beta band is more linked to attention (see Neuper and Pfurtscheller 2001; Cantero *et al.* 2002). The theta and delta bands are observed during drowsiness or slow wave sleep (see Spiegel *et al.* 2006). EEG records neuronal activity after it has undergone distortions due to the skull and tissue present between the site of activity generation and the electrode. Moreover, the signal present at the site of recording is the result of the interaction between various areas of the cortex. To characterize a cortical microcircuit, it is useful to identify more precisely the activity of a single neuron *in vivo*.

Neuronal activity *in vivo*. Steriade and collaborators (Steriade *et al.* 2001) used intracellular recordings in adult cats to show the various characteristics of neocortical neurons in awake state, slow wave sleep (SWS) and rapid eye movement sleep (REM, also called paradoxical sleep). They first showed that 50% of the recorded neurons were regular spiking and 24% were fast spiking when depolarized during quiet state *in vivo*. These results show a different distribution in the discharge responses from *in vitro* preparation observations (see Toledo-Rodriguez *et al.* 2002, recordings reported for juvenile rats) indicating that a single neuron firing pattern depends also on environmental factors and not only on intrinsic characteristics. This finding is further supported by the differential firing with respect to the site of stimulation on a neocortical PC (Schwindt and Crill 1999). However, the firing characteristics as such (AP shape, hyperpolarization, etc..) are similar to the *in vitro* observations.

There is in general no spontaneous firing in *in vitro* neocortical preparations. It is then of importance to know the stimulation frequencies that best mimic the neuronal activity *in vivo*. Cortical neurons *in vivo* have an average discharge frequency between 10 and 50 Hz depending on type and waking state (awake, SWS, REM). Regular spiking neurons (like PCs recorded for this thesis) do not change dramatically in their average frequency discharge across the different states (9.4 ± 1.7 Hz during waking, 11.8 ± 1.6 Hz in SWS; and 14.0 ± 2.8 Hz in REM sleep) compared to fast spiking neurons (like GABAergic interneurons) that tend to always discharge at a higher frequency (23.7 ± 6.1 during waking, 14.9 ± 4.1 in SWS and 30.6 ± 8.4 in REM sleep, Steriade *et al.* 2001). Although the *in vivo* recordings were performed in adult cats and the *in vitro* recordings presented in this thesis are performed in juvenile rats, the frequencies reported above give an idea of the order of magnitude of the frequencies that might be appropriate to study the synaptic characteristics between neocortical neurons. Moreover, it has recently been shown that neocortical neurons are similar in adult rats, adult cats and young rats (Ali *et al.* 2007).

Dynamic synaptic transmission. Synaptic connections are traditionally classified into three main categories; facilitating, linear and depressing connections. When the post synaptic potentials (PSPs) increase in amplitude during a pre-synaptic stimulation train, the connection is referred to as facilitating (Thomson *et al.* 1993a; Thomson *et al.* 1993b; Markram *et al.* 1998). When the consecutive PSPs in a train are smaller than the previous ones the connection is referred to as depressing (Markram *et al.* 1998, see Figure 3). When the PSP amplitudes are constant along the train, the connection is considered linear. More recent studies showed that there can be subdivisions of these categories depending on the facilitation/depression time constants ratio (Gupta *et al.* 2000). Along with the PSPs train dynamics, the amplitude of the post-synaptic potential is also a major characteristic of synaptic transmission. It depends on the number of synapses in the connection and on individual synapses strengths. The response amplitude at a synapse site is likely to depend on the number of post-synaptic receptors, as the amount of neurotransmitter released seems to saturate them (Jack *et al.* 1981; Edwards *et al.* 1990). The location of the synapses along the dendrite also determines the amplitude of the PSP response as membrane potential can undergo some attenuation when propagated along the dendritic tree (Stuart *et al.* 1997; Nevian *et al.* 2007).

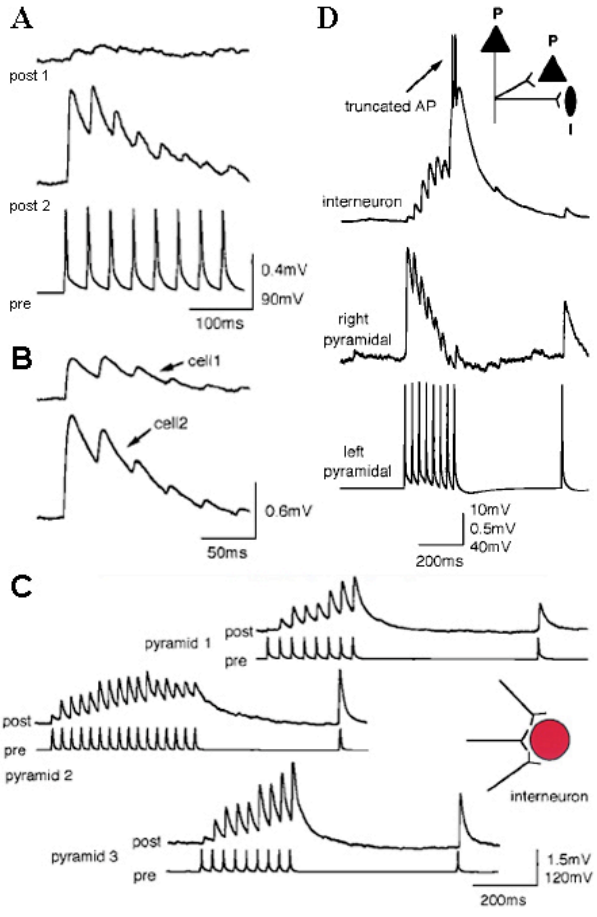

Figure 3 Depression and facilitation in neocortical synapses. A – Average excitatory post-synaptic potentials (EPSPs) of 30 trials at 30 Hz. The pre-synaptic cell (pre) was stimulated by a 30 Hz train of pulses (5 ms-500 pA) allowing a controlled action potential generation. The synapses on post-synaptic cell 1 (post1) had an electrotonic distance 3 times larger than on the post-synaptic cell 2 (post2). B – Differential synaptic transmission onto two PCs from a same pre-synaptic PC. The electrotonic distances were similar for both post-synaptic cells. Same stimulation as in *A*. C – Facilitation in the connections from PC to interneurons. Three pre-synaptic PCs elicited different facilitation dynamics onto the same postsynaptic interneuron. D – Facilitation on interneuron can be sufficient for one pre-synaptic PC to trigger APs in the postsynaptic interneuron. The same PC stimulation results in a depressing EPSP train in another PC. Adapted from (Markram *et al.* 1998).

Mechanisms underlying synaptic dynamics. The underlying mechanism for synaptic transmission has been shown to depend on the calcium entry at the pre-synaptic terminal. In the facilitation process, two subsequent APs generate a cumulative calcium influx at the pre-synaptic site thus increasing the probability of vesicle release (Pr) from the first spike to the second and inducing a larger amount of neurotransmitter released (Miledi and Slater 1966; Katz and Miledi 1968; Rahamimoff 1968; Thomson *et al.* 1993b). This can be achieved by either a cooperative action of calcium or by a calcium induced change in the conformation of the proteins involved in vesicle release (see Thomson 2003). In a facilitating synapse, the probability of release can generally be modelled as being low for the first AP and then increases for the subsequent APs of the train (Markram *et al.* 1998; Gupta *et al.* 2000). At first, it is tempting to think that Pr depends on the number of vesicles ready to be released. However the number of vesicles docked at the membrane is similar for both facilitating and depressing synapses (Xu-Friedman *et al.* 2001) indicating that either (1) the number of vesicles ready to be released is not proportional to the number of vesicles docked in the pre-synaptic bouton or (2) the release mechanism itself influences the probability of release after docking.

Synaptic transmission between neurons is mediated by more than one synapse (Deuchars *et al.* 1994; Markram *et al.* 1997a; Markram *et al.* 1998; Gupta *et al.* 2000; Silver *et al.* 2003). As a consequence, facilitation might also be due to a larger number of release sites recruited along the train of pre-synaptic APs (see Thomson 2003). The number of release sites activated by a given AP participates in the determination of the PSP amplitude. The measurement of the post-synaptic response would then give different results in case of a trial with many release sites recruited compared to a trial with few release sites activated. The number of failures must also be significantly higher in the case of connections with few release sites. Therefore measuring the failure rate and the coefficient of variation for a synaptic connection between two neurons gives an indication on the mechanism underlying its dynamics. If the number of failures is important, the synaptic dynamics might originate from a differential recruitment of synapses by the pre-synaptic AP train. The variation in the post-synaptic amplitude might also originate from a small amount of postsynaptic receptors. Simulations showed that, when treated statistically, a small amount of receptors induces a great variance in the proportion of receptors activated. As a consequence, less channels open, and the opening of these channels varies considerably as well (Faber *et al.* 1992).

These mechanisms are valid for both depressing and facilitating synapses as they can work in both directions depending on the original probability of release considered (see Thomson 2003).

Depression might not always depend on the release history. Release independent depression has been observed in hippocampus (Thomson and Bannister 1999), and somatosensory cortex (Fuhrmann *et al.* 2004). Although in the somatosensory cortex, the release independent depression component was extracted from the post-synaptic response, in hippocampal neurons the connections were depressing even when the first AP failed to elicit a response in the post-synaptic cell (Thomson and Bannister 1999). The authors suggest that this release independent depression might be due to rapid inactivation of N-type calcium channels. The first AP fails to release transmitter but inactivates channels in the closed state resulting in a smaller release (by for instance inactivating some sites for the second AP). Supporting this hypothesis, it had been previously shown that APs-like stimulations can inactivate N-type calcium channels during a 100 Hz train (McNaughton *et al.* 1998).

1.4 Models for synaptic transmission

Quantal analysis. One of the models describing the synaptic mechanism and giving tools to interpret depression and facilitation is quantal analysis. It originates from the study of the frog neuromuscular junction (Fatt and Katz 1952; Del Castillo and Katz 1954). The synaptic transmission at this junction is such that it allows the identification of post-synaptic potentials due to the relax of just one vesicle. Indeed, one quanta was estimated at 0.5-1.0 mV for a 70-80 mV global depolarization (Del Castillo and Katz 1954). The stochastic nature of neurotransmitter release with hundreds of release sites allows the use of a Poisson distribution based binomial model to describe many connections assumed to fit within the quantal hypothesis (see Thomson 2003). The parameters used for a binomial description are the quantal size q, the number of active sites n and the probability of release at these sites p. These parameters are not measurable directly in most of the synaptic connections but if they are invariants and if p is independent for each release site, a simple binomial model can be used (Faber and Korn 1991 and see Voronin 1993). The dependence upon n, p and q of the mean response amplitude M and the coefficient of variation CV of the response (being the standard deviation of the single responses amplitudes divided by M) are then:

$$M = npq \qquad CV = \left(\frac{1-p}{np}\right)^{1/2}$$

This model has been developed for connections with large response amplitudes such as in the neuromuscular junction. It is however widely used with relative success for central nervous system (CNS) connections. The number of release sites is generally more precisely measured by later ultrastructural investigations. The model can also be used either to determine n, p and q or to study the changes in these parameters during synaptic modification experiments. However, the experimental data are subject to a low signal to noise ratio with noise originating from the experimental equipment as well as from the studied tissue itself. This adds to the low response amplitudes recorded in the CNS (see Korn and Faber 1991). Finally, detailed analysis that might be more precise than the simple binomial model shown above requires more computation which increases the errors in the final results.

These considerations lead to the conclusion that quantal analysis can be a good approximation for CNS connections but the description of CNS synapses would require more adapted models to be adequate. Additionally, this model can only describe changes in the amplitude of the post-synaptic response. A more complete description of the temporal dynamics in response to pre-synaptic AP trains requires a different model.

A dynamic model. Synaptic connections recordings using the patch clamp technique are generally performed at the soma. The experimental and biological variabilities are fairly important when compared to individual, and in particular low probability, single-axon post-synaptic responses. To overcome this difficulty the averaging of several trials has been extensively used (generally between 5 and 50 trials per average, see for example Markram *et al.* 1998; Gupta *et al.* 2000). In addition, the dynamics of a connection can be computed from one set of trials provided the stimulation is an AP train of sufficient length (Tsodyks and Markram 1997). The model presented below, which we will refer to as the Tsodyks-Markram model, suggests a set of four parameters describing fairly accurately the functional synaptic transmission dynamics.

The absolute synaptic efficacy (ASE or A, in mV) refers to the maximum synaptic response amplitude that can be produced by the connection. It is defined as the amplitude of the post-synaptic potential that would be recorded if the probability of release would be 1. This can be linked to the quantal hypothesis by identifying A with the product of the quantal size, the number of release sites and the electrotonic attenuation factor (Markram *et al.* 1998).

The utilization of synaptic efficacy (U, dimensionless) is the proportion of synaptic resources available that is used after an AP discharge. The actual response measured at the soma for the first excitatory post-synaptic potential (EPSP) in the train is the product of U with A. It can be assimilated to the probability of release depending on the mechanism of frequency dependence (Markram *et al.* 1998), e.g. when the connection is only depressive (or, equivalently, the time constant for facilitation, see below, is close to zero). Indeed, the depression observed in neocortical connections is pre-synaptically mediated (Thomson *et al.* 1993a; Tsodyks *et al.* 1998) and as a consequence, the depression observed is due to lower neurotransmitter release. The absolute synaptic efficacy being constant (by definition) the parameter that varies with time during a sequence of pre-synaptic APs is the amount of neurotransmitter available represented in this model by the running value R. R is decreased at each AP in the train according to the parameter U.

The time constant for recovery from depression (τ_D, in s). When an AP is fired in the pre-synaptic neuron, the next amplitude is calculated by assuming that the available strength at that time point is the original strength (A) diminished by the transmitter amount that has just been released ($A \cdot U$). But this reduction due to an AP discharge is modified by the recovery from depression of the pre-synaptic terminal. This recovery is clearly seen when two APs are separated by few seconds as this time is sufficient for the pre-synaptic cell to recover and then the recorded EPSP is on average constant (the fluctuations observed on a trial to trial basis originate from the stochastic characteristic of vesicle release and receptor activation).

The time constant for recovery from facilitation (τ_F, in s). Facilitation is modelled by an increase in the utilization parameter and has been observed to decrease along an AP train. The parameter U described above is then the value for the first EPSP and a running value u, exponentially decreasing towards U after each stimulation, is used to model the subsequent EPSPs of the train. The increase in u is defined as $U(1-u)$ that synthesizes various models and ensure that $u < 1$ (Markram *et al.* 1998).

The algorithms used to determine these four parameters characterizing a given connection are (from Markram *et al.* 1998 and where R is fraction of synaptic efficacy available):

$$R_{n+1} = R_n\left(1 - u_n\right)\exp\left(\frac{-\Delta t}{\tau_D}\right) + 1 - \exp\left(\frac{-\Delta t}{\tau_D}\right)$$

$$u_{n+1} = u_n \exp\left(\frac{-\Delta t}{\tau_F}\right) + U\left(1 - u_n \exp\left(\frac{-\Delta t}{\tau_F}\right)\right)$$

$$EPSP_{amp\,n} = ASE_n \cdot R_n \cdot u_n \quad ; \quad R_1 = 1 - U$$

Where Δt is the time interval between two APs.

This model can be applied to EPSPs recorded in response to any pre-synaptic train. It (or similar versions) has been applied on regular, irregular and Poisson trains of pre-synaptic APs, always giving a very good fit to the experimental traces (Tsodyks and Markram 1997; Markram *et al.* 1998). The EPSP trains presented in this thesis are analysed with this model.

1.5 Scope of the thesis

The functional structure of the cortical column has been investigated for more than a century but still requires much efforts to be fully understood. The results presented in this thesis push further the understanding of the functional cortical column. In chapter 2 results concerning the *structural connectivity* of a special PC population will be presented. *Cortico-callosally projecting cells* have been identified with retrograde labelling and the connections among this population investigated. Along with the functional connectivity within this population, the morphological connections characteristics as well as single cell electrophysiological and morphological aspects will be exposed and compared to another PC population. This study outlines the differences among PC populations in the neocortex when classified according to their projection targets.

The *dynamics of the connectivity* has long been considered by looking at the change of existing connections. In chapter 3 a novel view of plasticity is presented with experiments that show the formation of new functional connections and complete pruning of existing connections in acute slices within hours. The so-called *microcircuit plasticity* is investigated in terms of its dependence on the various glutamate receptors and cell activations. Along with the characterization of the dynamics of newly formed and removed connections, existing connections changes in strength and dynamics are also investigated. These changes can be on the one hand spontaneously occurring when the slice is let without specific stimulation or pharmacology in standard artificial cerebro-spinal fluid (ACSF) or on the other hand induced by glutamate application (by perfusion in ACSF or puffing on the investigated cell cluster) over a period of time that can last up to 12 hours.

Although acute slices do exhibit only low rates of spontaneous activity and therefore are suitable for dissecting the direct connections between different neurons, some synapses do trigger post-synaptic action potentials. This phenomenon is briefly used for the investigation of *indirect connections* between thick tufted PCs presented in chapter 4.

This thesis gave rise to the following publications:

Jean-Vincent Le Bé and Henry Markram, “Spontaneous and evoked synaptic rewiring in the neonatal neocortex” (2006), PNAS, 103(35) 13214-13219.

Jean-Vincent Le Bé, Gilad Silberberg, Yun Wang and Henry Markram, “Morphological, Electrophysiological and Synaptic Properties of Corticocallosal Pyramidal Cells in the Neonatal Rat Neocortex” (2006), Cerebral Cortex, bhl127.

Jean-Vincent Le Bé and Henry Markram, “A new mechanism for memory: neuronal networks rewiring in the young rat neocortex”, Médecine/Sciences décembre 2006, 22(12), 1031-1033.

Jean-Vincent Le Bé, Tania Rinaldi and Henry Markram, “Altered synaptic rewiring in an animal model of autism”, in preparation with additional experiments.

2 Synaptic connectivity in sub-populations of PCs

2.1 Introduction

PCs are homogenous in terms of their gross morphology compared to the inhibitory interneurons. However, their axon projection targets are relatively heterogeneous. The vast majority of interneurons, both excitatory and inhibitory, project their axons locally within or close to the cortical column (Lubke *et al.* 2000 and see Markram *et al.* 2004). PCs on the other hand, project both locally and to other brain areas (Hubener and Bolz 1988; Farinas and DeFelipe 1991; Kasper *et al.* 1994a; Cho *et al.* 2004).

Classifying the PCs. The first morphological studies using retrograde tracers showed that a given PC projects either to cortical areas or to sub-cortical targets but not to both (Catsman-Berrevoets *et al.* 1980; Hallman *et al.* 1988). It was also shown that PCs in the visual cortex do not project to both the claustrum and the LGN (LeVay and Sherk 1981). This leads to the conclusion that projection target is a good criterion for PC sub-populations classification. PCs in these various sub-populations differ in their morphology and intrinsic cellular electrical properties. The projection targets might also determine the PCs embedding in the cortical column in terms of their synaptic connectivity. All of these differences will shape the functional roles that these neurons play in the microcircuit and affect the output to their respective brain regions.

Morphology varies with target. Differences in the morphology of PCs projecting to various targets have already been identified (Katz 1987; Hubener and Bolz 1988). The gross neuron shape features (the pyramidal-like soma and the apical dendrite growing towards the pia) are conserved across PC sub-populations, but more specific features differ from a sub-population to another. PCs that project to the thalamus and the superior colliculus are located in layer V and have a large soma compared to other PCs. Their apical dendrites extent up to layer I forming a dendritic tuft there (Katz 1987; Hubener and Bolz 1988; Markram *et al.* 1997a). These cells typically have on average 5 basal dendrites coming out of the soma (Kasper *et al.* 1994a; Kasper *et al.* 1994c; Markram *et al.* 1997a). These morphological features seem to be quite typical of the superior-colliculus or thalamic projecting PCs as, when the area is retrogradely labelled for these targets, unmarked cells present untufted apical dendrites (Kasper *et al.* 1994a).

PCs projecting to the contralateral hemisphere have also been carefully studied (Catsman-Berrevoets *et al.* 1980; Hubener and Bolz 1988; Kasper *et al.* 1994a; Christophe *et al.* 2005). The cell soma is also pyramidal shaped, although smaller and located in all layers except layer I. The apical dendrite does not reach layer I when the cell body is located in layer V and there are typically 3 to 5 basal dendrites (Kasper *et al.* 1994a; Kasper *et al.* 1994c). This morphology is not exclusive to the cortico-callosal cells since small untufted or slender PCs (Larkman and Mason 1990) are common in layer V, and retrograde labelling from the opposite hemisphere does not mark all the cells displaying this specific morphology (Kasper *et al.* 1994a). In more superficial layers, callosally projecting cells have a small soma and an apical dendrite terminating in layer I, but most of the PCs within this layer have a similar morphology. The main difference between neocortical PC sub-populations is in their axonal pattern (see Bannister 2005) and hence in their projection characteristics. Although they are

by far the most numerous neurons, PCs are not the only neurons marked by retrograde labelling.

Cortico-callosal neurons in the neocortex. Retrograde labelling with Diamidino Yellow marked various shapes of neurons across all the 6 layers of the neocortex (Martinez-Garcia *et al.* 1994). This study was done in the rat visual cortex, but spiny stellate cells labelled by retrograde tracers are also found in the cat's visual cortex (Vercelli *et al.* 1992). This latter study also suggests that the spiny stellate cells might be PCs in early stages of development and that the apical dendrite is pruned between P6 and P10. Cortico-callosal neurons are found in all the layers of the neocortex, mainly in layer III. The other layers where the cortico-callosal neurons are most represented are the layer V in rodents and layer VI in the cat (see Innocenti 1986). The cortico-callosal cells project mainly to the area homotopic to the one they are located in but some heterotopic projections have been observed in the infragranular layers (see Innocenti 1986).

Physiology varies with target. Early studies on the physiology of neurons in the neocortex showed three major characteristics (McCormick *et al.* 1985). An early classification divided the neurons into intrinsically bursting cells (IB) that start with a burst of APs in response to a depolarizing step current, regular spiking cells that respond to a depolarizing step current with regular firing at moderate frequency (241±102 $Hz.nA^{-1}$, mean±SD, McCormick *et al.* 1985) and fast spiking cells that respond with a regular firing at higher frequency (549±261 $Hz.nA^{-1}$, McCormick *et al.* 1985). However, the fast spiking cells presented in this study were likely to be GABAergic. Fast spiking behaviour had already been shown and was further confirmed to be characteristic to some GABAergic cells (Chagnac-Amitai and Connors 1989; Kawaguchi and Kubota 1998; Wang *et al.* 2002; Wang *et al.* 2004). Another study confirmed the dual firing pattern of the PCs (Chagnac-Amitai *et al.* 1990).

Studies using retrogradely labelled neurons (Katz *et al.* 1984) showed more detailed neuronal physiologies that are characteristic to projection targets. Kasper and collaborators (Kasper *et al.* 1994a) showed that the cortico-callosally projecting cells are regular spiking, and their smaller size induces a higher input resistance compared to the intrinsically bursting superior colliculus projecting cells with a larger size and a smaller input resistance. Other studies confirmed that these electrophysiological differences between PC sub-populations were partly correlated with the neuron's morphological characteristics (Kasper *et al.* 1994a; Christophe *et al.* 2005).

The bursting versus non-bursting classification is controversial and might not be related only to the projection target but also to variance within the same sub-population as well as developmental stage. It is shown further throughout this thesis that the cortico-callosally projecting cells in young animals can have an initial bursting behaviour and that the large thalamic projecting neurons can be regular spiking (also consistent with other studies: Kasper *et al.* 1994c; Christophe *et al.* 2005). The differences and the apparent shift between the populations characteristics can be explained by the difference in the species and ages of the animals used (Kasper *et al.* 1994b). This transition from bursting to non-bursting might even be more continuous and depend on other parameters. Work by Schwindt and collaborators (Schwindt and Crill 1999) showed that the mechanism for bursting depend on the calcium concentration in the cell and that bursting and non-bursting responses can be obtained from the same cell depending on the method used for the stimulation (somatic depolarization or extracellular pharmacological stimulation). Neuronal migration during brain development might influence the input patterns and hence the firing behaviour. On another hand, calcium might flow differently between juvenile and adult neurons, also influencing the firing pattern.

Synapses depend on target. The way the cells are embedded in the cortical column differs between PC sub-populations and would be of functional relevance. How are they interconnected with other neurons in the microcircuit? What is the synaptic distribution on the neuron? What is the balance between excitation and inhibition? Work done by Farinas and DeFelipe in 2001 showed that the cortico-callosally projecting cells receive more and have a denser repartition of symmetrical axo-somatic synapses than the thalamic projecting cells (Farinas and DeFelipe 1991). Symmetrical synapses are known to originate from inhibitory interneurons (Ribak 1978; Fairen and Valverde 1980; Freund *et al.* 1983; Hendry *et al.* 1983; Somogyi *et al.* 1983) and are the most numerous synapses on the PCs somata (Freund *et al.* 1983). This difference in inhibition together with the synaptic connectivity for specific projection targets PCs are yet to be investigated with electrophysiological recordings.

Retrograde Labelling. TTCs have been extensively studied (Katz 1987; Thomson *et al.* 1993a; Markram 1997; Markram *et al.* 1998; Kalisman *et al.* 2005) and are well recognizable by their specific morphology observed with an infra-red differential interference contrast (IR-DIC) microscope (see Figure 4). The early studies based on morphology used horseradish peroxydase as the retrograde marker (Schofield *et al.* 1987; Games and Winer 1988 and see Innocenti 1986) that can only be processed on fixed tissue and therefore limited the investigation to morphology. The use of latex microspheres (Katz *et al.* 1984; Katz and Iarovici 1990) that are retrogradely transported by the axons allows electrophysiological recordings of target-specific PCs. This technique highlighted differences in the electrophysiology between PCs that project to different brain areas (Kasper *et al.* 1994a; Christophe *et al.* 2005).

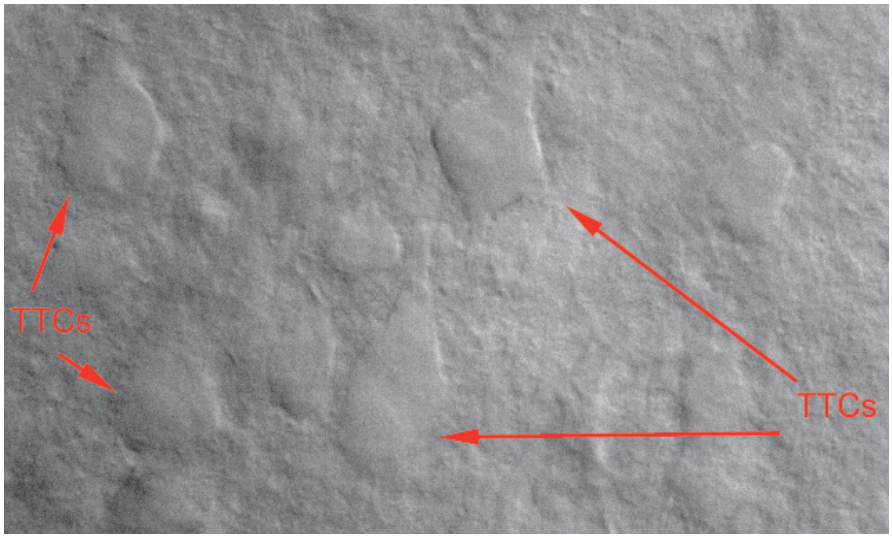

Figure 4 Infrared differential interference contrast of a portion of the somatosensory cortex. TTCs are indicated by red arrows. They are clearly differentiable from the other, smaller, cells present in the area.

The paper presented in section 2.5 reports the examination of the morphological, electrophysiological and synaptic properties of cortico-callosal PCs in layer V of the somatosensory cortex of young wistar rats (P13-P16). With the use of multi electrode patch clamp equipment, up to 4 neurons were simultaneously recorded. Identification of the callosal PCs was done by retrograde labelling with fluorescent latex microbeads. Pre-synaptic neurons were stimulated with trains of APs allowing the extraction of the Tsodyks-Markram model

parameters of post-synaptic responses (as presented in section 1.4 on page 17). TTCs were also recorded and their connections dynamics and rates compared with the labelled cortico-callosal neurons. As reported above, the morphological and intrinsic electrophysiological properties of the cortico-callosally projecting cells (CCPs) have already been described in some detail. The synaptic properties of this sub-population of PCs is however unknown and of crucial importance to understand the role these cells play in the neocortex.

2.2 Materials and Methods

Injections. CCPs labelling was done by injections of fluorescent microbeads (Lumafluor, 4x diluted in nano-pure water) into the left hemisphere of P11 (postnatal 11 days) Wistar rats (Figure 1*A* of the paper in section 2.5). These beads are retro-transported by the axons that terminate at the site of injection. The rats were anaesthetized with an intraperitoneal injection of Fentanyl-Medetomidine (mixed from Fentanyl IV solution at 0.05mg ml^{-1} and Domitor solution at 1mg ml^{-1} and completed with saline solution to get a 10ml kg^{-1} injection and 0.3mg kg^{-1} for both products). They were then fixed on a stereotaxic table (Stoelting co., Illinois) and their head skin opened with a scalpel sagittally from between the eyes to between the ears. The skin was then gently pushed aside and the skull cleaned with a dry cotton piece. The smooth skull was then pierced at the injection sites with a Neolus 25G x 5/8'' syringe needle (Terumo Europe N.V., Leuven, Belgium). It was then cleaned again and the beads were injected with a Hamilton syringe inserted 1 mm below the skull surface. A volume of 0.5 µl per site was injected in three sites 1 mm lateral and 0 ± 1 mm from Bregma in the left hemisphere (Somatosensory cortex, S1). In order to get a good diffusion at the injection site the syringe was retracted 60 s after the end of the injection. The wound was then glued with chirurgical glue (Histoacryl, Braun Aesculap) and the rats awakened with Atipamezole-Naloxone (1mg kg^{-1} and 0.1mg kg^{-1} respectively, mixed from Antisedan solution at 5mg ml^{-1} and Narcan solution at 0.4mg ml^{-1} and completed with saline to get a 10ml kg^{-1} injection). After complete awakening (~20 min) the rats were returned to their mother's cage. All animal experimentations were performed under the Swiss guidelines for animal experiments.

Slicing. Three days following the injection of beads, the rats were rapidly decapitated and sagittal slices (300 µm thick) of the right hemisphere were cut in artificial cerebro-spinal fluid (ACSF) on a slicer HR2 (Sigmann Elektronik, Heidelberg). The hemisphere was glued at the surface of the sagittal plane onto a block, which was mounted at an angle of 10° such that the blade cut from the upper part of the cortex towards the caudal border and down towards the midline. Slices were incubated for 15 to 30 min at 35°C and then left at room temperature (20-22°C). The ACSF contained (in mM): 125 NaCl, 2.5 KCl, 25 D-glucose, 25 $NaHCO_3$, 1.25 NaH_2PO_4, 2 $CaCl_2$ and 1 $MgCl_2$.

Fluorescence and IR-DIC microscopy. Neurons in somatosensory cortex were identified using IR-DIC microscopy (Figure 5*A* below and Figure 1*C* of the paper in section 2.5), with an upright microscope (BX 51WI, Olympus, fitted with a 60x LUMPlan FI, Japan objective). The recorded neurons were selected up to 50 µm below the slice surface. The fluorescent beads were identified using the same microscope with a filter cube for GFP (Figure 5*B* below and Figure 1*B* of the paper in section 2.5). Both fluorescence and IR-DIC images were taken by a camera (VX 55, Till Photonics) and displayed on a monitor (WV-BM 1410, Panasonic). The cells identified under the fluorescence were marked on the monitor with the z coordinates given by the micro-manipulators (SM-55, Luigs and Newmann) and could then be identified with certainty in the IR-DIC imaging for patch clamp recordings (Figure 5*C* below and Figure 1*D* of the paper in section 2.5).

Electrophysiological recordings. Somatic whole-cell recordings were performed at 35°C and signals were amplified using Axoclamp-2B amplifiers (Axon Instruments, USA). Voltages were recorded with pipettes containing (in mM): 110 potassium gluconate, 10 KCl, 4 ATP-Mg, 10 phosphocreatine, 0.3 GTP, 10 Hepes (pH 7.3, 310 mOsm adjusted with

sucrose) and 0.5% biocytin. The pipettes were pulled with a Flamming/Brown micropipette puller P-97 (Stutter Instruments CO, USA). The scaled output of the amplifier was connected to an ITC device (ITC-18, Instrutech Co, Port Washington, New York, USA) connected to an Apple computer running Igor Pro (Wavemetrics). The junction potential between the ACSF and the solution in the pipettes was around -10mV. The recordings were made without correction for it.

Biocytin labelling. The recording pipettes were filled with 5 mg ml^{-1} of biocytin that was perfused into the neurons during recording. Following the recording, the slices were fixed for at least 24 hours in a cold phosphate buffer (100 mM, pH 7.4) containing 2% paraformaldehyde and 1% glutaraldehyde and 0.3% picric acid. Thereafter, the slices were rinsed and then transferred into a phosphate-buffered 3% H_2O_2 to block endogenous peroxidases. After rinsing in the phosphate buffer, slices were incubated overnight at 4°C in an avidin-biotinylated horseradish peroxidase (ABC-Elite, Vector Labs; 5% A, 5% B and 0.25% Triton X-100). Subsequently, sections were rinsed again in the phosphate buffer and developed with diaminobenzidine (DAB substrate kit, Vector Labs) under visual control using a stereomicroscope (Leica) until all processes of the cells were clearly visible. Finally, the reaction was stopped by transferring the sections into the phosphate buffer. After rinsing in the phosphate buffer, slices were mounted in an aqueous mounting medium.

Reconstruction. The stained cells were reconstructed under light microscope using Neurolucida software (Microbrightfield). Reconstructed neurons and connections underwent quantitative analysis using NeuroExplorer (MicroBrightField). The quantitative morphometric analysis is based on multiple parameters derived from the dendrites and axons of reconstructed neurons. Putative contacts were identified according to the following criteria: (i) only the contacts formed by axonal swellings (boutons) were considered; (ii) the same plane of focus (microscope lens with x60 magnification, numerical aperture = 0.9; resolution along the Z-axis = 0.37 μm) is used. This requires the boutons and soma/dendrite/axon to be membranes within <0.5 μm of each other; (iii) if a dendrite is thick (>2 μm) with many spines, then a greater distance between the bouton and dendrite is allowed, providing that the course of the axon bent towards or ran parallel to the dendrite. When a putative contact was located, it was systematically double-checked through the eye-pieces to confirm the screen based identification. The staining procedure results in ~25% shrinkage of the slice thickness and ~10% anisotropic shrinkage along the X and Y axes. Only the shrinkage of thickness was corrected.

Electrophysiological analysis. The AP onset is measured as the time point where the second derivative with respect to time of the voltage trace is maximum, i.e. where the deflection of the curve is maximum. The end of the AP falling phase is measured as the time point where the modulus of the falling rate becomes lower than 5 Vs^{-1}.

The EPSP onset was calculated by linear extrapolation from the 20-80% maximum amplitude linear fitting on the average trace of 80 single sweep events. These onset points were then automatically marked on the graph for visual verification. The latency of the single EPSP is defined as the time lapse between the top of the pre-synaptic AP and the EPSP onset. The coefficient of variation (CV) of the EPSP amplitude was calculated based on the measured amplitudes of each of the 80 single events triggered.

Model for synaptic dynamics. In order to analyze quantitatively the synaptic connections, a model of dynamic synaptic transmission was used (Markram *et al.* 1998 and see section 1.4). Fitting the responses to the model yielded four parameters: the time constant of recovery from

depression, τ_D; the time constant of recovery from facilitation, τ_F; utilization of synaptic resources as used analogously to Pr (e.g., release probability), U; and the absolute strength, ASE, of the synaptic connection (defined as the response when U equals 1). After the 5th EPSP of a given train the response typically reaches a steady-state amplitude considered to calculate the steady-state vs frequency (f) relationship. The frequency at which this curve matches a 1/f function is the limiting frequency. Tsodyks and Markram (Tsodyks and Markram 1997) showed that if the pre-synaptic cell fires above the limiting frequency, the average post-synaptic depolarization will remain constant. The same study demonstrated that as lowering the calcium concentration increases the limiting frequency, this frequency is pre-synapticaly dependent and estimated by: $f \approx 1/(\tau_D \bullet U)$.

2.3 Results

The results are presented extensively in the paper in section 2.5. A brief summary of the most important results is given below.

Thirty-nine P11 Wistar rats were injected with fluorescent microbeads into the left primary sensory cortex (S1) and 476 marked cells were recorded in the right S1. Paired recordings were performed for cells which somata were separated by less than 100µm. The cortico-callosally projecting cells of the neocortical layer V (CCPs) have a lower release probability compared to the TTCs. This implies a tendency for a more linear dynamics within the CCPs sub-population compared to the dynamics within the TTCs sub-population (see Figures 6 and 7 of the paper). Additionally, the connectivity is about 4 times higher in the TTCs sub-population. The single EPSP characteristics (such as amplitude, rise time and time constant of voltage decay from the EPSP peak to the rest membrane potential) are similar for both populations (Figure 4 of the paper).

CCPs in layer V have an untufted apical dendrite (Figure 1*E* and 3*A* of the paper) as it is shown by the Sholl distance analysis on the Figure 3*B* of the paper. The main axonal trunk descends vertically to the white matter but two major features can be distinguished for the axons collaterals in the cortical sheet. 70% of the CCPs have an axon collateral extending parallel to the apical dendrite and 80% have two collaterals extending horizontally just below the proximal dense axonal arborisation (see Figure 3*A* and *F* of the paper). Connected CCPs pairs have typically 4.0±0.3 putative synapses located on average at 130±18µm from the soma along the dendrite and 80% of the contacts are on basal dendrites.

Single cell electrophysiology revealed that CCPs have two distinct firing patterns. One half of the cells have an initial burst of 2-3 APs when a square current pulse is injected into the soma. The other half does not have this burst. The current-discharge average slope is 13±19 $Hz.nA^{-1}$ for the non-bursting CCPs and 40±30 $Hz.nA^{-1}$ for the bursting cells (mean±SD, $p<0.05$, Student t-test).

2.4 Discussion

This study describes the morphological, electrophysiological and synaptic properties of a sub-population of neocortical PCs, the CCPs. The small size of the cells and hence the high input resistance together with the short untufted apical dendrite terminating in layer II-III are consistent with previous results (Katz 1987; Hubener and Bolz 1988; Christophe *et al.* 2005). In comparison with the TTCs electrophysiological properties, the CCP APs are smaller in amplitude and of a longer duration. The CCPs firing threshold is higher than the TTCs suggesting that CCPs are less excitable. However, with a higher input resistance, both phenomena might compensate each other resulting in the similar current-discharge slope observed for the two populations (see table 1 in the paper). The high standard deviation in the current-discharge slope distribution for the CCPs suggest a differential behaviour for two sub-groups within that population that could be related to the bursting versus non-bursting CCPs observed. Although the current-discharge slope distribution does not show two clear peaks, there is a significant difference between the average current-discharge slope for the bursting CCPs and the non-bursting CCPs. None of these differs significantly from the TTC average current-discharge slope. The burst mechanism rather than the excitability of the cells might be at the origin of this difference. The standard deviation remains however large despite the split of the CCPs population into two groups. This indicates that the CCPs have a large variability in their excitability regardless of their bursting or non-bursting initial response.

Synapses between CCPs have a lower probability of release than between TTCs. Moreover, CCPs are 4 time less interconnected than the TTCs. This suggests, given the more phasic reaction, that TTCs might have a more integrative role. Indeed, when the TTCs sub-population receives a signal, the beginning of this signal will be propagated into the population but later information might be lost unless the circuit is given a time for the synapses to recover from depression. The signal given out by the TTCs subpopulation is then likely to be importantly modified. On the contrary, the low connected linear responding CCPs sub-population is more likely to amplify slightly the input signal but above all to transmit it with minimum distortion. These cells would then give a read out of their home cortical column to the opposite hemisphere counterpart.

In the line of other publications (see Innocenti 1986 for a review), the area of the cortex labelled was shown to be homotopic to the site of injection in the opposite hemisphere although some labelling of adjacent areas have been noted but to a lesser extent. This suggests that the CCPs main role is to transmit the information about the computation performed by their cortical column to the cortical column that is symmetrically placed in the neocortex. These cells therefore might play a role of synchronisation across the hemispheres at the level of the cortical column localized in similar functional areas for both sides of the neocortex.

A deficiency in the corpus callosum or in the CCPs population gives rise to impairments in bilateral vision (Gott and Saul 1978), bimanual movements (Eliassen *et al.* 2000) and language skills (Gazzaniga *et al.* 1989). This suggests that synchronisation at the cortical column level via CCPs is essential for proper function of various cortical modalities.

Future developments. The connectivity across populations has not been examined in this study. A first step would be to patch pairs of CCPs-TTCs identified by retrograde labelling. If the hypothesis of the read-out role of CCPs is correct, these connections should be quite

frequent and with a linear dynamics. The connectivity across other PC sub-populations should also be studied carefully in the same manner. This could be achieved with double retrograde labelling of the neocortical PCs as microbeads containing different fluorescence wavelengths are commercially available (Lumafluor, Naples, FL). These studies would reveal further the role of the various PCs sub-populations and would also give more information about the component of cortical computation that is sent to the various targets. Inhibition is another important aspect of the neocortical microcircuit, which must be studied with respect to the different PC sub-populations. In order to fully understand the integration of the different PC subtypes in the neocortical microcircuit, it is important to study the inhibitory pathways that characterize them.

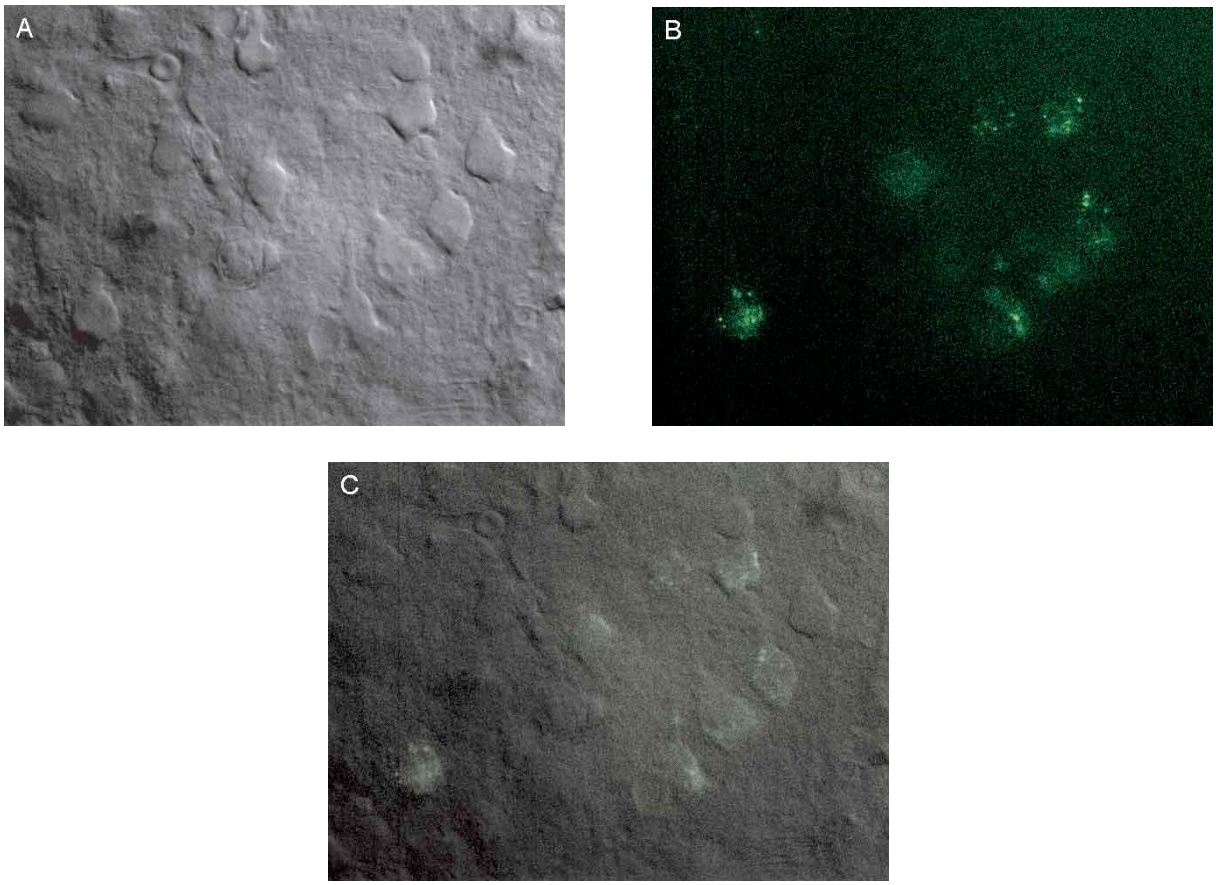

Figure 5 Density of labelled cortico-callosal cells in rat neocortex. A – Infrared differential interference contrast (IR-DIC) image of rat neocortex after bead injection in the contralateral cortex. B – The same area as in *A* under green fluorescence. The beads are visible as small green dots. C – Merge of *A* and *B* showing that the CCPs are quite present in the neocortex.

2.5 The publication

Cerebral Cortex Advance Access published November 23, 2006

Cerebral Cortex
doi:10.1093/cercor/bhl127

Morphological, Electrophysiological, and Synaptic Properties of Corticocallosal Pyramidal Cells in the Neonatal Rat Neocortex

Jean-Vincent Le Bé[1], Gilad Silberberg[1,2], Yun Wang[3] and Henry Markram[1]

[1]Laboratory of Neural Microcircuitry, Brain Mind Institute, Ecole Polytechnique Fédérale de Lausanne (EPFL), Lausanne 1015, Switzerland, [2]Nobel Institute for Neurophysiology, Department of Neuroscience, Karolinska Institute, Stockholm, Sweden and [3]Division of Neurology Research, Caritas St Elizabeth's Medical Center, Tufts University, Boston, MA, USA

Neocortical pyramidal cells (PCs) project to various cortical and subcortical targets. In layer V, the population of thick tufted PCs (TTCs) projects to subcortical targets such as the tectum, brainstem, and spinal cord. Another population of layer V PCs projects via the corpus callosum to the contralateral neocortical hemisphere mediating information transfer between the hemispheres. This subpopulation (corticocallosally projecting cells [CCPs]) has been previously described in terms of their morphological properties, but less is known about their electrophysiological properties, and their synaptic connectivity is unknown. We studied the morphological, electrophysiological, and synaptic properties of CCPs by retrograde labeling with fluorescent microbeads in P13–P16 Wistar rats. CCPs were characterized by shorter, untufted apical dendrites, which reached only up to layers II/III, confirming previous reports. Synaptic connections between CCPs were different from those observed between TTCs, both in probability of occurrence and dynamic properties. We found that the CCP network is about 4 times less interconnected than the TTC network and the probability of release is 24% smaller, resulting in a more linear synaptic transmission. The study shows that layer V pyramidal neurons projecting to different targets form subnetworks with specialized connectivity profiles, in addition to the specialized morphological and electrophysiological intrinsic properties.

Keywords: corpus callosum, neocortex, pyramidal neurons, synaptic connections

Introduction

Transfer of information between the 2 neocortical hemispheres is essential for a variety of cognitive processes, such as perception, memory, attention, and learning (Engel et al. 1991; Matsuzaka et al. 1999; Eliassen et al. 2000; Aboitiz et al. 2003; Quigley et al. 2003). Information is directly transferred between the 2 neocortical hemispheres by axons of a specialized subpopulation of neocortical pyramidal cells (PCs) via the corpus callosum. Neocortical PCs exhibit a large diversity, which is mainly evident in their different morphological properties (Simons and Woolsey 1984; Hirsch et al. 1998) and projection targets (Katz 1987; Hubener and Bolz 1988; Kasper et al. 1994; Zhang and Deschenes 1997; Thomson and Bannister 2003). Layer V PCs project to various targets, including subcortical nuclei (White and Hersch 1982; Cho et al. 2004), cortical regions in the same hemisphere (Zhang and Deschenes 1998), and the contralateral hemisphere (Katz 1987; Hubener and Bolz 1988). The differences in the morphological properties of the different PC subpopulations (Hubener and Bolz 1988; Tsiola et al. 2003; Vercelli et al. 2004; Yuste 2005) suggest that they integrate cortical activity differently, thus conveying different aspects of the cortical activity to the various efferent targets. The electrophysiological and synaptic properties of the different PC subpopulations are also likely to affect their respective functions.

Corticocallosally projecting cells (CCPs) project to the contralateral hemisphere via the corpus callosum. They are characterized by a small soma and a short apical dendrite that does not display a tuft in layer I, strikingly different from the extensively studied layer V thick tufted PCs (TTCs) that have a big soma and a thick apical dendrite forming tuft dendrites in layer I and project their axons to the tectum, brainstem, and the spinal cord (Hubener and Bolz 1988; Kasper et al. 1994). Previous reports showed electrophysiological (Kasper et al. 1994; Christophe et al. 2005) and genetic (Christophe et al. 2005) differences between the TTCs and the CCPs. A systematic study of the CCPs synaptic properties is however still lacking. In this study, CCPs were selectively labeled by retrograde injection of fluorescent microbeads to the contralateral hemisphere and then recorded by multineuron whole-cell recordings followed by 3-dimensional morphological reconstruction for detailed characterization. We describe here the morphological, electrophysiological, and synaptic properties of corticocallosal PCs in layer V of the rat somatosensory neocortex.

Materials and Methods

Injections

CCPs labeling was done by injections of fluorescent microbeads (Lumafluor, Naples, FL, 4× diluted in nano-pure water) into the left hemisphere of P11 (postnatal 11 days) Wistar rats (Fig. 1*A*). These beads are retrotransported by the axons that terminate at the site of injection. The rats were anesthetized with an intraperitoneal injection of Fentanyl-Medetomidine (mixed from Fentanyl IV solution at 0.05 mg mL^{-1} and Domitor solution at 1 mg mL^{-1} and completed with saline solution to get a 10 mL kg^{-1} injection and 0.3 mg kg^{-1} for both products). They were then fixed on a stereotaxic table (Stoelting Co., Wood Dale, IL) and their head skin opened with a scalpel sagittally from between the eyes to between the ears. The skin was then gently pushed aside, and the skull cleaned with a dry cotton piece. The smooth skull was then pierced at the injection sites with a Neolus 25G × 5/8″ syringe needle (Terumo Europe N.V., Leuven, Belgium). It was then cleaned again, and the beads were injected with a Hamilton syringe inserted 1 mm below the skull surface. A volume of 0.5 μL per site was injected in 3 sites 1 mm lateral and 0 ± 1 mm from Bregma in the left hemisphere (somatosensory cortex, S1). In order to get a good diffusion at the injection site, the syringe was retracted 60 s after the end of the injection. The wound was then glued with chirurgical glue (Histoacryl, Braun Aesculap, Tuttlingen, Germany) and the rats awakened with Atipamezole–Naloxone (1 mg kg^{-1} and 0.1 mg kg^{-1}, respectively, mixed from Antisedan solution at 5 mg mL^{-1} and Narcan solution at 0.4 mg mL^{-1} and completed with saline to get a 10 mL kg^{-1} injection). After complete awakening (~20 min), the rats were returned to their mother's cage. All animal experimentations were performed under the Swiss guidelines for animal experiments.

Slicing

Three days following the injection of beads, the rats were rapidly decapitated, and sagittal slices (300 μm thick) of the right hemisphere

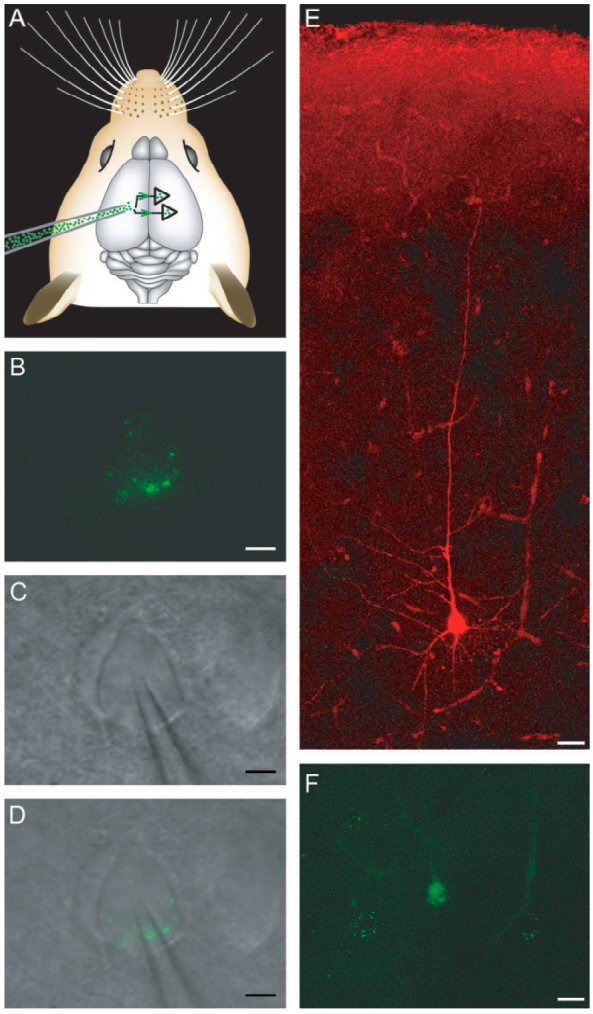

Figure 1. Isolation of the corticocallosally projecting PCs. (*A*) Schematics of the beads injection procedure. The beads are injected in layer V of the left hemisphere cortex. They then undergo retrograde transport (green arrows) to the right hemisphere (used for recordings) marking the cells projecting via the corpus callosum. (*B*) High-magnification picture of a retrograde-labeled pyramidal neuron. The green dots are the ~0.2 μm beads. Scale bar 5 μm. (*C*) The same view as in (*B*) but under IR-DIC imaging, showing the cell and the patch pipette. (*D*) Merge of (*B*) and (*C*). (*E*) Low-magnification fluorescence view of the cell in (*B*), (*C*), (*D*) filled with alexa red by the patch pipette. Scale bar 20 μm. (*F*) Low magnification of the region containing the cell mentioned (in plain green due to overlap with alexa red spectrum in the green region). Other cells marked with beads are present in the area showing the possibility to obtain paired recordings of the identified population. Scale bar 20 μm.

were cut in artificial cerebrospinal fluid (ACSF) on a slicer HR2 (Sigmann Elektronik, Heidelberg, Germany). The hemisphere was glued at the surface of the sagittal plane onto a block, which was mounted at an angle of 10° such that the blade cut from the upper part of the cortex toward the caudal border and down toward the midline. Slices were incubated for 15–30 min at 35 °C and then left at room temperature (20–22 °C). The ACSF contained (in mM) 125 NaCl, 2.5 KCl, 25 D-glucose, 25 $NaHCO_3$, 1.25 NaH_2PO_4, 2 $CaCl_2$, and 1 $MgCl_2$.

Fluorescence and infrared differential interference contrast (IR-DIC) Microscopy

Neurons in somatosensory cortex were identified using IR-DIC microscopy (Fig. 1*C*), with an upright microscope (BX 51WI, Olympus, fitted with a 60× LUMPlan FI, Japan objective). The recorded neurons were selected up to 50 μm below the slice surface. The fluorescent beads were identified using the same microscope with a filter cube for green fluorescent protein (Fig. 1*B*). Both fluorescence and IR-DIC images were taken by a camera (VX 55, Till Photonics, Gräfelfing, Germany) and displayed on a monitor (WV-BM 1410, Panasonic, Osaka, Japan). The cells identified under the fluorescence were marked on the monitor with the *z* coordinates given by the micromanipulators (SM-55, Luigs and Neumann, Ratingen, Germany) and could then be identified with certainty in the IR-DIC imaging for patch-clamp recordings (Fig. 1*D*).

Electrophysiological Recordings

Somatic whole-cell recordings were performed at 35 °C, and signals were amplified using Axoclamp-2B amplifiers (Axon Instruments, Molecular Devices, Union City, CA). Voltages were recorded with pipettes containing (in mM) 110 potassium gluconate, 10 KCl, 4 ATP-Mg, 10 phosphocreatine, 0.3 GTP, 10 *N*-2-hydroxyethylpiperazine-*N*′-2-ethanesulfonic acid (pH 7.3, 310 mOsm adjusted with sucrose), and 0.5% biocytin. The pipettes were pulled with a Flamming/Brown micropipette puller P-97 (Sutter Instruments Co, Novato, CA). The scaled output of the amplifier was connected to an ITC device (ITC-18, Instrutech Co, Port Washington, NY) connected to an Apple computer running Igor Pro (Wavemetrics, Portland, OR). The junction potential between the ACSF and the solution in the pipettes was around −10 mV. The recordings were made without correction for it.

Biocytin Labeling

The recording pipettes were filled with 5 mg mL^{-1} of biocytin that was perfused into the neurons during recording. Following the recording, the slices were fixed for at least 24 h in a cold phosphate buffer (100 mM, pH 7.4) containing 2% paraformaldehyde and 1% glutaraldehyde and 0.3% picric acid. Thereafter, the slices were rinsed and then transferred into a phosphate-buffered 3% H_2O_2 to block endogenous peroxidases. After rinsing in the phosphate buffer, slices were incubated overnight at 4 °C in an avidin-biotinylated horseradish peroxidase (ABC-Elite, Vector Labs, Burlingame, CA; 5% A, 5% B, and 0.25% Triton X-100). Subsequently, sections were rinsed again in the phosphate buffer and developed with diaminobenzidine (DAB substrate kit, Vector Labs) under visual control using a stereomicroscope (Leica, Wetzlar, Germany) until all processes of the cells were clearly visible. Finally, the reaction was stopped by transferring the sections into the phosphate buffer. After rinsing in the phosphate buffer, slices were mounted in an aqueous mounting medium.

Reconstruction

The stained cells were reconstructed under light microscope using Neurolucida software (MicroBrightField, Magdeburg, Germany). Reconstructed neurons and connections underwent quantitative analysis using NeuroExplorer (MicroBrightField). The quantitative morphometric analysis is based on multiple parameters derived from the dendrites and axons of reconstructed neurons. Putative contacts were identified according to the following criteria: (i) only the contacts formed by axonal swellings (boutons) were considered; (ii) the same plane of focus (microscope lens with 60× magnification, numerical aperture = 0.9; resolution along the *z* axis = 0.37 μm) is used. This requires the boutons and soma/dendrite/axon to be membranes within <0.5 μm of each other; (iii) if a dendrite is thick (>2 μm) with many spines, then a greater distance between the bouton and dendrite is allowed, providing that the course of the axon bent toward or ran parallel to the dendrite. When a putative contact was located, it was systematically double-checked through the eyepieces to confirm the screen-based identification. The staining procedure results in ~25% shrinkage of the slice thickness and ~10% anisotropic shrinkage along the *x* and *y* axes. Only the shrinkage of thickness was corrected.

Electrophysiological Analysis

The action potential (AP) onset is measured as the time point where the second derivative with respect to time of the voltage trace is maximum, that is, where the deflection of the curve is maximum. The end of the AP falling phase is measured as the time point where the modulus of the falling rate becomes lower than 5 V s^{-1}.

The excitatory postsynaptic potential (EPSP) onset was calculated by linear extrapolation from the 20–80% maximum amplitude linear fitting on the average trace of 80 single sweep events. These onset points were then automatically marked on the graph for visual verification. The latency of the single EPSP is defined as the time lapse between the top of the presynaptic AP and the EPSP onset. The coefficient of variation (CV) of the EPSP amplitude was calculated based on the measured amplitudes of each of the 80 single events triggered.

Model for Synaptic Dynamics

In order to analyze quantitatively the synaptic connections, a model of dynamic synaptic transmission was used (Markram et al. 1998). Fitting the responses to the model yielded 4 parameters: the time constant of recovery from depression, τ_D; the time constant of recovery from facilitation, τ_F; utilization of synaptic resources as used analogously to Pr (e.g., release probability), U; and the absolute strength, ASE, of the synaptic connection (defined as the response when Pr equals 1). After the 5th EPSP of a given train, the response typically reaches a steady-state amplitude considered to calculate the steady-state versus frequency (f) relationship. The frequency at which this curve matches a $1/f$ function is the limiting frequency. Tsodyks and Markram (1997) showed that if the presynaptic cell fires above the limiting frequency, the average postsynaptic depolarization will remain constant. The same study demonstrated that as lowering the calcium concentration increases the limiting frequency, this frequency is presynaptically dependent and estimated by $f \approx 1/(\tau_D \times Pr)$.

Results

Thirty-nine P11 Wistar rats were injected with fluorescent latex microbeads into layer V of the somatosensory cortex (S1). Rats appeared fully recovered within 2 days following the injection. The microbeads were clearly visible in acute slices under fluorescence microscopy, enabling selective recordings from neighboring (<100 μm somatic distance) CCPs (Fig. 1 *A,F*). A total of 476 marked cells were patched and filled with biocytin. The neuron somata were small and pyramidal shaped with a slender apical dendrite projecting toward the pia. Neurons with soma located in lower layer V had an apical dendrite projecting to layer II/III, whereas about 80% of the neurons located in more superficial layers had an apical dendrite reaching layer I (Fig. 1*E*). Labeled cells were visible in all the layers from layer II to layer VI in an area symmetrical to the injection site.

Single-Cell Electrophysiology

The response of CCPs to a step current injection was either an initial AP or a burst of 2–3 APs followed by a pause before firing again (Fig. 2*G*, defined as burst adapting) or an initial AP or burst followed by a regular spiking train (Fig. 2*H*). Both behaviors were observed at high and low current injections. Their small somata and dendrites are expected to yield a relatively high input resistance and indeed, the input resistance was 183 ± 67 MΩ (all values are given as mean ± standard deviation [SD], n = 22, Fig. 2*A,B*, Table 1), and the membrane time constant in response to a negative pulse (Δ pulse) was 20 ± 6 ms (Fig. 2*D*, Table 1). In response to a step current injection, CCPs displayed slow after-hyperpolarization (Fig. 2*C*) of 7.1 ± 3.2 mV. The spiking threshold was −32 ± 6 mV (Fig. 2*F*), and on about half of the cells, an initial burst was present (Fig. 2*F*). A typical AP had an amplitude of 60 ± 5 mV, a duration at half amplitude of 1.9 ± 0.3 ms, a rise time of 1.0 ± 0.2 ms, and a fall time of 3.2 ± 0.6 ms (Fig. 2*E*). Values for second APs in a train and other intrinsic parameters are given in Table 1.

CCP versus TTC Single-Cell Electrophysiology

In order to compare the single-cell electrophysiology of the CCPs with the TTCs, we recorded from 35 TTCs using the same protocol of Figure 2. The CCPs have an AP amplitude significantly smaller than the TTCs (60 ± 5 mV, n = 22 vs. 63 ± 5 mV, n = 35, respectively, mean ± SD). This difference is even larger in the second AP of a train generated by a depolarizing step current (45 ± 11 mV vs. 63 ± 6 mV). On the contrary, the AP duration is about 1.2 ms longer for the CCPs (4.3 ± 0.6 ms vs. 3.1 ± 0.5 ms for the first AP and 7.2 ± 1.2 ms vs. 6.0 ± 0.7 ms for the second AP in a train). The input resistance is 3.6 times larger in the CCPs (183 ± 67 MΩ vs. 51 ± 15 MΩ), but the membrane time

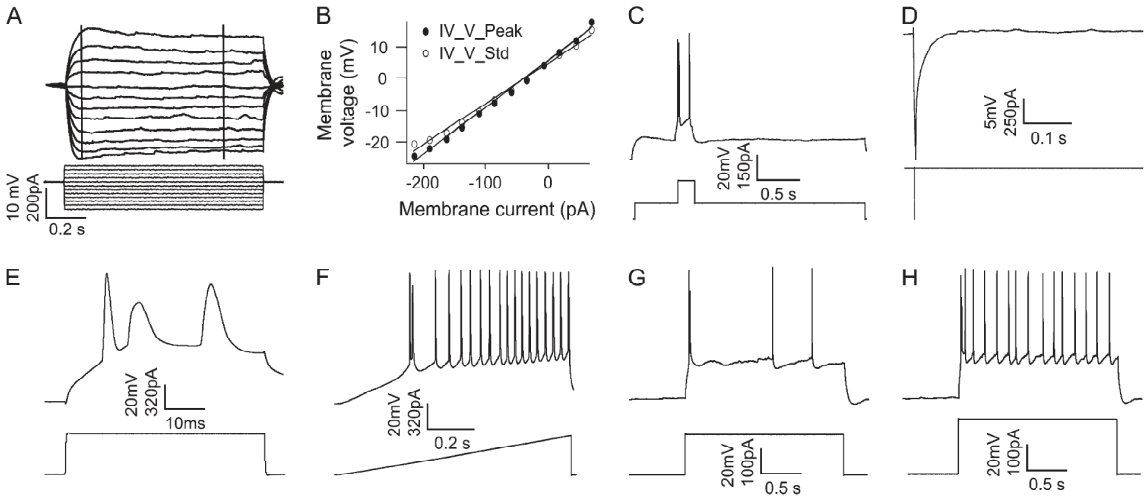

Figure 2. Single CCP electrophysiology. Recorded neurons are held at a membrane potential of −70 mV in current-clamp configuration. (*A*) Injected current steps and their corresponding voltage responses. (*B*) IV graph of the current–voltage relationship protocol described in (*A*). (*C*) Voltage response and current stimulation for slow after-hyperpolarization potential. (*D*) Voltage response and current stimulation of a short (5 ms) hyperpolarizing current injection used to determine the membrane time constant. (*E*) Voltage response and current stimulation of high temporal resolution used to determine the AP waveform. (*F*) Voltage response and current stimulation of a ramp to determine the discharge threshold. (*G*) Voltage response and current stimulation just above threshold to determine the threshold response to a long depolarizing pulse. (*H*) Same as in (*G*) but for more depolarized stimulation.

Table 1
Electrophysiological properties of the CCPs and the TTCs

	CCP (n = 22)	TTC (n = 35)
Access (MΩ)	23.7 ± 5.4	21.9 ± 4.9
First AP in train		
AP amplitude (mV)	59.6 ± 5.5	63.0 ± 5.3*
AP duration (ms)	4.29 ± 0.64	3.09 ± 0.52***
AP duration at half amplitude (ms)	1.93 ± 0.31	1.35 ± 0.24***
AP rise time (ms)	1.05 ± 0.16	0.80 ± 0.15***
AP fall time (ms)	3.24 ± 0.55	2.29 ± 0.41***
Fast AHP (mV)	−2.2 ± 4.1	3.7 ± 3.5***
Second AP in train		
AP amplitude (mV)	45 ± 11	63 ± 6***
AP duration (ms)	7.2 ± 1.2	6.0 ± 0.7***
AP duration at half amplitude (ms)	2.87 ± 0.88	2.06 ± 0.35***
AP rise time (ms)	1.99 ± 0.39	1.25 ± 0.26***
AP fall time (ms)	5.2 ± 1.1	4.7 ± 0.7
IV analysis		
Time to hyperpol peak (s)	0.194 ± 0.033	0.417 ± 0.430**
Input resistance for peak (MΩ)	228 ± 92	64 ± 19***
Input resistance for steady state (MΩ)	183 ± 67	51 ± 15***
Maximum sag (mV)	6.6 ± 3.9	5.8 ± 3.4
Decay time constant for Δ pulse (ms)	20.0 ± 5.8	17.5 ± 4.7
AP threshold (mV)	−32.3 ± 5.6	−39.4 ± 2.6***
Slow AHP (mV)	7.1 ± 3.2	8.6 ± 2.9
Step current		
Average delay to first spike (s)	0.031 ± 0.013	0.026 ± 0.012
Current-discharge slope (Hz nA^{-1})	27.6 ± 28.5	26.2 ± 5.7
Initial burst interval (s)	0.052 ± 0.047	0.081 ± 0.049*

Note: Mean ± SD, *P < 0.05, **P < 0.01, ***P < 0.001, P value is from Student t-test; AHP – after hyperpolarization.

constant after a hyperpolarizing spike is similar for both populations (20 ± 6 ms vs. 18 ± 5 ms). CCPs had a higher discharge threshold (-32 ± 6 mV vs -40 ± 3 mV), as extracted from a response to a ramp current injection (Fig. 2 F). Both populations have a similar mean current-discharge slope although its variation is much higher in the CCPs population than for the TTCs (28 ± 28 Hz nA^{-1} for CCPs and 26 ± 6 Hz nA^{-1} for TTCs). The initial burst interval is significantly smaller in the CCPs (50 ± 50 ms vs. 80 ± 50 ms) showing the tendency for some cells of this population to discharge with an initial burst in response to a depolarizing step current. The distribution of this interval for the CCPs is not showing 2 distinct groups indicating that the transition between bursting and not-bursting behavior is continuous in the CCPs population (bursting on Fig. 2*F* and not-bursting on Fig. 2*G*). None of the TTCs recorded showed this initial burst. The complete data set is given in Table 1.

Morphology of the Corticocallosal Cells

Consistent with previous reports (Katz 1987; Hubener and Bolz 1988; Christophe et al. 2005), the morphological differences of CCPs from TTCs were already obvious under light microscopy by the smaller soma and the untufted apical dendrites (Fig. 3*A*,*F*). These differences in the dendritic arborization are further quantified by the total dendritic tree surface (4800 ± 300 μm^2 for the CCPs vs. 33 000 ± 3000 μm^2 for TTCs) and by the dendritic Sholl distance (Fig. 3*B*), in which the number of intersections crossing concentric circles centered on the soma are counted (Fig. 3*A*). The Sholl analysis provides a quantitative estimate of the arborization of an axonal or dendritic tree. A greater number of crossings at a given distance compared with another indicate that it is more likely for the neuron to send outputs or receive inputs at that distance. The dendritic Sholl distance distribution of CCPs displayed a single peak within a radius of 100 μm from soma (Fig. 3*B*, red). The TTCs Sholl distance distribution shows clearly the tuft at a distance between 700 μm and 980 μm from the soma (Fig. 3*B*, gray). Moreover, the more extended dendritic tree of the TTCs is also visible on the Sholl distribution as the plot of Figure 3*B* is scaled by a factor of 0.51 for the TTCs. The axonal Sholl distance reflected the CCPs axons dense projection below the soma within a radius of 200 μm (Fig. 3*C*). Most of the cells had multiple primary axonal collaterals (collaterals directly emerged out from the main axonal stem, 7 ± 3). One of them often projected up ascending in parallel to the apical dendrite (70%, 15/22 reconstructed), with an averaged length of about 400 μm. Below the dense projection zone illustrated by the Sholl distance analysis, CCPs axons typically project 2 primary axonal collaterals horizontally extending within the layer VI (80%, 17/22 reconstructed, Fig. 3*A*). The main axonal trunk descends vertically into the white matter, presumably projecting to the opposite hemisphere. A summary of the morphological parameters is presented in Table 2.

Synaptic Connections between CCPs

In order to study the CCPs synaptic properties, we recorded simultaneously from labeled neurons with soma lying within a lateral distance of 100 μm. The probability to find a connection between 2 CCPs in acute slices was 3.15% (40 connections out of 1272 pairs tested). A single presynaptic AP induced an EPSP with amplitude of 0.8 ± 0.6 mV (Fig. 4*D*, mean ± SD). The latency (Fig. 4*C*), defined as the time lapse between the top of the AP and the EPSP onset, was 1.4 ± 0.8 ms (Fig. 4*D*). The 20–80% rise time was 2.8 ± 1.0 ms (Fig. 4*D*), and the decay time constant to rest membrane potential from the EPSP maximum amplitude (Tau) was 47 ± 25 ms (Fig. 4*D*). The mean number of synapses per connection obtained with the CV analysis was 4.6 ($n = [1–Pr_m]/[Pr_m \times CV_m^2]$, Pr_m: mean probability of release equivalent to U [see Materials and Methods], Fig. 6*D*, CV_m = mean CV, Fig. 5*C*). Morphological analysis yielded 4.0 ± 1.3 putative contacts per connection, in agreement with the CV analysis. Putative contacts between CCPs were mainly formed on basal dendrites (80%), at a branching order of 3.4 ± 0.2 (67.3% of total were formed on basal dendrites at a branching order higher than 3), a geometric distance of 129 ± 20 μm, and an electrotonic distance (see Materials and Methods) of 0.15 ± 0.02 (n = 14). The number of failures was relatively small and comparable to previously found values for other PC to PC connections (12 ± 11%, n = 23 [Thomson et al. 1993; Markram et al. 1997]). Despite this low failure rate, the observed CV was quite high (0.58 ± 0.24, n = 23). Weak synaptic connections displayed high trial-to-trial variability, as observed by the negative correlations between the mean EPSP size and the failure rate and CV (correlation index –0.73 and –0.74, respectively) and the positive correlations between the CV and failure rates (correlation index 0.92). These correlations show that the amplitudes of the CCPs to CCPs EPSPs depend on the number of synapses rather than on the probability of release. Among the correlations between the number of contact points, the distance of the contacts from the soma along the dendrites, the distance between the cell soma and the amplitude of the EPSP, only 3 were above 0.4. The correlation indices are 0.62 between the number of contact and the distance separating soma, 0.46 between the amplitude of the EPSP and the number of contact points, and 0.42 between the EPSP amplitude and the distance separating soma. It is worth to notice that given the small range of the data obtained for the soma separation distance (80 ± 40 μm, n = 14, mean ± SD) and the number of contact points

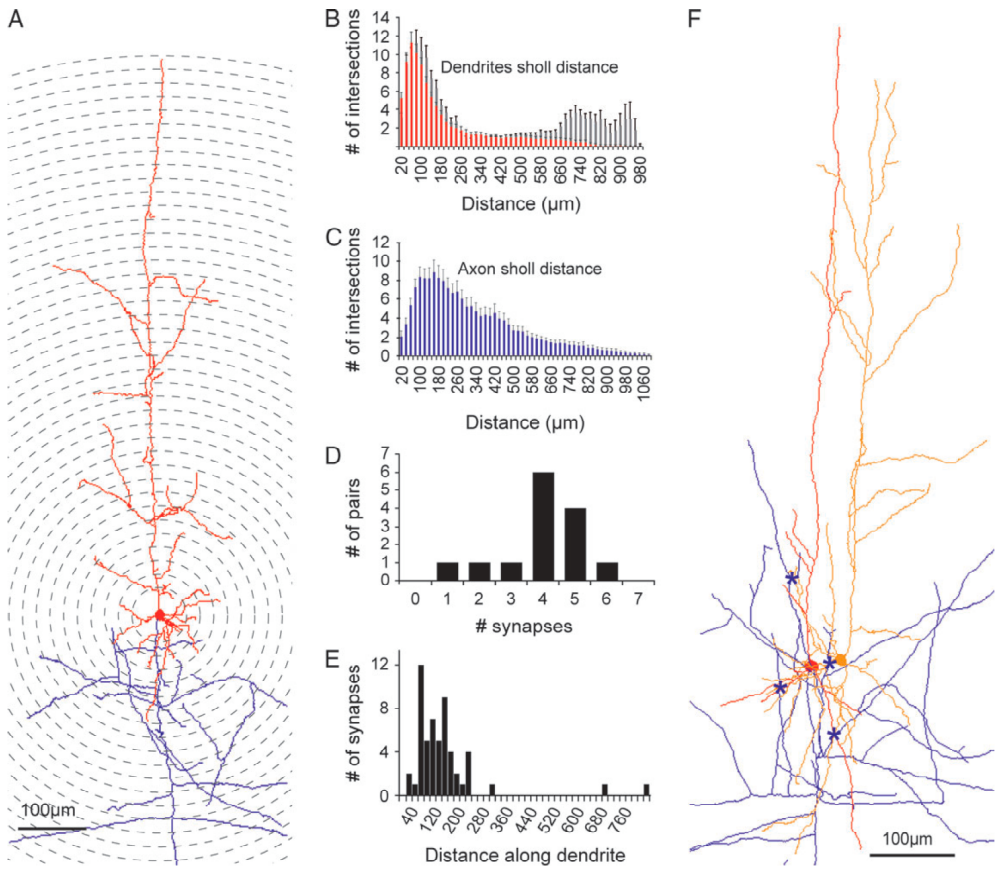

Figure 3. Morphological characteristics of single cell and connections in the CCP population. (*A*) Reconstruction of a single CCP showing the untufted apical dendrite and the circles defining the Sholl distances. Axon in blue and dendrites and soma in red. (*B*) Dendrite Sholl analysis. The distribution designates the number of times the circle centered on the soma with a radius of the Sholl distance crosses a dendrite (cf., *A*) ($n = 23$). Front in red: CCPs, behind in gray normalized with a factor of 0.51: TTCs (*C*) Axon Sholl analysis ($n = 23$), same as in (*B*). (*D*) Distribution of putative contacts in the population. A total of 4.0 ± 0.3 putative contacts per connection (mean ± SEM, $n = 14$). (*E*) Distribution of the distance between the soma and the putative contacts along the dendrites 130 ± 18 µm (mean ± SEM, $n = 55$). (*F*) Reconstruction of a pair of connected CCPs. Presynaptic axon in blue and dendrites in red and orange. Stars show the location of the identified putative contacts (axodendritic contact points with a bouton at the touch site).

Table 2
Morphometric properties of the corticocallosal PCs

	Mean	SEM	*n*
Dendritic tree surface (µm^2)	4800	300	23
Apical dendritic length (µm)	2973	1285	23
Basal dendrite number	5.2	1.5	23
Maximum branching order			
Apical dendrite	13.6	4.5	23
Basal dendrite	5.4	2	23
Axon	9.8	2.7	23

(Fig. 3*D*), more data would be required to reach any strong conclusion on this issue.

We used presynaptic trains of APs at various frequencies to characterize the dynamic properties of synaptic connections between CCPs (Figs 4*B* and 6). The synaptic responses were fitted using the model for synaptic dynamics, allowing for the extraction of the release probability and time constants of recovery from depression and facilitation (Markram et al. 1998) (see Materials and Methods and Fig. 6*B*). Synaptic connections between CCPs had low release probabilities (0.39 ± 0.14, range 0.04–0.61, $n = 23$, Fig. 6*D* top right panel), exhibited short-term depression (depression time constant: 690 ± 410 ms, Fig. 6*D* bottom left panel) and only little facilitation (facilitation time constant 44 ± 103 ms, Fig. 6*D* bottom right panel). We used presynaptic trains of different frequencies to extract the limiting frequency of CCP synapses (see Materials and Methods), which was found to be approximately 4 Hz (Fig. 6*C*).

CCP versus TTC Connectivity

We recorded from 24 synaptically connected TTCs pairs to perform a quantitative comparison with CCP pairs. TTCs were identified under IR-DIC microscopy by their large soma and thick apical dendrites. Neurons were biocytin filled via the patch pipette during recordings, and a later confirmation of the stained TTCs was obtained under light microscopy (as in Markram et al. 1997). The number of probed pairs was 222, giving 11% of connected pairs. This shows that the CCPs are 3–4 times less connected than the TTCs. A chi-square test yielded a P value of 8.10^{-17}. The EPSP amplitudes had a tendency to be smaller for the CCP synapses compared with TTC synapses (0.8 ± 0.2 mV for CCPs and 1.2 ± 0.2 mV for TTCs, mean ± standard error of the mean [SEM]).

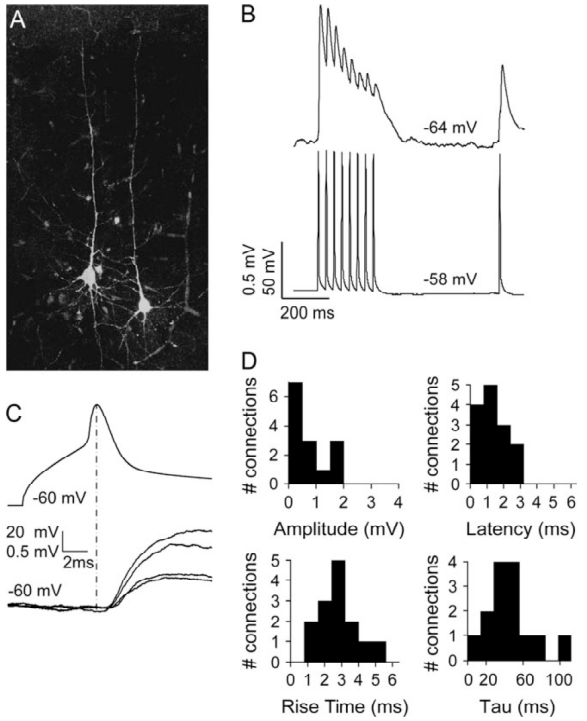

Figure 4. CCP connectivity: population response to a single AP. (*A*) Confocal image of a pair of layer V CCPs. (*B*) EPSP (top trace) recorded in response to the presynaptic cell stimulation of 8 APs at 30 Hz and a recovery test spike 500 ms later (bottom trace). Membrane potentials are given in the middle of the traces. (*C*) Single AP stimulated in the presynaptic cells (top trace) and 4 examples of trial-to-trial EPSP (bottom trace). The dashed line indicates the reference point for the latency measurement. Membrane potentials are given near the traces. (*D*) Population distribution of CCP single AP EPSP (80 trials per cell). Amplitude 0.8 ± 0.2 mV, latency 1.4 ± 0.2 ms, rise time 2.8 ± 0.3 ms, Tau = 47 ± 7 ms (membrane potential decay time constant from the top of the EPSP to rest) (mean ± SEM, n = 13 cells).

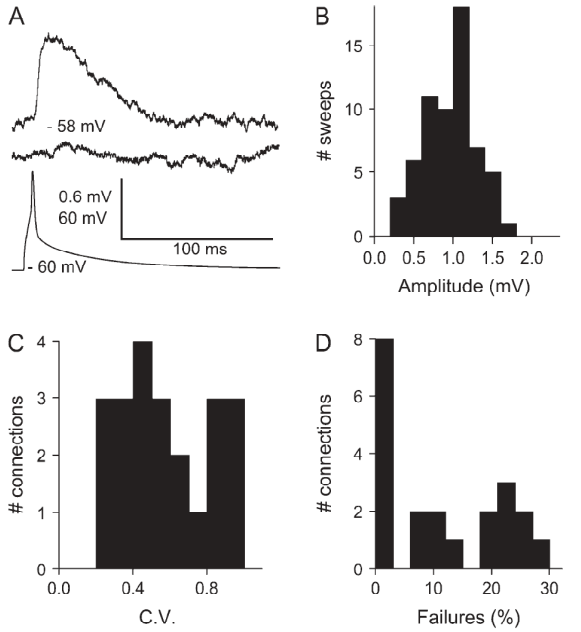

Figure 5. CCP connectivity: trial-to-trial response to a single AP. (*A*) Example of a successful EPSP, a failure and the corresponding presynaptic AP. Membrane potentials are given in the middle of the traces. (*B*) Distribution of the amplitudes for one cell across the trials (80 trials, 0.99 ± 0.06 mV, mean ± SEM). (*C*) Distribution of the CV for the CCP population (0.58 ± 0.05, n = 22). (*D*) Distribution of the failures for the CCP population (12 ± 2%, n = 22).

The onset latency for EPSPs was 1.4 ± 0.2 ms for CCPs and 1.2 ± 0.3 ms for TTCs; the 20–80% rise time was 2.8 ± 0.3 mV for the CCPs and 3.6 ± 0.6 ms for the TTCs; the synaptic decay time was 47 ± 7 ms for the CCPs and 54 ± 4 ms for the TTCs (mean ± SEM, n = 14 for CCPs and n = 12 for TTCs). None of these values was significantly different (P value larger than 0.2 in a 2-tailed t-test, data summarized in Table 3). Short-term plasticity was also compared between CCPs and TTCs (Fig. 7*A*,*B*) using the model for synaptic dynamics (see Materials and Methods). The only significantly different parameter was the probability of release (0.39 ± 0.03 vs. 0.51 ± 0.02 for CCPs and TTCs, respectively, mean ± SEM, P < 0.01 Fig. 7*C*, top panel). TTCs are interconnected by a disynaptic inhibitory pathway (Fig. 7*D*, first, second, and third panels) (Silberberg and Markram 2004; Rinaldi et al. 2005), which is activated following a presynaptic burst discharge. Such disynaptic inhibitory responses were not observed between CCPs, in contrast to their high prevalence between TTCs (Fig. 7*D*).

Discussion

Our study describes the properties of a subpopulation of neocortical pyramidal neurons projecting to the contralateral hemisphere. Whole-cell recordings from groups of layer V CCPs were obtained following retrograde labeling of the contralateral hemisphere and their morphological, electrophysiological, and synaptic properties were extracted. In agreement with previous reports (Katz 1987; Hubener and Bolz 1988; Mercer et al. 2005), CCPs had shorter and thinner apical dendrites, smaller soma, and higher input resistance than the thick tufted layer V PCs. In addition, the AP amplitude of the CCPs was smaller, and the AP duration was longer in the CCPs than in the TTCs. The discharge threshold was higher in the CCPs suggesting a lesser excitability of this PC type. We speculate that together with the AP duration, this lesser excitability could compensate for the higher input resistance and hence explain the similar current-discharge slope between the 2 populations.

Previous studies showed that some neurons in the guinea pig adult neocortex tend to discharge with an initial burst in response to a depolarizing step current (Connors et al. 1982). In a previous study, PCs that were morphologically undistinguishable exhibited discharge with or without an initial burst (McCormick et al. 1985). Another study reported that the large PCs (like the TTCs described here) displayed an initial burst discharge, whereas small PCs (closer to the CCPs) presented only a regular spiking behavior in the somatosensory cortex of 1-month-old rats (Chagnac-Amitai et al. 1990). Later, it was revealed that the bursting behavior of the TTCs originated from dendritic stimulations and regular firing originated from somatic stimulations (Schwindt and Crill 1999). Our results indicate that a variation of discharge behavior is true for the CCPs in the juvenile somatosensory neocortex. However, there are clear morphological and electrophysiological differences between the TTCs and the CCPs. Indeed, the main differences are in the shorter apical dendrite, larger input resistance, longer AP

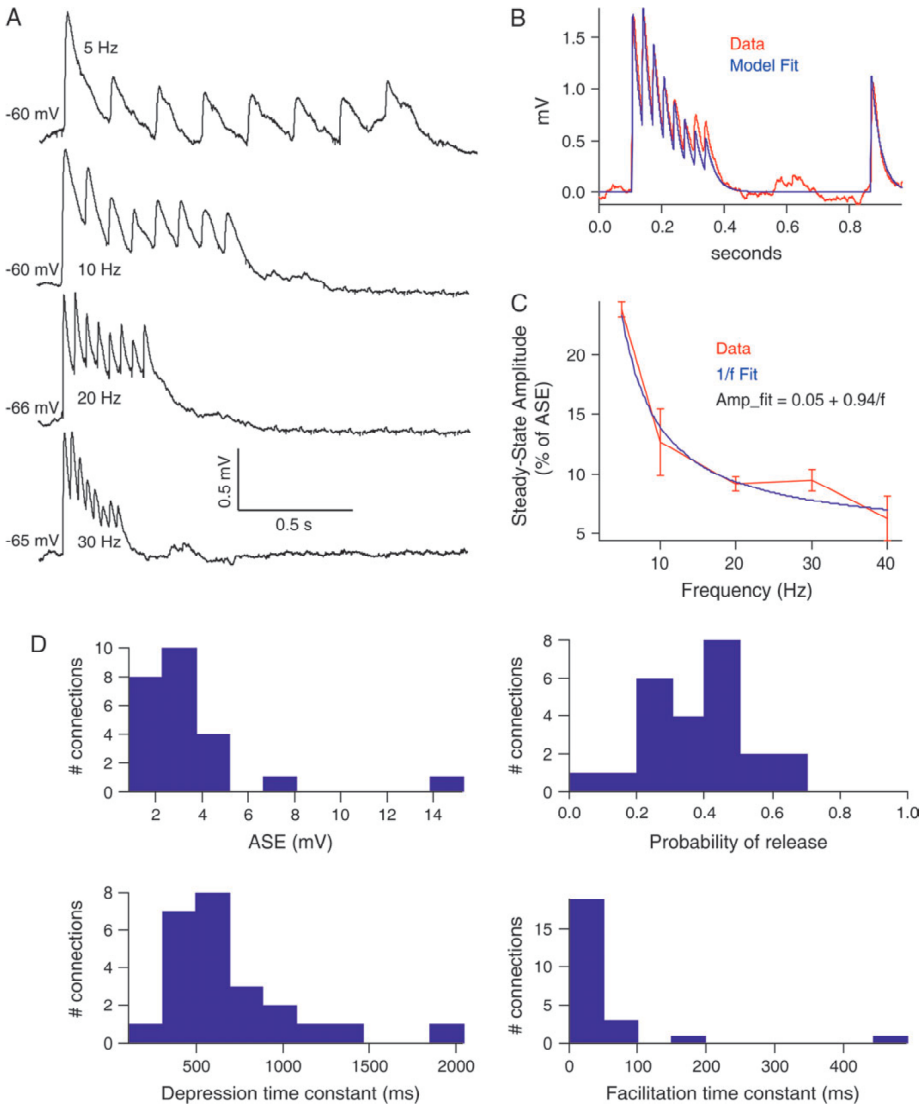

Figure 6. CCP connectivity: response to a train of APs. (*A*) Frequency dependence of EPSPs in response to a train of 8 APs at 5, 10, 20, and 30 Hz. Membrane potentials are given at the beginning of the traces. (*B*) Red trace: actual data for one connection averaged over 30 trials. Blue trace: Tsodyks–Markram model fit of the data. (*C*) Frequency dependence of the steady-state amplitude (last 3 EPSPs of the trains shown in panel *A* averaged and divided by the corresponding ASE). Blue trace: inverse frequency fit of the data trace, as given by the equation for Amp_fit. (*D*) Distributions of the parameters extracted by the Tsodyks–Markram model. ASE is the absolute synaptic efficacy, that is, the amplitude of the EPSP if the probability of release U was 1. ASE = 3.4 ± 0.6 mV, U = 0.39 ± 0.03, τ_D = 690 ± 90 ms, τ_F = 44 ± 21 ms (mean ± SEM, n = 23).

Table 3
Comparison of the synaptic properties between CCPs and TTCs

	CCP	TTC	*P* value
Number of putative contacts/connection	4.0 ± 0.3	5.5 ± 1.1[a]	<0.005
Amplitude (mV)	0.8 ± 0.2	1.2 ± 0.2	>0.02
Latency (ms)	1.4 ± 0.2	1.2 ± 0.3	>0.07
Rise time (20–80%, ms)	2.8 ± 0.3	3.6 ± 0.2	>0.02
Decay time (ms)	47 ± 7	54 ± 4	>0.03
ASE (mV)	3.4 ± 0.6	3.8 ± 0.4	>0.06
U	0.39 ± 0.03	0.51 ± 0.02	<0.01
τ_D (ms)	690 ± 90	620 ± 30	>0.03
τ_F (ms)	44 ± 21	13 ± 4	>0.01

Note: Student *t*-test was used for the statistical comparison.
[a]Data obtained from Markram et al. (1997).

duration, smaller AP amplitude, and the presence of an initial burst for the CCPs compared with the TTCs. The mechanism underlying bursting was suggested to be dependent on the synchronicity of the sodium spike with a dendrite generated calcium spike (Schwindt and Crill 1999). The bursting behavior of some CCPs reported here might depend on various intrinsic properties that are related to the dendritic calcium spike. Intrinsic neuronal properties depend on the developmental stage of the tested animals, which may also be a reason for the variability in firing patterns recorded in different studies.

Synaptic connections between pairs of CCPs were characterized and compared with those observed between TTCs. Synaptic connections between CCPs differed in their low

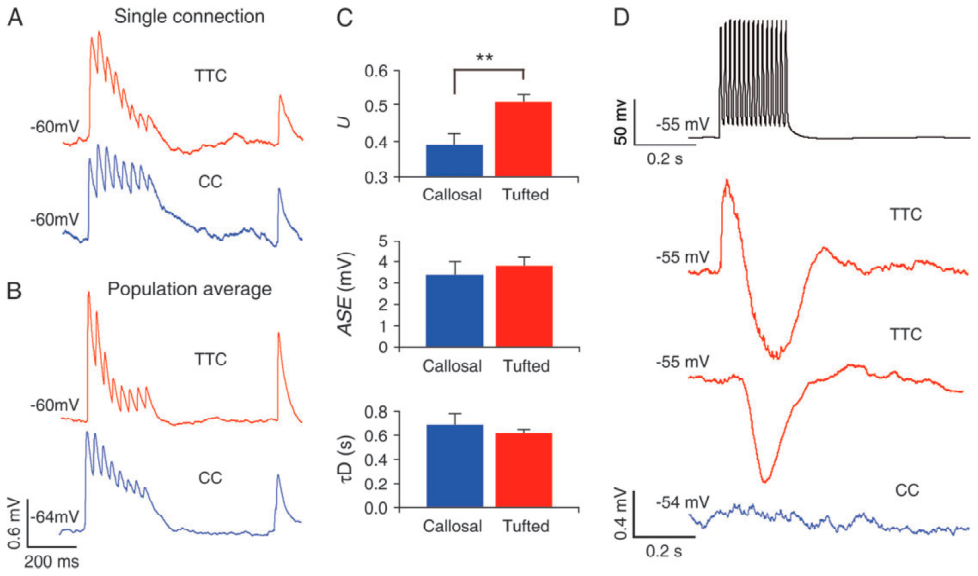

Figure 7. Comparison of CCP connection dynamics with the TTC. (*A*) Comparison of an EPSP response to an 8 APs train at 30 Hz followed by a recovery test AP 500 ms later. Red trace: TTC single connection and blue trace: CCP single connection. Membrane potentials are given at the beginning of the traces. (*B*) Same as (*A*) but traces are population averages ($n = 13$ for CCPs and $n = 10$ for TTCs). (*C*) Parameters extracted by the Tsodyks–Markram model. $^{**}P < 0.01$, CCP $n = 23$, TTC $n = 24$ (CCP: $U = 0.39 \pm 0.03$, ASE = 3.4 ± 0.6 mV, $\tau_D = 690 \pm 90$ ms; TTC: $U = 0.51 \pm 0.02$, ASE = 3.8 ± 0.4 mV, $\tau_D = 620 \pm 30$ ms, mean ± SEM). (*D*) Disynaptic connection between PCs mediated by an interneuron. First panel shows a presynaptic stimulation used to evoke the disynaptic connection (15 APs at 70 Hz). Second and third panels show a TTC disynaptic inhibitory response with and without a direct monosynaptic connection, respectively. Fourth panel shows a CCP response, whereas another CCP was stimulated at 70 Hz. No disynaptic connections were observed between CCPs. Membrane potentials are given at the beginning of the traces.

connection probability, smaller EPSP amplitudes, and lower release probabilities. Disynaptic inhibition was not observed between CCPs pairs, compared with the large probability for these connections between TTCs. Our results show that in addition to differences in the morphological and electrophysiological properties, subpopulations of PCs within the same neocortical column and layer also display different properties of connectivity.

The short untufted apical dendrites of CCPs as well as the narrow span of their basal dendrites suggest that, unlike TTCs, they integrate inputs in a relatively narrow range. This is further supported by the almost complete absence of dendritic arborization in layers II/III, in which long-range horizontal intracortical connections are abundant (Fitzpatrick 1996; Chisum and Fitzpatrick 2004). CCPs do not display a dendritic tuft in layer I, suggesting that they also do not receive top–down inputs (Rockland and Virga 1989; Cauller and Connors 1994; Cauller et al. 1998). The untufted aspect of the CCPs apical dendrite is not a developmental feature due to incomplete dendritic growth because the dendritic arborization is already completed by the end of the first postnatal week (Wise and Jones 1976). Further, untufted morphology also exist in adult animals (Kasper et al. 1994). Putative contacts between CCPs were mainly located on basal dendrites, similar to those formed between TTCs, but different from those formed between corticostriatal PCs (Morishima and Kawaguchi 2006). Comparing with the TTC connections (5.5 ± 1.1, $n = 19$) (Markram et al. 1997), the CCPs formed a significantly smaller number of putative contacts in a connection (4.0 ± 0. 3, $n = 14$; $P < 0.005$, Student *t*-test). Connections between TTCs had 63% of contacts located on basal dendrites, and 37.5% of all contacts were formed on basal dendrite at an order higher than 3 (Markram et al. 1997) innervating to a greater extent the apical dendrite than the CCPs (80% of contacts on basal dendrites and 67.3% of contacts were on basal dendrites at a branching order higher than 3). The mean geometrical distance between the soma and the contact points tends to be larger in TTCs (201 ± 62 μm compared with 129 ± 20 μm for CCPs); however, the mean electrotonic distance is similar for both cell types as TTCs contacts are located at a mean electrotonic distance of 0.13 ± 0.03 (Markram et al. 1997) (0.15 ± 0.02 for CCPs).

The connection probability between CCPs was much lower than observed between TTCs, indicating different connectivity patterns for PCs in somatosensory cortex projecting to different targets. Similar differences in connectivity probabilities were observed between PCs in the prefrontal cortex projecting to different targets (Morishima and Kawaguchi 2006). The sparse connectivity between CCPs suggests that they may primarily be driven by other sources of excitation such as PCs from other subpopulations within layer V or from other layers. The connectivity between CCPs and other subclasses of PCs is, however, yet to be investigated. Given the differences reported here between the CCPs and TTCs circuits, it is very likely that there is an asymmetry in the connections between the PCs subpopulations (Thomson and Bannister 2003). The inhibitory network signaling to CCPs should also be considered in face of the specific excitatory connectivity pattern. Previous studies showed that Martinotti cells provide inhibition primarily to layers I and IV (Wang et al. 2004). These interneurons also mediate a disynaptic feedback loop within the TTCs population (Silberberg and Markram 2004). We did not observe any disynaptic inhibitory responses between CCPs, suggesting that the inhibitory connectivity also differs for various PC subpopulations.

This hypothesis is supported by a morphological study of the inhibitory synapses onto the TTCs and CCPs populations (Farinas and DeFelipe 1991) in the cat visual cortex that shows a higher axosomatic inhibitory synapses density on the CCPs. This population would then be less innervated distally and more somatically than the TTCs. The differential distribution of inhibitory synapses between cell populations projecting to different target has also been shown in the monkey (Lund et al. 2001), indicating that this projection target specificity for inhibition might not be specific to species.

Most synaptic properties, such as onset latency, kinetics, depression, facilitation, were similar for connections between CCPs and between TTCs. However, connections between CCPs were weaker and had lower release probabilities, following the same tendency of very low interconnectivity in this subpopulation.

This low interconnectivity suggests a reduced integration capacity of the CCP population as compared with the thick tufted pyramidal network. The rather linear dynamics of the connections between CCPs also suggests a different functional role in the neocortex compared with the TTCs. The narrower dendritic field of the CCPs further indicates that this population mainly receives and processes information present in the microcolumn and the neighboring layers, thus integrating inputs from a smaller area than the TTCs. We therefore speculate that CCPs contribute less to the processing within the column than TTCs and perform minimal transformation of the information processed before sending it to the opposite hemisphere. The CCP cells therefore appear to be well suited to act as read out neurons of the columns for the opposite hemisphere.

Notes

Conflict of Interest: None declared.

Address correspondence to email: henry.markram@epfl.ch

References

Aboitiz F, Lopez J, Montiel J. 2003. Long distance communication in the human brain: timing constraints for inter-hemispheric synchrony and the origin of brain lateralization. Biol Res. 36:89–99.

Cauller LJ, Clancy B, Connors BW. 1998. Backward cortical projections to primary somatosensory cortex in rats extend long horizontal axons in layer I. J Comp Neurol. 390:297–310.

Cauller LJ, Connors BW. 1994. Synaptic physiology of horizontal afferents to layer I in slices of rat SI neocortex. J Neurosci. 14: 751–762.

Chagnac-Amitai Y, Luhmann HJ, Prince DA. 1990. Burst generating and regular spiking layer 5 pyramidal neurons of rat neocortex have different morphological features. J Comp Neurol. 296:598–613.

Chisum HJ, Fitzpatrick D. 2004. The contribution of vertical and horizontal connections to the receptive field center and surround in V1. Neural Netw. 17:681–693.

Cho RH, Segawa S, Okamoto K, Mizuno A, Kaneko T. 2004. Intracellularly labeled pyramidal neurons in the cortical areas projecting to the spinal cord. II. Intra- and juxta-columnar projection of pyramidal neurons to corticospinal neurons. Neurosci Res. 50:395–410.

Christophe E, Doerflinger N, Lavery DJ, Molnar Z, Charpak S, Audinat E. 2005. Two populations of layer v pyramidal cells of the mouse neocortex: development and sensitivity to anesthetics. J Neurophysiol. 94:3357–3367.

Connors BW, Gutnick MJ, Prince DA. 1982. Electrophysiological properties of neocortical neurons in vitro. J Neurophysiol. 48: 1302–1320.

Eliassen JC, Baynes K, Gazzaniga MS. 2000. Anterior and posterior callosal contributions to simultaneous bimanual movements of the hands and fingers. Brain. 123(Pt 12):2501–2511.

Engel AK, Konig P, Kreiter AK, Singer W. 1991. Interhemispheric synchronization of oscillatory neuronal responses in cat visual cortex. Science. 252:1177–1179.

Farinas I, DeFelipe J. 1991. Patterns of synaptic input on corticocortical and corticothalamic cells in the cat visual cortex. I. The cell body. J Comp Neurol. 304:53–69.

Fitzpatrick D. 1996. The functional organization of local circuits in visual cortex: insights from the study of tree shrew striate cortex. Cereb Cortex. 6:329–341.

Hirsch JA, Gallagher CA, Alonso J-M, Martinez LM. 1998. Ascending projections of simple and complex cells in layer 6 of the cat striate cortex. J Neurosci. 18:8086–8094.

Hubener M, Bolz J. 1988. Morphology of identified projection neurons in layer 5 of rat visual cortex. Neurosci Lett. 94:76–81.

Kasper EM, Larkman AU, Lubke J, Blakemore C. 1994. Pyramidal neurons in layer 5 of the rat visual cortex. I. Correlation among cell morphology, intrinsic electrophysiological properties, and axon targets. J Comp Neurol. 339:459–474.

Katz LC. 1987. Local circuitry of identified projection neurons in cat visual cortex brain slices. J Neurosci. 7:1223–1249.

Lund JS, Griffiths S, Rumberger A, Levitt JB. 2001. Inhibitory synapse cover on the somata of excitatory neurons in macaque monkey visual cortex. Cereb Cortex. 11:783–795.

Markram H, Lubke J, Frotscher M, Roth A, Sakmann B. 1997. Physiology and anatomy of synaptic connections between thick tufted pyramidal neurones in the developing rat neocortex. J Physiol. 500(Pt 2):409–440.

Markram H, Wang Y, Tsodyks M. 1998. Differential signaling via the same axon of neocortical pyramidal neurons. Proc Natl Acad Sci USA. 95:5323–5328.

Matsuzaka T, Ono K, Baba H, Matsuo M, Tanaka S, Kamimura N, Tsuji Y. 1999. Quantitative EEG analyses and surgical outcome after corpus callosotomy. Epilepsia. 40:1269–1278.

McCormick DA, Connors BW, Lighthall JW, Prince DA. 1985. Comparative electrophysiology of pyramidal and sparsely spiny stellate neurons of the neocortex. J Neurophysiol. 54:782–806.

Mercer A, West DC, Morris OT, Kirchhecker S, Kerkhoff JE, Thomson AM. 2005. Excitatory connections made by presynaptic corticocortical pyramidal cells in layer 6 of the neocortex. Cereb Cortex. 15:1485–1496.

Morishima M, Kawaguchi Y. 2006. Recurrent connection patterns of corticostriatal pyramidal cells in frontal cortex. J Neurosci. 26:4394–4405.

Quigley M, Cordes D, Turski P, Moritz C, Haughton V, Seth R, Meyerand ME. 2003. Role of the corpus callosum in functional connectivity. Am J Neuroradiol. 24:208–212.

Rinaldi T, Silberberg G, Markram H. 2005. Enhanced monosynaptic and disynaptic connectivity in the neonatal microcircuit of an animal model of Autism. Abstract viewer/Itinerary Planner. Washington (DC): Society for Neuroscience Poster No. 448.2.

Rockland KS, Virga A. 1989. Terminal arbors of individual "feedback" axons projecting from area V2 to V1 in the macaque monkey: a study using immunohistochemistry of anterogradely transported Phaseolus vulgaris-leucoagglutinin. J Comp Neurol. 285:54–72.

Schwindt P, Crill W. 1999. Mechanisms underlying burst and regular spiking evoked by dendritic depolarization in layer 5 cortical pyramidal neurons. J Neurophysiol. 81:1341–1354.

Silberberg G, Markram H. 2004. Di-synaptic inhibition between pyramidal neurons via Martinotti cells in neocortical layer V. Abstract viewer/Itinerary Planner. Washington (DC): Society for Neuroscience Poster No. 508.7.

Simons DJ, Woolsey TA. 1984. Morphology of Golgi-Cox-impregnated barrel neurons in rat SmI cortex. J Comp Neurol. 230:119–132.

Thomson AM, Bannister AP. 2003. Interlaminar connections in the neocortex. Cereb Cortex. 13:5–14.

Thomson AM, Deuchars J, West DC. 1993. Large, deep layer pyramid-pyramid single axon EPSPs in slices of rat motor cortex display paired pulse and frequency-dependent depression, mediated presynaptically

and self-facilitation, mediated postsynaptically. J Neurophysiol. 70:2354–2369.

Tsiola A, Hamzei-Sichani F, Peterlin Z, Yuste R. 2003. Quantitative morphologic classification of layer 5 neurons from mouse primary visual cortex. J Comp Neurol. 461:415–428.

Tsodyks MV, Markram H. 1997. The neural code between neocortical pyramidal neurons depends on neurotransmitter release probability. Proc Natl Acad Sci USA. 94:719–723.

Vercelli AE, Garbossa D, Curtetti R, Innocenti GM. 2004. Somatodendritic minicolumns of output neurons in the rat visual cortex. Eur J Neurosci. 20:495–502.

Wang Y, Toledo-Rodriguez M, Gupta A, Wu C, Silberberg G, Luo J, Markram H. 2004. Anatomical, physiological and molecular properties of Martinotti cells in the somatosensory cortex of the juvenile rat. J Physiol. 561:65–90.

White EL, Hersch SM. 1982. A quantitative study of thalamocortical and other synapses involving the apical dendrites of corticothalamic projection cells in mouse SmI cortex. J Neurocytol. 11: 137–157.

Wise SP, Jones EG. 1976. The organization and postnatal development of the commissural projection of the rat somatic sensory cortex. J Comp Neurol. 168:313–343.

Yuste R. 2005. Origin and classification of neocortical interneurons. Neuron. 48:524–527.

Zhang ZW, Deschenes M. 1997. Intracortical axonal projections of lamina VI cells of the primary somatosensory cortex in the rat: a single-cell labeling study. J Neurosci. 17:6365–6379.

Zhang ZW, Deschenes M. 1998. Projections to layer VI of the posteromedial barrel field in the rat: a reappraisal of the role of corticothalamic pathways. Cereb Cortex. 8:428–436.

3 Rewiring of the neocortical microcircuit

3.1 Introduction

A remarkable property of the neocortex is the high adaptability and plasticity both at the synaptic and circuit levels (see Buonomano and Merzenich 1998). Learning and memory are currently believed to originate from the long lasting changes in various properties of synaptic transmission (Morris 2003; Pastalkova *et al.* 2006; Whitlock *et al.* 2006).

The original Hebbian hypothesis for memory formation and consolidation started to find its experimental support when various brain areas necessary for memory were identified. The hippocampus has long been thought to be necessary for memory as many observations of a missing hippocampus reported memory impairments (Henderson *et al.* 1973; Jarrard 1975; Handelmann and Olton 1981; Olton and Feustle 1981; Press *et al.* 1989; Grady *et al.* 1995). It has later been shown that this structure is necessary for specific memories but is not required for others. For example, rats with an altered hippocampus undergoing a task requiring spatial and contextual learning were shown to behave with a significant reduction of information retention. On the contrary, the same injury did not affect the rats learning capabilities in the case of a task involving non-spatial learning (Jarrard 1993).

Another brain structure that plays an important role in learning and memory is the amygdala (Miserendino *et al.* 1990 and see Davis 1992; Lavond *et al.* 1993). On one hand, the amygdala is believed to be a major player in the emotions (Adolphs *et al.* 1994; Morris *et al.* 1996 and see Aggleton 1992) and on the other hand, emotions play a particularly important role in memory and learning (see Damasio 2001). The everyday life experience already shows evidences of the role of emotion in information retention. A special, emotionally connoted event is more easily remembered than any event, even more recent, that lack emotional imprinting.

Although there are some structures that play key roles in memory formation, the current thinking is that memory and learning require changes across the whole brain. Various parts of the brain seem however to be dedicated to specific aspects of memory. For instance, the medial-temporal lobe seems to be linked to episodic memory whereas the temporal cortex is likely to be responsible for semantic-like memory (see Miyashita 2004). On another hand, working memory seems to use several brain areas (see Kaldy and Sigala 2004).

The cortical representations of the sensory inputs are also modified with experience. Hebbian plasticity provides a mechanism for the formation and the modification of sensory topographic representation maps such that adjacent sensors are likely to be activated simultaneously and hence activate cortical neurons whose synaptic interaction might be increased by the common sensory input. Sensory inputs of a same stimulation modality will eventually form their common area of signal processing in the cortex (see Buonomano and Merzenich 1998).

Long term potentiation. The experiments searching for the cellular basis of learning and memory, based on Hebb's law, concentrated on long term potentiation (LTP, Bliss and Lomo 1973). LTP is defined as the increase of a synaptic strength originating from a high frequency (tetanic) stimulation and lasting for a long period (Bliss and Lomo 1973; Brown *et al.* 1988). The synaptic strength was in the early experiments measured extracellularly as the slope of the synaptic response to the stimulation of afferent fibres (typically the CA3 afferent fibres on

the CA1 neurons of the hippocampus). The response was relatively constant across trials. Directly after the tetanic stimulation, the synaptic response greatly increases and then weakens to a steady level that is of steeper slope than the original synaptic response. The difference between the baseline before the stimulation and the steady response after the tetanus is referred to as LTP (see Bliss and Collingridge 1993).

The justification of LTP as the cellular mechanism for memory lies in the common features shared by memory and LTP. Both phenomena are rapidly induced by a specific stimulus. They are also, and importantly, long lasting and display a continuous expression on reiteration of the original stimulus (see Bliss and Collingridge 1993; Izquierdo 1994). Animals undergoing successive learning tasks were displaying LTP-like phenomenon in their brains (Berger 1984; Sharp *et al.* 1985; Skelton *et al.* 1985).

In addition to the functional features, LTP and memory share common pharmacological dependences. Impairments due to inhibition of NMDA receptors by 2-amino-5-phosphono-pentanoic acid (AP5) or inhibition of AMPA receptors by 6-cyano-7-nitroquinoxaline-2,3-dione (CNQX) as well as inhibition of metabotropic receptors by (RS)-α-methyl-4-carboxyphenyl-glycine (MCPG) are common to LTP and memory. On another hand, memory was stimulated and LTP enhanced after exposure to glutamate or to picrotoxin, a $GABA_A$ receptor antagonist (see Izquierdo 1994; Izquierdo and Medina 1995).

Recent experiments gave for the first time a direct evidence of synaptic potentiation based memory mechanism. Whitlock *et al.* (Whitlock *et al.* 2006) report experiments where one trial inhibitory avoidance learning potentiated hippocampal CA1 neurons. Adult rats were trained with the inhibitory avoidance task where they learned on a one-trial basis to avoid dark environment as they were given an electric shock when running into the dark side of a box. A single row 8-electrodes recording array was implanted in their hippocampus prior the behavioural experiment. This array allowed the stimulation of the Shaffer collaterals and multiple recordings of the resulting EPSPs in the CA1 region. Whitlock and collaborators showed that the EPSPs recorded at some electrodes (but not all) were potentiated after the one-trial learning. Additionally, when they tried to induce LTP *in vivo* after the training via the same electrode array, the EPSPs amplitude increase was smaller for the synapses potentiated with the training compared to the synapses that were not. This induction of LTP by the one-trial learning on the one side and the saturation of LTP on the other side lead the authors to the conclusion that LTP is required for the one-trial learning in the inhibitory avoidance task.

Role of calcium and NMDA receptors. Although many receptors are involved in synaptic plasticity when observed via LTP, the most studied is the NMDA receptor. Ca^{2+} influx through NMDA receptors has two effects, the depolarization of the cell observed directly electrophysiologically (Clark *et al.* 1997) and the triggering of calcium dependent mechanisms such as Calcium/Calmodulin-dependent Kinase (CaMK) signalling pathway (Lledo *et al.* 1995), protein kinase C (PKC) signalling pathway (see Linden and Routtenberg 1989) or gene expression (see Morgan and Curran 1988) that are the starting points of some mechanisms increasing the response in the post-synaptic cell (like the insertion of new ionotropic receptors). The application of calcium chelators in the post-synaptic cell showed that calcium increase is required to generate potentiation (Kimura *et al.* 1990). Similarly, NMDA antagonist application also significantly reduces LTP (Reymann *et al.* 1989). The action potential in the post-synaptic cell is increasing the Ca^{2+} concentration in dendrites via voltage gated calcium channels (Markram *et al.* 1995). The combined influx of calcium via NMDARs and voltage gated channels is then adapted to trigger the long term changes in the synaptic strength. This mechanism is very close to the original suggestion of Hebb.

Additionally, the various voltage gated calcium channels interact and differentially vary

the calcium concentration in the dendrites. Non-linear summation of calcium concentration when different calcium sources are activated has a number of functional consequences (Kaiser *et al.* 2004; Sjostrom and Hausser 2006). It has been shown that the increase in dendritic calcium due to synaptic activity is localized within 8µm of the synaptic site (Kaiser *et al.* 2004; Polsky *et al.* 2004). This local increase together with the non-linear dynamics are very likely related to the non-linear activation of adjacent dendritic areas (Polsky *et al.* 2004) that has been shown to be responsible for differential and locally controlled plasticity at distal dendrites (Sjostrom and Hausser 2006).

Trafficking of AMPA receptors. AMPA receptors are the principal receptors involved in rapid post-synaptic response to pre-synaptic glutamate release. Although AMPA receptors concentration is higher at the post-synaptic sites, they are also found on the cellular membrane outside of the post-synaptic density (Tardin *et al.* 2003; Groc *et al.* 2004). The original mechanism proposed for synaptic plasticity was the trafficking of AMPA receptors between the intracellular milieu and the membrane (see Malinow and Malenka 2002). This motility is suggested to be triggered by NMDA receptor activation and calcium influx. On top of that phenomenon, a lateral trafficking of AMPA receptors already inserted in the membrane have been observed (Tardin *et al.* 2003; Ashby *et al.* 2004; Groc *et al.* 2004). This trafficking of AMPA receptors has also been suggested in synapses that were not generating any EPSP in the normal resting membrane potential. These synapses, composed of only NMDA receptors and referred to as "silent-synapses", could receive AMPA receptors at their post-synaptic membrane and then become fully functional synapses (Liao *et al.* 1995).

Spike timing dependent plasticity (STDP). The mechanisms of synaptic plasticity described above are dependent on activity patterns that trigger various signalling pathways. The original paradigms functionally inducing plasticity were based on a high frequency and long lasting stimulation. These stimulations are closer to an epileptic activity than to a normal behaviour (compare to physiological activity, see section 1.3). Moreover, the massive stimulation of adjacent fibres is not very likely to happen *in vivo*. Another disadvantage of extracellular electrical stimulation is that many pre-synaptic neurons and neuron types are stimulated, and there is no knowledge regarding the identity of the pre-synaptic neuron.

More precise experiments using calcium imaging and patch clamp recordings in the hippocampus have shown that the calcium signal was supra-linearly summed when an AP and an EPSP were simultaneously triggered in a dendrite (Magee and Johnston 1997). This increased calcium signal was correlated with synaptic potentiation since the calcium channels antagonists nimodipine and Ni^{2+} inhibited the induced LTP. NMDA receptors also seem to take part in the induced LTP, although some of the potentiation was still present even with 100µM of AP5. These experiments gave strong support to the Hebbian theory of synaptic plasticity with stimulations that were closer to the physiological conditions.

At the same time, Markram and collaborators showed that neocortical synapses between neuron pairs can be differentially modified depending on the timing of pre- and post-synaptic firing (Markram *et al.* 1997b). This study showed that synchronous depolarization of the post-synaptic neuron with pre-synaptic firing was not sufficient to induce LTP. Additionally, they showed that not only the post-synaptic action potential generation was necessary to induce LTP but also the timing of this post-synaptic discharge was important. Indeed, if the post-synaptic AP is triggered within a window of 10 ms before the pre-synaptic one, the synapse undergoes long-term depression (LTD). On the contrary, if the post-synaptic cell fires 10 ms after the pre-synaptic one, the synapse undergoes LTP (Figure 6a). This timing dependence is now referred to as "Spike-Timing Dependent Plasticity" (STDP) (Froemke *et al.* 2005; Letzkus *et al.* 2006 and see Abbott and Nelson 2000; Bi and Poo 2001). Additionally, this

discovery showed the importance of synchronicity in synaptic plasticity. This precise timing for synaptic plasticity was further supported by the evidence that the post-synaptic AP trigged calcium influx differentially influence the mechanisms of insertion or removal of AMPA receptor (Wyllie and Nicoll 1994; Barria *et al.* 1997; Lu *et al.* 2001). If the influx of calcium due to the cell discharge occurs before the activation of NMDA receptors, different signalling pathway might be activated and AMPA receptors might be removed (Mulkey *et al.* 1993; Chung *et al.* 2000).

STDP depends on synapse type. Spike timing dependence of synaptic modification has already been studied in various brain areas and species. Although in most cases plasticity is observed, the timing-rules and direction (depression or potentiation) vary across brain areas and neuronal types. Following are some examples of STDP in different areas and species.

In the dentate gyrus of the rat hippocampus, LTP has been observed when the post-synaptic stimulation was synchronous or delayed up to 20 ms with respect to the pre-synaptic firing (Levy and Steward 1983). Extra-cellular recordings in the guinea pig CA1 region of the hippocampus showed that simultaneous stimulation and stimulation of the test volley up to about 40 ms after the conditioning tetanus also results in LTP (Gustafsson and Wigstrom 1986). A later experiment in the same animal with intracellular recordings and extracellular stimulation showed that a depolarizing step current in the recorded cell within 100 ms after or simultaneous to the EPSP elicited by the extracellular stimulation was sufficient to generate LTP (Gustafsson *et al.* 1987). In cultures of dissociated rat glutamatergic neurons, intracellular recordings showed that LTP could be obtained with stimulation of the post-synaptic cell within 20 ms after the pre-synaptic cell activation and LTD could be obtained with the post-synaptic cell stimulation within 20 ms before the pre-synaptic activation. It was further shown that strong synapses were less sensitive to LTP than weak ones but LTD was similar at both types of synapses (Figure 6a, Bi and Poo 1998). The same time window of plasticity was observed in Xenopus retinotectal projections with intracellular recordings and extracellular stimulation (Zhang *et al.* 1998).

In rat hippocampal slice cultures, however, the same tendency of potentiation and depression as in cortical acute slices was observed but with an asymmetrical time window. Indeed, whereas LTP could be induced with the pre-synaptic firing up to 20 ms before the post-synaptic firing, LTD could be induced with a reversed delay up to 200 ms (Debanne *et al.* 1998, Figure 6b). Similarly, in connections of layer II-III PCs in adult rat somatosensory cortex, the LTP and LTD windows have been shown to be asymmetric. Intracellular recordings with extracellular stimulations showed that LTP was induced when the post-synaptic spike was delayed up to 15 ms (but failed at longer intervals) after the EPSP whereas LTD was induced even when the post-synaptic spike preceded the EPSP by 100 ms (Feldman 2000, Figure 6b).

In the electrosensory lobe of the mormyrid electric fish, qualified as a “cerebellum-like” structure, intracellular recordings of extracellular stimulations showed LTP when the additional stimulation was fired simultaneous or up to 50 ms before the EPSP. Symmetrically, LTD was elicited when the additional stimulation followed the EPSP by up to 50 ms (Bell *et al.* 1997). This result is in opposition to the previously mentioned studies where the conditioning stimulus needed to follow the synaptic response in order to get LTP (Figure 6c).

Interestingly, the connections between spiny stellate cells of young rats barrel fields were only showing LTD regardless of the sequence of firing of the pre- and post-synaptic cells (Figure 6e). Whole cell recordings and stimulations in acute slices showed further that this LTD was AMPA and NMDA independent and group II metabotropic glutamate receptors were required (Egger *et al.* 1999).

In GABAergic synapses of cultures and slices of rat hippocampus the spike timing

dependent plasticity is quite different from the glutamatergic synapse. The order in which the pre- and post-synaptic cells are fired is not as important as the plasticity is symmetrical with respect to the axis of synchronicity. Potentiation is induced within a window of ±20 ms of synchronicity and if the cells fire within a longer interval, the synapses undergo LTD (Woodin *et al.* 2003, Figure 6d).

Additionally, the glutamatergic to GABAergic neurons connections were not affected by spike timing (Bi and Poo 1998).

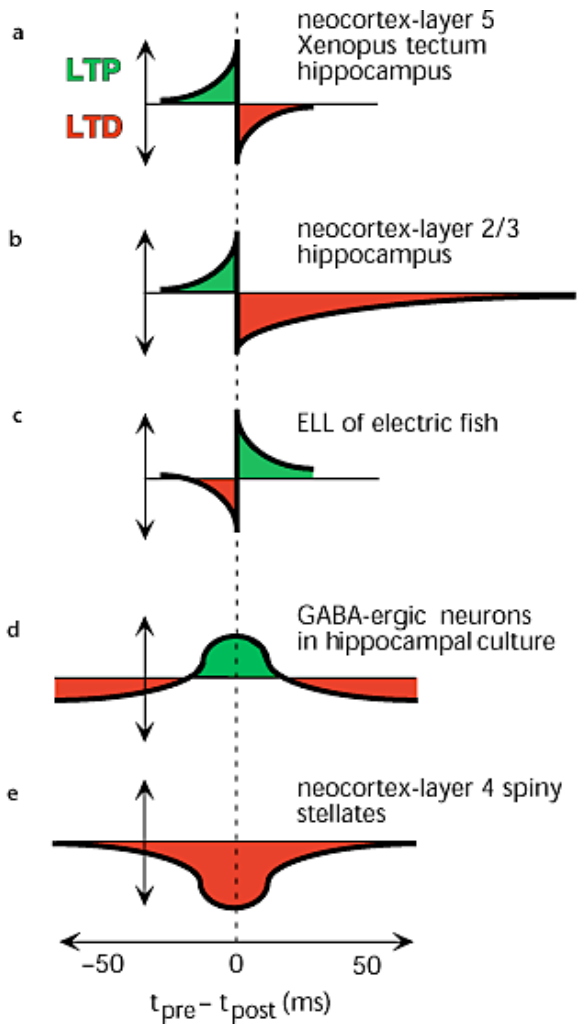

Figure 6 Spike timing dependent plasticity varies with cells, species and brain areas. The horizontal axis is showing the time difference from the pre-synaptic activation minus the post-synaptic activation. Axis label give an indication of the order of magnitude of the values and is not intended to give precise results. Illustration from Abbott and Nelson 2000.

STDP depends on synapse location. The neuron membrane potential is not simultaneously modified across the dendritic tree by a back-propagating AP. The back-propagating signal arrives later to distal dendrites and it is modified in shape and amplitude (Spruston *et al.* 1995, and see Johnston and Wu 1997). Early STDP experiments were done by somatic stimulations and recordings. Later studies showed that the time window required for STDP depends on the post-synaptic dendritic location (Froemke *et al.* 2005). In case of a synapse close to the soma (<50µm) the STDP time windows are rather symmetrical for LTD and LTP, within ±50 ms

pre- and post-synaptic time delay. However, at more distal synapses (>100µm away from the soma), the time windows for STDP start at almost +200 ms for depression (pre-synaptic spike 200 ms after the post-synaptic spike) but LTP can be induced only if the interval is within -30 ms (Froemke *et al.* 2005).

The stimulation pattern in the post-synaptic cell also induces differential LTP. Letzkus and collaborators showed that at synapses from layer II-III to layer V PCs, a burst of action potentials (even two APs) in the post-synaptic cell could elicit LTP where a single AP failed (Letzkus *et al.* 2006). Moreover, the timing required for this burst-induced plasticity depends on the location of the synapse on the dendrite. For proximal dendrites, the post-synaptic burst generated LTP when initiated 10 ms after the pre-synaptic firing, and generated LTD when initiated 10 ms before. At distal dendritic synapses the induction of LTP and LTD are switched (Letzkus *et al.* 2006; Sjostrom and Hausser 2006). This switch probably originates from differential calcium dynamics in the distal dendrites following back-propagating APs (Larkum *et al.* 1999). Additionally, the membrane voltage at the synapse influences the direction of plasticity. More depolarized membrane induces a shift of the timing window towards LTP (Letzkus *et al.* 2006; Sjostrom and Hausser 2006).

A recent study of STDP induced in spines of layer II-III PCs showed that the variations of intracellular calcium concentration were similar for LTP and LTD (Nevian and Sakmann 2006). The direction of plasticity was due to the time of activation of metabotropic glutamate receptors (mGluRs) that trigger endocannabinoid synthesis via phospholipase C activation. If mGluRs are activated after the voltage dependent Ca^{2+} influx, the signalling pathway is triggered and LTD induced. On the contrary, if the voltage dependent Ca^{2+} influx is enhanced by NMDA activation the synapse is potentiated (Nevian and Sakmann 2006).

Apart from the exact timing required to elicit STDP, the firing rate is also an important factor. A minimum firing rate has been shown to be required for some protocols (10Hz, Markram *et al.* 1997b) and most studies were performed using firing rates of 50-100Hz (Gustafsson and Wigstrom 1986; Magee and Johnston 1997) or a prolonged depolarization (Gustafsson *et al.* 1987; Debanne *et al.* 1998).

Redistribution of synaptic efficacy. The amplitude of any given post-synaptic response depends on the release probability (or U in the Tsodyks-Markram model) as well as the overall synaptic strength (ASE). In order to properly study synaptic plasticity it is therefore important to study the modification of these two factors independently. Most LTP experiments were performed by observing changes in single synaptic responses (evoked by low frequency stimulation), which do not allow for the separation of these two components.

Paired-recordings in the rat neocortex showed that subsequent EPSPs in a train are differentially modified following Hebbian pairing (Markram and Tsodyks 1996a; Markram and Tsodyks 1996b). On the one side, the first EPSP in the train increased while the second one decreased after pairing. On the other side, stationary EPSPs (with steady-state amplitude) seemed not to be affected by the pairing protocol when the frequency of the AP train is above 25 Hz (Markram and Tsodyks 1996a). These observations lead the authors to propose the concept of "Redistribution of Synaptic Efficacy". Indeed, LTP was induced for the firsts EPSPs in the train but subsequent EPSPs seemed to have undergone LTD. The interpretation for this observation is that the utilization factor (equivalent to release probability) increases following pairing, even if no changes are observed in the absolute synaptic efficacy strength. This leads to a larger first response, leaving a smaller amount of resources for subsequent APs (Markram and Tsodyks 1996a; Markram and Tsodyks 1996b). It seems that the biological mechanism underlying this plasticity differs from the LTP due to an overall increase in the synaptic strength, in which case the EPSP train would increase as a whole. The plasticity presented here is likely to be caused by a pre-synaptic change in release probability.

Synaptic transmission is a dynamic and complex phenomenon and does not only depend on synaptic strength. In order to fully understand synaptic plasticity it is important to investigate changes in other synaptic parameters such as the time constants governing its dynamics (depression and facilitation time constants).

The role of mGluRs in plasticity. mGluRs in PC spines were shown to be involved in differential plasticity with respect to the spike timing of the pre- and post-synaptic neurons (Nevian and Sakmann 2006). The role of mGluRs in synaptic plasticity has been investigated for more than a decade, with increasing specificity regarding the subtypes of receptors and ligands. LTP in hippocampus could be induced by a common activation of group I and II mGluRs (Bortolotto and Collingridge 1993; O'Connor *et al.* 1995) presumably triggering a calcium dependent mechanism (Bortolotto and Collingridge 1995) or by non-specific mGluR activation that seems to be NMDA receptor independent (Bortolotto *et al.* 1994; Rossi *et al.* 1996). This mGluR induced LTP required the post-synaptic cell to be depolarized and was closely related to NMDA receptor LTP (O'Connor *et al.* 1995). However, LTD was also observed after mGluR activation and some studies showed that the intra-cellular mechanisms were quite different between NMDA and mGluR mediated LTD (O'Mara *et al.* 1995; Oliet *et al.* 1997).

The induction of synaptic modification by mGluR could also have a pre-synaptic origin. Various studies showed that mGluRs have a differential role in glutamate release. Non-specific agonists could equally elicit facilitated (Bezzi *et al.* 1998; Moroni *et al.* 1998) or depressed (East *et al.* 1995; Cozzi *et al.* 1997) glutamate release. More detailed experiments using specific group I, II or III mGluRs agonists showed that group I mGluRs were involved in the increase of glutamate release (Bezzi *et al.* 1998; Herrero *et al.* 1998; Moroni *et al.* 1998), whereas group II and III mGluRs were involved in the decrease of glutamate release (Vazquez *et al.* 1995; Di Iorio *et al.* 1996; Herrero *et al.* 1996).

To further illustrate the diversity of mechanisms where mGluR are involved, it was shown that group I mGluRs are necessary for LTP in an NMDA dependent manner both in the hippocampus (Fitzjohn *et al.* 1996) and in the cingulate cortex (Hedberg and Stanton 1996). However, still in the hippocampus, group I mGluR can also be involved in a form of LTD called depotentiation (Zho *et al.* 2002).

Additionally, an elegant electrophysiological study involving various group-specific mGluR antagonists in the medial vestibular nuclei demonstrated the differential role the three receptor groups play (Grassi *et al.* 2002). The authors showed that group II and III mGluRs activation resulted in the prevention of LTP by reducing glutamate release. They also highlighted a differential role of the two receptors of the group I mGluRs. Indeed, mGluR1 was shown to be required for LTP whereas mGluR5 (the other receptor in the group I) was shown to prevent LTP (Grassi *et al.* 2002). Even though this study was not performed in the cerebral cortex it shows the complex and differential roles mGluRs play in synaptic plasticity.

To further illustrate the contrasting actions of mGluRs in the brain, it is worth mentioning that mGluR5 knock-out mice show memory impairments in the Morris water maze and in fear-conditioning tests (Lu *et al.* 1997). The study by Lu *et al.* further shows that the CA1 region of the hippocampus displayed LTP reduction while the CA3 region was intact. This difference in brain region specificity of mGluRs has also been shown in the hippocampus *in vitro*. Indeed, LTP induction in the mossy fibre contrasts with CA1 LTP by its independence upon NMDA receptor activation (Zalutsky and Nicoll 1990).

These complex and diversified actions of mGluRs will require further detailed and more targeted investigations in order to identify their differential roles in the various cells domains and brain regions in which they are located. The study presented in this chapter shows different aspects of synaptic and circuit plasticity that can be induced by mGluR activation.

The variety of mGluR roles as well as the diversity in spike timing dependent plasticity show the large variability in synaptic plasticity. All these studies where however focused on the changes in existing synapses properties. Synapses are formed and pruned during development following neuronal formation and migration in the various cortical layers. However, learning and memory occurs throughout the entire life. Do the cellular mechanisms for this life-long capability only include changes of existing synapses? Recent experiments showed that spines of superficial layers PCs are very active and can grow, stabilize or retract during the animal activity (Trachtenberg *et al.* 2002; Holtmaat *et al.* 2005; Holtmaat *et al.* 2006). These observations are however only morphological and lack the functional evidence for newly formed synaptic connections (although it is quite likely that the spines' movement follows some functional signal).

There is an *all-to-all morphological connectivity* among TTCs such that multiple axo-dendritic appositions exist between any given pair of TTCs whose somata are within the same cortical column (Kalisman *et al.* 2005). The *functional connectivity* for the same neuronal population is however only around 10-15%. The difference between functional connections and morphological close appositions lies in the presence or not of axonal boutons. There is then a possibility for the synaptic connections to be "turned on" and "turned off" provided a bouton is formed or reabsorbed and post-synaptic receptors are inserted or retracted. This possibility implies a potential complete rewiring of the microcircuit at limited morphological and energetic costs.

To test this hypothesis, up to 7-neurons clusters of TTCs were patched and the connectivity of this local microcircuit recorded both in terms of connection proportion and existing connections dynamics. The patch pipettes were then retracted within 20 min after obtaining whole-cell configuration in the first neuron, in order to minimise the washout of the internal milieu. The slice was then left in the recording chamber for 12 hours and the exact same neurons were re-patched for a second recording.

The changes observed in the connectivity of TTCs clusters within 12 hours, both under control conditions and following the application of various pharmacological agents are described in this chapter.

3.2 Materials and Methods

Electrophysiological recordings. Young (12-14 postnatal day) Wistar rats were rapidly decapitated and their brains removed and sliced in an artificial cerebro-spinal fluid (ACSF) containing (in mM): 125 NaCl, 2.5 KCl, 25 D-glucose, 25 $NaHCO_3$, 1.25 NaH_2PO_4, 2 $CaCl_2$ and 1 $MgCl_2$. The sagittal somatosensory cortex brain slices were then perfused with 35°C ACSF for the whole experiment. Somatic multiple whole-cell recordings were made and signals were amplified using Axoclamp-200B amplifiers (Axon Instruments, USA) and digitized via an ITC-18 interface (Instrutech, Great Neck, NY, USA) to an Apple computer running Igor Pro (Wavemetrics). Voltages were recorded with pipettes filled with an intra-cellular solution (ICS) containing (in mM): 100 potassium gluconate, 10 KCl, 4 ATP-Mg, 10 phosphocreatine, 0.3 GTP, 10 Hepes and 5mg ml^{-1} of biocytin (pH 7.3, 310 mosmol l^{-1}, adjusted with sucrose). The pipettes were pulled with a Flamming/Brown micropipette puller P-97 (Stutter Instruments CO, USA). All animal experiments were done under the authorization number 1550 of the "Service Vétérinaire de l'Etat de Vaud".

Clusters of 6-7 layer 5 thick tufted pyramidal cells (TTCs) were patched a first time ("before") and their connectivity recorded using successively, for each cell, a train of 30Hz action potentials followed by a recovery test spike 500ms later. The stimulation was repeated 30 times and the averaged trace used for analysis. Recordings were obtained ~2hours after slicing in an attempt to avoid the initial increase in synapses reported due to slicing (Kirov *et al.* 1999). Within 20 min the pipettes were withdrawn and the slice was left in the recording chamber with various conditions. For the spontaneous condition we continued perfusing only ACSF. Evoked 1 was ACSF in the presence of 50 mM sodium glutamate 2 secons puffs 100 µm above the cell cluster every minute (Figure 1*C*,*D* of the paper in section 3.5). Evoked 2 was ACSF perfused with 100µM sodium glutamate (Sigma-Aldrich, St-Louis, MO, USA) (Figure 1*E* of the paper). The various antagonists conditions correspond to the slice perfused with ACSF containing the antagonists concentrations described below and glutamate puffing on the cluster.

The monitor display from the Zeiss Axioscope and Hamamatsu CCD camera were used to capture IR-DIC images, define landmarks and find the same cell cluster 12–14 hours later (Figure 1*A* of the paper). The microscope focus on the cells was also maintained through the experiment. The cells were then re-patched and the same stimulation protocol executed to monitor the connectivity in the new state ("after"). After recording, the slices were fixed and ABC stained and since biocytin was used in the first and second patchings, we could double check that the same cluster was patched for each experiment (Figure 1*B* of the paper). In one case, when the IR-DIC localization of the cluster was not convincing, 2 clusters were clearly seen corresponding to the "before" and "after" patching sessions. This shows that the biocytin is preserved in the cell even after more than 12 hours in the recording chamber.

The electrophysiological responses were analysed off-line (Igor) and the Markram-Tsodyks model was used on the averaged traces to determine synaptic properties. The model yields the absolute synaptic efficacy (A) that is the total amount of resources the unperturbed presynaptic neuron has over all its synapses (expressed in mV measurable in the post-synaptic neuron). It then also yields the utilization of synaptic efficacy (ranged between 0 and 1) which is the fraction of the resources used by one action potential. The first EPSP size is the product of A with the utilization of synaptic efficacy. As A is the total amount of resources and the depression in TTCs is mostly presynaptically mediated (Thomson *et al.* 1993a; Tsodyks *et al.* 1998), A is equivalent to the number of release sites multiplied by the quantum size. The EPSP size is then A multiplied by the probability of release (Pr). Consequently, the utilization

of synaptic efficacy is equivalent to the probability of release which is then derived directly from the fitting of the model on the averaged traces.

The condition of 12 hours old slices was excellent (Figure 1*A* of the paper) with high visibility, no change in patchability (reflection of slice health), normal break-in resting potentials and normal discharge behaviour and no change in input resistances.

Histological procedure. Following the recording, the 300 µm slices were fixed for at least 24 hours in a cold 0.1 M phosphate buffer (100 mM, pH 7.4) containing 2% paraformaldehyde and 1% glutaraldehyde and 0.3% picric acid. Thereafter, the slices were rinsed and then transferred into a phosphate-buffered 3% H_2O_2 to block endogenous peroxidases. After rinsing in the phosphate buffer, slices were incubated overnight at 4°C in an avidin-biotinylated horseradish peroxidase (ABC-Elite, Vector Labs, Burlingame, CA; 5% A, 5% B and 0.25% Triton X-100). Subsequently, sections were rinsed again in the phosphate buffer and developed with diaminobenzidine (Vector Labs) under visual control using a stereomicroscope (Leica, Wetzlar, Germany) until all processes of the cells were clearly visible. Finally, the reaction was stopped by transferring the sections into the phosphate buffer. After rinsing in the phosphate buffer, slices were mounted in an aqueous mounting medium.

Pharmacology. The following pharmacological agents were used: tetrodotoxin (TTX; Alomone Labs, Jerusalem, Israel) 0.5 µM (a sodium channel blocker), 6-cyano-7-nitroquinoxaline-2,3-dione (CNQX; Sigma-Aldrich, St-Louis, MO, USA) 20 µM (an AMPA receptors antagonist), D-2-amino-5-phosphonopentanoic acid (D-AP5; Tocris, Ellisville, MO, USA) 20 µM (a NMDA receptors antagonist), 2-methyl-6-(phenylethynyl)pyridine (MPEP; Tocris, Ellisville, MO, USA) 4µM (a metabotropic glutamate receptor 5 (mGluR5) antagonist), DL-2-amino-3-phosphopropinionic acid (DL-AP3; Tocris, Ellisville, MO, USA) 100µM (a group I metabotropic glutamate receptor antagonist), (2S)-α-Ethylglutamic acid (EGLU; Tocris, Ellisville, MO, USA) 100µM (a group II metabotropic glutamate receptor antagonist) and (RS)-α-Cyclopropyl-4-phosphonophenylglycine (CPPG; Tocris, Ellisville, MO, USA), 20µM (a group III metabotropic glutamate receptor antagonist).

For complementary experiments not presented in the paper, Dihydroxyphenilglycine (DHPG; Tocris, Ellisville, MO, USA) was used in order to mimic the protocols with glutamate puffing. The required concentration was calculated by multiplying the 50mM of glutamate puffing by the ratio between the glutamate and the DHPG IC_{50}s (IC_{50}=0.7µM and 3.9µM for L-glutamate and DHPG respectively see Pin and Acher 2002). 100 mM of DHPG was puffed for 2 seconds every minute just above the slice without additional stimulation to the cluster. The maximum concentration was used and was still below the corresponding concentration that was calculated from the IC_{50} ratio. It is to compensate the difference with glutamate that DHPG was puffed for 2 seconds every minute just at the surface of the slice (compared with the glutamate puffed 100µm above the slice for the same timing). A specific mGluR5 agonist would have been preferable, but could not be used because the concentrations required to mimic the glutamate effect were too high for the available products solubility. In addition to DHPG, KCl (1mM) was puffed with the same timing at a position close to the DHPG containing pipette in order to generate action potential firing in the cells.

O-Phospho-L-serine (L-SOP; Tocris, Ellisville, MO, USA) 50µM, a group III mGluR agonist was perfused for some experiments. SP600125 (5µM; Tocris, Ellisville, MO, USA), a specific inhibitor of the C-Jun N-terminal kinase (JNK) and BAPTA (500µM; Sigma-Aldrich, St-Louis, MO, USA) a calcium chelator, were used inside the pipettes. In these last experiments, 4 out of the 7 pipettes were filled with the specific blocker mixed in ICS and the others with regular ICS. The stimulation protocol used on top of the intra-cellular

pharmacology application was Evoked 2.

Statistical tests. Student T-tests were used on the Gaussian-like distributions such as the distribution of the probability of release, the paired pulse ratio distributions, the changes in A and the natural logarithm of A "before" vs A "after". The comparison of A "before" and A "after" was made with a Kolmogorov-Smirnov test (KS test). The proportion of emergences, disappearances and the proportion of reciprocal emergences were tested using the Chi square test. As the connections hit rates, the proportions of emergences and disappearances were estimated as being the proportion of connections observed in the respective conditions (as opposed to the number of connections not observed, i.e. not present, not emerged or not disappeared) the standard errors of the mean were calculated on the base of a binomial distribution:

$$SEM = \sqrt{\frac{p(1-p)}{n}}$$

Indices and formulations. The Emergence index was calculated as:

$$E_i = \frac{\#\,connections\ that\ emerged}{\#\,remaining\ possible\ connections}$$

where

$$\#\,remaining\ possible\ connections = (\#\,possible\ connections) - (\#\,connections\ at\ first\ recording)$$

The Disappearance index was calculated as:

$$D_i = \frac{\#\,connections\ that\ disappeared}{\#\,connections\ at\ first\ recording}$$

The connection hit rate is the number of connections divided by the number of neuron pairs considered.

The conditional reciprocal connections hit rate is the number of neuron pairs reciprocally connected divided by the total number of connected pairs.

Valproic acid (VPA) treated animals. Wistar rats (Charles River Laboratories, L'Arbresle, France) were mated and pregnancy determined by the presence of a vaginal plug on embryonic day 1. Sodium salt of valproic acid (NaVPA, Sigma) was dissolved in 0.9% saline to get a concentration of 150 mg/ml, pH 7.3. Treated rats were injected 500mg/kg of NaVPA intraperitonally on gestational day 12.5, control rats were untreated. Delivery of this dose to rats during embryogenesis has been shown to result in maximum levels of total valproic acid in maternal plasma in less than 1 hour, with a mean plasma elimination half life of 2.3 hours. Dams were housed individually and were allowed to raise their own litters. The offsprings were used for experiments on postnatal day 12 to 14. Experiments with treated rats were don with the Evoked 2 protocol.

3.3 Results

The major results of this section are in the paper in section 3.5. A summary of the most important results is presented below.

Rewiring in the neonatal neocortex. New connections were formed, existing connections disappeared or were being modified in strength between the "before" and the "after" recordings for all the experimental conditions used. In the spontaneous condition, 4±1% of unconnected pairs "before" were connected "after" and 13±7% of connected pairs disconnected in the same period of time. The Evoked 1 and Evoked 2 significantly increased the rate of emergence of connections (E_i=16±3% and 14±3% respectively, $p<0.01$ for both) and tended to decrease the rate of disappearance but without significance (D_i=6±4% and 7±5% respectively). The overall connection rate in the cluster of neurons was doubled after the 12-hours glutamate stimulation (14% of connected pairs at the first recording vs. 29% after the stimulation). The connections that appeared between the "before" and "after" recordings were weaker (1.5±0.1mV vs 2.4±0.1mV, $p<0.001$) and with a smaller probability of release (0.36±0.01 vs 0.45±0.01, $p<0.001$) compared to the connections recorded "before". The connections that disappeared were also weaker (1.1±0.3mV vs 2.4±0.1mV, $p<0.001$) but with a normal probability of release (0.43±0.03 vs 0.45±0.01).

As glutamate triggers the apparition of new connections, various glutamate receptors antagonists were perfused into the bath while the cluster was stimulated with glutamate puffing. Additionally, as glutamate puffing generated AP discharge in the cells, the sodium channel blocker tetrodotoxin (TTX) was also perfused in a series of experiments. These experiments showed that both mGluR5 and AP discharge are required for the new connections to be formed as the proportion of unconnected pairs in the first recording that were connected after 12 hours was significantly reduced towards spontaneous levels of appearance with the perfusion of TTX or 2-methyl-6(phenylethynyl)pyrine (MPEP, an mGluR5 selective antagonist) (E_i=6±2% and 7±2% respectively).

The dynamics of the existing connections was unchanged after 12 hours in the recording chamber even with glutamate stimulation. However, the absolute synaptic efficacy spontaneously increased. This increase was further enhanced with glutamate stimulation. The various pharmacological products perfused while the cluster was stimulated with glutamate puffing showed that again AP firing and mGluR5 are required for the enhancement of synaptic efficacy. Additionally AMPA and NMDA receptors are also contributing to this increase in connection strength. The experiments with antagonists of group I mGluRs also showed a requirement of this group for plasticity of existing connections. The inhibition of group III mGluRs showed a tendency for these receptors to diminish the synaptic strength although this was not significant. We will see below that complementary experiments with group III mGluRs confirm this tendency.

Some complementary results that were not published are given in the following paragraphs.

Time course for microcircuit rewiring. The Evoked 1 protocol was used for 4-hours glutamate stimulations. Within this period of time, 6±2% (mean±SEM, n=140 unconnected pairs "before") of unconnected pairs were connected "after". These new connections had the same dynamics as the connections that appeared after 12 hours (A=1.3±0.3 mV and U=0.37±0.06, n=8, vs. A=1.5±0.1 mV and U=0.35±0.01 respectively, mean±SEM). No

significant difference in dynamics was observed between the connections that appeared in 4 hours and those that were present at first recording, probably because of the small number of emerged connections in the 4 hours protocol. Only one connection among the 28 present at first recording disappeared at the second recording (after 4 hours). This does not allow any statistical treatment nor a temporal investigation. However, the emergence proportions have been analyzed together with the 12 hours results and are displayed in Figure 7. A first approximation linear fitting gave a rate of 1.3±0.2% new connections per hour (assuming that no connections are emerging within the first minutes of stimulation).

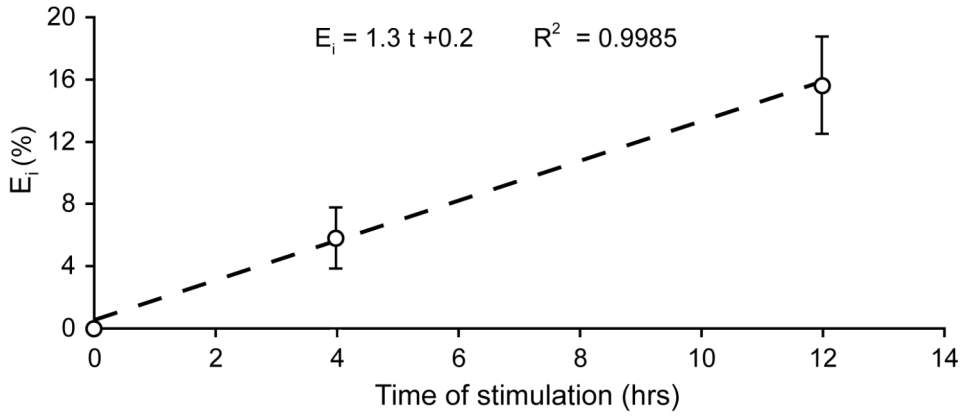

Figure 7 Time course of the emergence of new connections. Glutamate stimulation by puffing 50 mM NaGlut for 2s every minute. Pipette positioned 100µm above the cluster of interest. Mean±SEM.

In four hours of stimulation the increase in absolute synaptic efficacy was: ΔA = 1.0±0.2 mV (mean±SEM, n=54 connected pairs in both recordings). The linear extrapolation for the two points at 8 and 12 hours intersects the ΔA axis at 0.7 mV (Figure 8). As a consequence, assuming a linear increase in A would mean that the very first stimulations would result in an increase in A of 30% (0.7 mV over 2.4 mV).

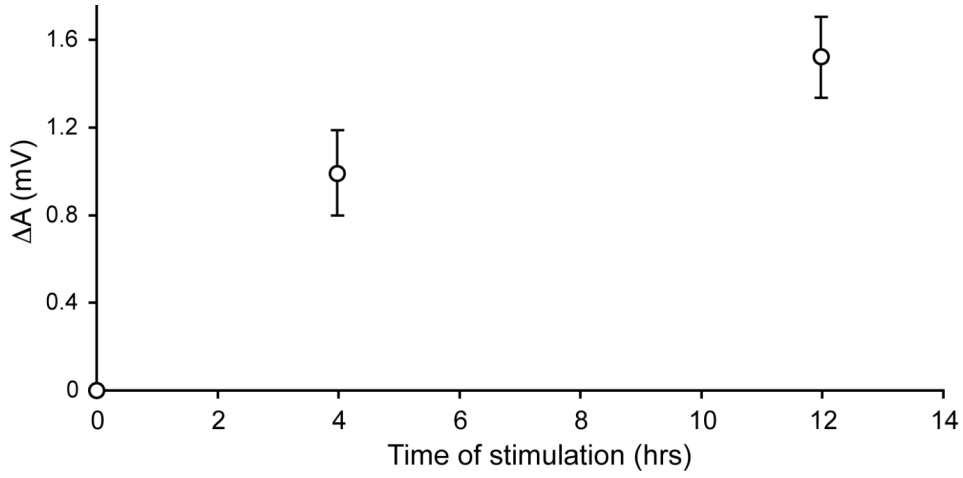

Figure 8 Time course of the variation of the absolute synaptic efficacy. Glutamate stimulation by puffing 50 mM NaGlut for 2s every minute. Pipette positioned 100µm above the cluster of interest. Mean±SEM.

Complementary experiments with extra-cellular pharmacology. The spontaneous appearance of connections (without any glutamate stimulation) was not significantly affected by TTX (6±3%, n=50 vs. 4±1%, n=182, mean±SEM for ACSF perfusion with and without 0.5 µM TTX respectively, Figure 9*A*). Similarly, the change in the absolute synaptic efficacy of already existing connections did not seem to be modified either (1.2±0.5 mV, n=14, vs. 1.0±0.2 mV, n=41 with and without TTX respectively, Figure 9*B*).

As MPEP, an mGluR5 antagonist, significantly reduces the creation of new connections, an agonist of group I mGluRs has been perfused in the bath to try to induce the creation of new connections. DHPG puffing did not trigger new connection formation nor increased the efficacy of existing synapses (E_i =5±2%, n=103 vs 4±1% and A=0.9±0.3 mV, n=25 vs 1.0±0.2 mV for DHPG and spontaneous respectively, Figure 9). Additionally, some experiments were performed with an increase in activity triggered by KCl puffing. This gave rise to only one new connection over the 5 clusters probed. This rate is below the spontaneous appearance and might be the result of some other effects induced by KCl.

The perfusion of DHPG together with the puffing of KCl induced significantly more emergences than the spontaneous condition (11±3%, n= 129, vs 4±1% for DHPG+KCl and spontaneous respectively, $p<0.05$, χ^2 test, Figure 9*A*). The emergence index with this condition did not reach the values obtained with glutamate stimulation (Figure 9*A*), but, as mentionned above, KCl puffing might interfere with the mechanism inducing the creation of new connections. The increase in synaptic efficacy was not significantly affected by the combined actions of DHPG and KCl (ΔA=0.6±0.1 mV, n=39 vs ΔA=1.0±0.2 mV for DHPG+KCl and spontaneous respectively, Figure 9*B*).

When perfused in ACSF without any glutamate stimulation, L-SOP did not modify the rate of emergence of new connections (E_i=3±2%, n=96 vs 4±1% for L-SOP and spontaneous respectively, Figure 9*A*). The glutamate stimulation induced emergence of new connections was not affected either by the increased stimulation of group III mGluRs (E_i=18±3%, n=159 vs 16±3%, n=135 for glutamate puffing with and without L-SOP perfusion respectively Figure 9*A*).

The group III mGluRs activation resulted in a reduction in synaptic efficacy during the 12-hours plasticity both with and without glutamate stimulation. In the case of perfusion of L-SOP only, the overall synaptic efficacy was even decreased from the first recording to the recording 12 hours later (ΔA=–0.3±0.2 mV, n=22, vs 1.0±0.2 mV for L-SOP and spontaneous respectively, $p<0.001$, Student T-Test, Figure 9*B*). This shows that group III mGluRs activation results in long term synaptic depression. Even when glutamate was puffed on the cluster, condition that has been shown to significantly increase the augmentation of synaptic efficacy, the group III mGluRs agonist significantly reduces this potentiation (ΔA=0.9±0.2 mV, n= 59, vs 1.5±0.2 mV, n=63 for glutamate puffing with and without L-SOP perfusion respectively, $p<0.05$, Student T-Test, see Figure 9*B*).

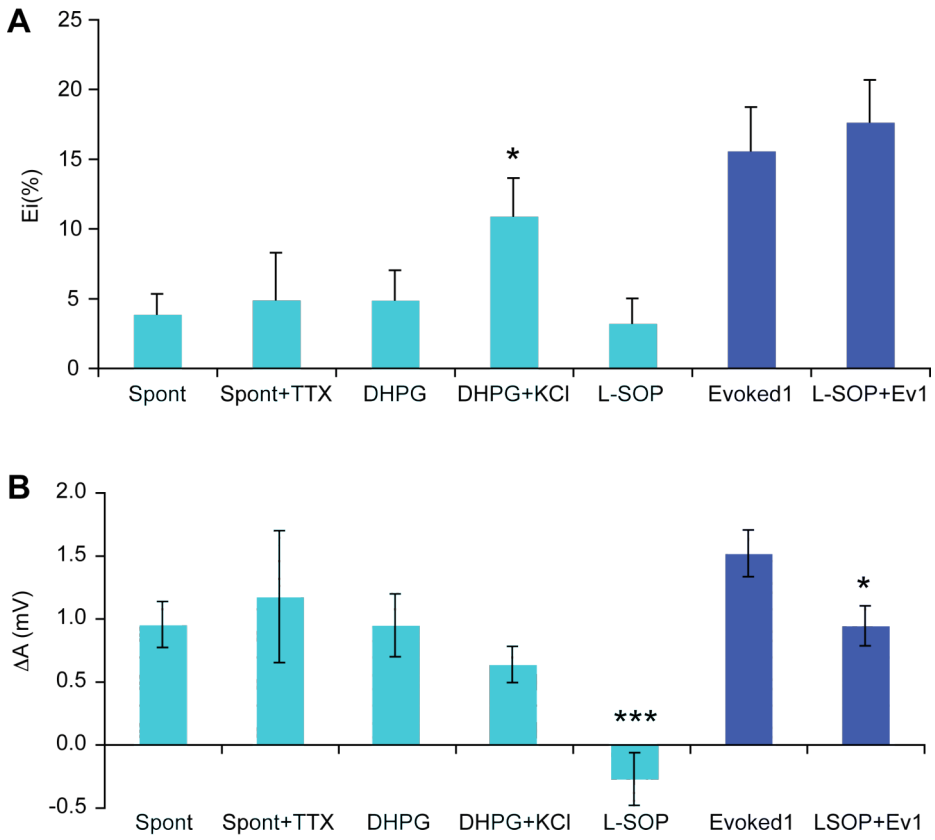

Figure 9 Agonists actions on the proportion of new connections and the change in synaptic efficacy. A – Emergence index (E_i) variation induced by various agonists applications. The group I mGluR action conjugated to cluster activation by KCl induced a significant increase in the emergence of new connections. *p<0.05, χ^2 test. B – Variation in the absolute synaptic efficacy induced by agonist stimulation. The group III agonist L-SOP significantly reduced the increase in synaptic efficacy both with and without glutamate stimulation. ***p<0.001, *p<0.05, Student T-Test.

Preliminary results with intra-cellular pharmacology. The cells were separated into four groups. The potentially new pre-synaptic cells blocked or unblocked by pharmacology and the potentially new post-synaptic cells blocked or unblocked. An emergence index was calculated for each group. For both conditions, the unblocked cells had a similar E_i for pre- and post-synaptic cells (E_i= 14±3%, mean±SEM, for the four groups n=130 for the post-synaptic side, n=131 for the pre-synaptic side, Figure 10).

No significant difference in the emergence indices was found in this set of experiments. However, a tendency for a reduction of new connections on post-synaptic cells after JNK inhibition by SP600125 was observed (E_i=8±3%, n=65, Figure 10*A*) as well as a tendency for a reduction of new connections in the pre-synaptic cell after partial Ca^{2+} chelation with BAPTA (E_i=12±3%, n=104, Figure 10*B*).

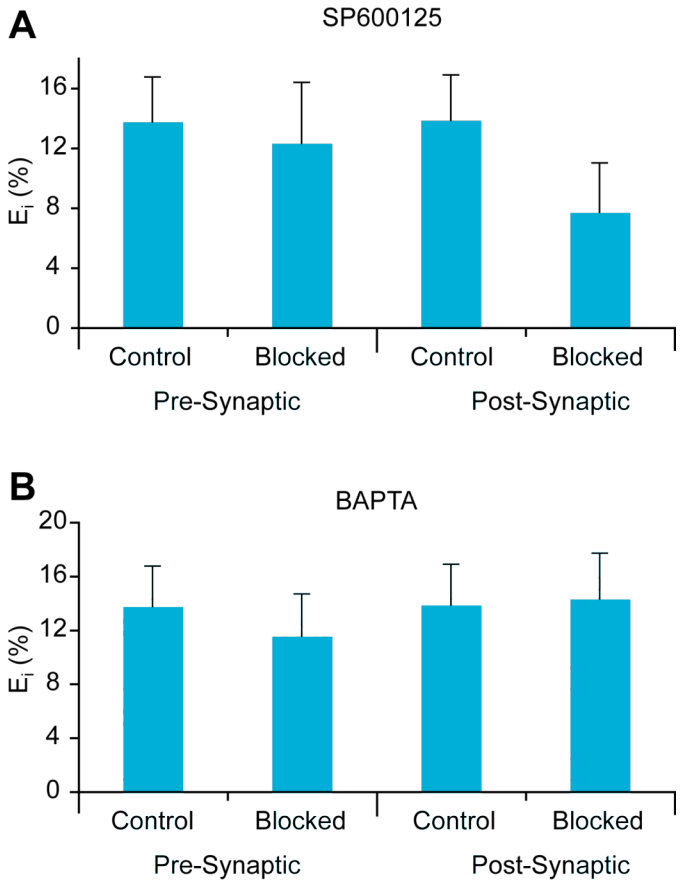

Figure 10 Interfering with the intra-cellular pathway. A – Emergence index for cells that were patched without (Control) and with (Blocked) 5 µM of SP600125 in the recording pipette. The potential new pre-synaptic and post-synaptic cells were analyzed separately. B – Same as in *A* but with or without 500µM of BAPTA in the recording pipette.

Microcircuit plasticity in the valproic acid rat model of autism. In typical 7 patch recordings, neurons are separated by 20 to 200µm. A binning of the connectivity was then performed to separate the cells closer than 50 µm from those 50-100µm apart. A tendency for hyper-connectivity for nearby cells was observed (11±4% vs. 18±3%, n=76 and 156 for control and treated rats respectively, Figure 11*A*). This tendency for hyper-connectivity was not observed for distances between 50µm and 100µm (16±4% vs. 14±3%, n=94 and 112 for control and treated rats respectively, Figure 11*A*) in accordance with previous results (Rinaldi *et al.* 2007b).

Hyper-plasticity was observed in 12 hours long term potentiation (ΔA=1.1±0.2 mV vs. 1.9±0.2 mV, n=47 and 53, $p<0.01$ for control and treated rats respectively, Figure 11*B*). Our results show that VPA treatment not only induces changes in the connectivity of the neocortical microcircuit, but also affects the mechanisms governing microcircuit plasticity.

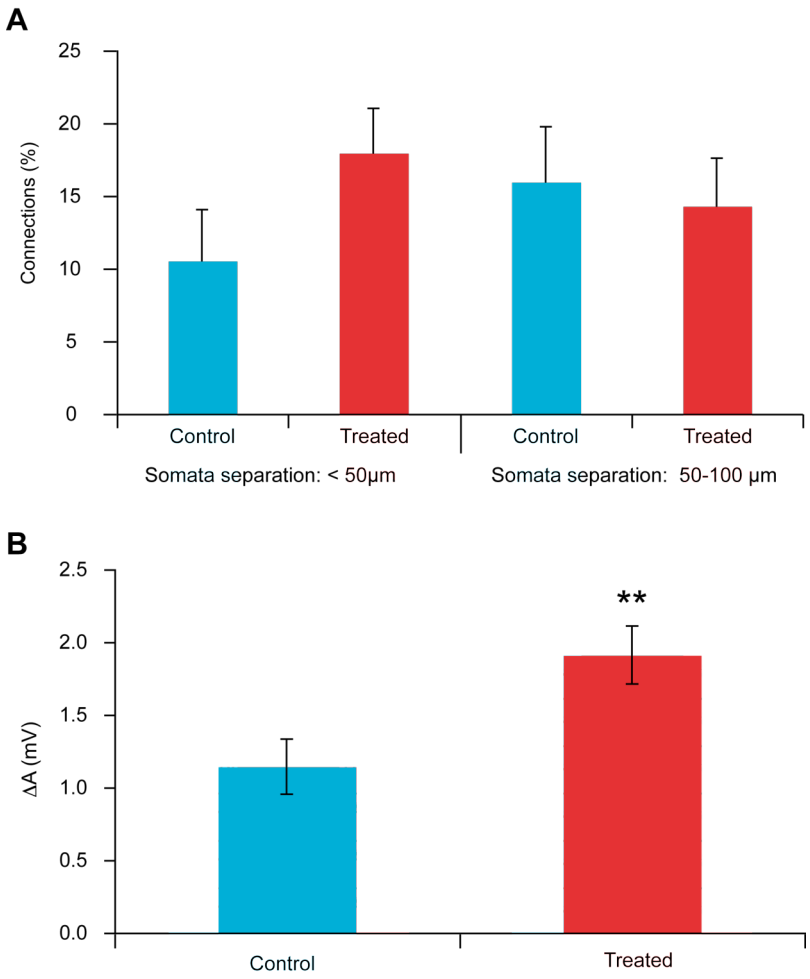

Figure 11 Hyper-connectivity and hyper-plasticity in VPA treated rats. A – Proportion of connections between layer V TTCs whose somata are separated by less than 50µm (left) and between 50 and 100µm (right). B – Variation in absolute synaptic efficacy for control and VPA treated rats under a stimulation of 12 hours perfusion of 100µM glutamate. **p<0.01

Preliminary results on the emergence and removal of connections in VPA treated animals are presented here. The emergence index tends to be reduced for nearby TTCs in treated rats (E_i=15±4% vs. 9±3%, n=68 and 110 for control and treated rats respectively, Figure 12). However, for TTCs whose somata were separated by 50-100µm, the emergence index was similar (E_i=10±3% vs. 9±3%, n=80 and 82 for control and treated respectively, Figure 12).

The emerged connections characteristics in the treated animals were similar to the one observed in control animals. Both U and A were smaller in the new connections compared to the normally observed connections "before" (A_{before}=2.4±0.1 mV, $A_{control}$=1.4±0.2 mV and $A_{treated}$=1.7±0.2 mV; U_{before}=0.45±0.01, $U_{control}$=0.33±0.03 and $U_{treated}$=0.35±0.03).

No disappearance has been observed in any of the 7 clusters probed in treated rats among the 34 connections recorded "before". This is to be compared with the 3 connections that disappeared among the 42 connections recorded "before" in control rats.

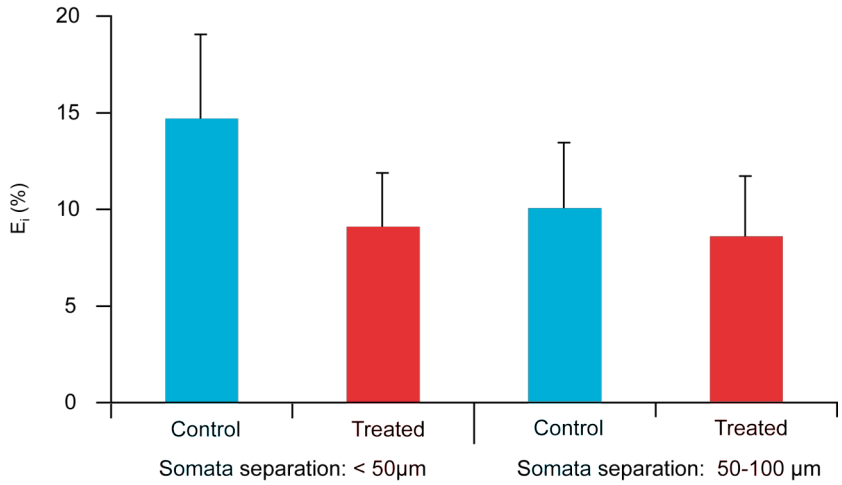

Figure 12 Emergence of connections in VPA treated rats. Emergence indices for pairs of TTCs whose somata are located within 50µm (left) and between 50 and 100µm (right) in both control and VPA treated rats.

3.4 Discussion

Direct connections between TTCs. The connection modifications observed in the microcircuit rewiring has been investigated at synaptic connections between TTCs. These synapses are excitatory and depressing with negligible facilitation. The connection probability between two TTCs whose somata are separated by ~100µm is ~15% (589 connections for 3907 pairs tested for this study). The fitting of the Tsodyks-Markram model gives an average absolute synaptic efficacy of 2.4±2.2 mV (mean±SD), a utilization of synaptic efficacy of 0.46±0.13, a recovery time constant from depression of 500±40 ms and a facilitation time constant of 60±180 ms. The median for this latter is 10 ms indicating that although there is a high mean, the vast majority of facilitation time constants is small. Over the 513 connections analysed, there was no correlation between the various parameters (coefficients between -0.03 and -0.3).

TTCs have also been recorded for the study presented in chapter 2. The connection rate for these experiments is 11%, on average A=3.8±0.4mV, U=0.51±0.02 and τ_D=620±30ms. The differences between these values and the values obtained for the microcircuit rewiring experiments originate from the method used to collect the data. In the experiments of chapter 2, the cells were patched and tested for connections with a few trials. If the connection was not visible on these trials the cluster was abandoned and another one investigated. This technique has been applied both for CCPs and TTCs investigations within this study. In the case of the experiments investigating the microcircuit rewiring, which data are summarised above, the cell clusters were systematically recorded. This allowed the analysis of smaller connections and explains the difference in absolute synaptic efficacy. The other parameters differences might be due to a sample size effect. Indeed, more than 500 connections were analysed for the microcircuit plasticity study whereas only 25 connections have been analysed for the CCPs study. It is worth noticing, however, that in the CCPs study the sample size was similar for the two populations compared. These differences highlight the importance of performing the control experiments in the same frame of a given new protocol to avoid artificial differences.

Rewiring in the neonatal neocortex. New functional synaptic connections are formed in neocortical acute brain slices within 12 hours. This apparition of new connections is not due to the recovery from slicing (Kirov *et al.* 1999) as the first recording was done 2 hours after the dissection. Glutamate stimulation led to a nearly 4-fold increase in the formation of new connections compared to the rate of emergence in a quiescent slice. On another hand, about 10% of connected pairs disconnected in the 12 hours period. Some variation in this disconnection rate has been observed under the different conditions but the small number of pre-existing connections did not allow the determination of any significant difference. This suggests that overall stimulation of the cluster generates a burst of new connections without a counter-balancing removal of existing connections.

The new connections formed within the 12 hours period were weaker, with synaptic efficacy (A) and the utilization factor (U) significantly smaller than in existing connections at the first recording. The depression time constant was unchanged. In contrast, connections that disappeared had a normal U parameter but a smaller A. These targeted disappearances further indicate that the neuron pairs disconnected because of a functional phenomenon and not an experimental procedure.

These observations suggest that a new experience enhancing the activity of a microcircuit gives rise to a rapid formation of new connections. These immature connections

are given a test period to become mature via the redistribution of synaptic efficacy (exposed in section 3.1) and then the mature but weak (and presumably not required) connections are removed in a second phase (not investigated in these experiments).

The number of boutons per connection is likely to be smaller for the emerged connection as they are weaker. Kalisman *et al.* (Kalisman *et al.* 2005) reported a linear regression of 0.41±0.12 mV/bouton. Connections recorded "before" have an average first EPSP amplitude of 1.08±0.07mV (amp of the first EPSP = A•U and A=2.4±0.1mV and U=0.45±0.01) yielding an average number of boutons per connection (calculated from the linear regression and the average) of 2.6±0.9 boutons/connection. The emerged connections have an average first EPSP amplitude of 0.34±0.03mV (A=1.5±0.1mV and U=0.36±0.01) resulting in the estimation of 0.8±0.3 boutons/connection. This suggests that new connections are visible with the activation of only one synapse. As reported in (Kalisman *et al.* 2005) the unconnected pairs have twice less boutons per connection than the connected pairs but the numbers of proximal axo-dendritic appositions are similar. As a consequence, the emerged connections can be the result of the activation of synapse where a bouton is already present. In order to determine the differences between the boutons present at unconnected pairs and the functional ones and consequently to determine the sequence of activation of a synapse, a more detailed investigation of the bouton content at the various stages of synapse maturation should be undertaken.

Time course for microcircuit rewiring. 4-hours of glutamate stimulation is sufficient to trigger the emergence of new connections in a neocortical microcircuit. It might be possible to observe new connections emerging in shorter periods of time although this might be experimentally difficult as the first estimate of the rate of emergence is 1.3% per hour. This linear extrapolation has been done with the two measured data points and the assumption that the regression should pass through the origin. This is likely to be the case as the emergence of new connections require metabotropic receptor activation as well as some mechanism such as bouton formation that require time. Therefore the first minutes of stimulation most likely result in an emergence index of 0%.

The linear extrapolation in the increase in synaptic efficacy does not pass through the origin and cuts the y-axis at about 0.7mV. This suggests that either the increase in synaptic efficacy is significant from the first stimulations (and then the linear extrapolation is appropriate) or that the time course for the variation in A is not linear and its rate tends to decrease with time. It is hard to compare directly the estimation of a rapid increase in synaptic efficacy of 0.7mV with previous LTP experiments as the synapse strength increase varies with the protocol. Moreover, some protocols result in an increase in the release probability and not in the absolute synaptic efficacy (Markram and Tsodyks 1996a). It would be necessary to measure the increase in A at another time point to conclude on the dynamics of the increase in A with the protocols used in this study. If alternatively the interpretation of a non-linearity in this evolution is true, the tendency would then be a decrease in the augmentation rate of A. This could be explained by the limited size of a synapse and the limited number of synapses per connection. The connections strengths could not grow indefinitely and it seems that the connections amplitudes recorded in these experiments might be close to the maximum that can be reached. The same argument could be raised for E_i but the small proportion of connected pairs (15%) allows a large increase in the number of connections before being limited by morphological constraints. Moreover, the emergence of new connections could be later counter-balanced by the removal of existing connections. This is only an assumption, as the number of disconnected cells observed (1/28 and 6/57 for 4 hours and 12 hours of glutamate puffing respectively) is too small to have any statistical significance. The reason for this small amount can be twofold: On the one hand the sustained

stimulation is artificial and can correspond to a particular transient physiological regime where connections are being massively created without down-regulation. On the other hand, the same stimulation could generate disconnection of neuron pairs but may require a longer stimulation period.

These results regarding the temporal aspects of microcircuit plasticity provide some insight into the dynamics of this phenomenon, which could be related to behavioural phenomena. However, experiments with stimulations lasting less than 12 hours would be required for a finer resolution of the connections' emergence dynamics. The complete dynamics of microcircuit reorganization would require experiments with stimulation lasting for more than 12 hours in order to see how the circuit would regulate this increase in connectivity and connections strength.

Complementary experiments with extra-cellular pharmacology. The perfusion of TTX without any glutamate stimulation did not result in any change of the emergence index nor of the variation in synaptic efficacy. The spontaneous changes might then be of a different origin than most of the changes evoked by glutamate (as TTX reduces the proportion of new connections when the cluster is stimulated with glutamate). As seen above, there is a number of functionally unconnected pairs with a bouton at the axo-dendritic appositions. The number of boutons is however significantly smaller than for connected pairs but there might be some mechanisms of bouton activation that are already at a later stage than the point where action potential activation is required. This spontaneous bouton activation might then be the final phase of the process suggested here that was started when the animal was still living. Here again a more detailed investigation of bouton maturation would highlight the various stages suggested by our results.

Activation of group I metabotropic receptors alone is not sufficient to significantly increase the emergence index from the spontaneous emergences. This is somehow expected as it was shown that the inhibition of mGluR5 and the blocking of spiking activity both results in a significant decrease in the emergence index. Similarly, the activation of the cell cluster by KCl does not increase the emergence index. In this case, it could have been expected to have some more important effect as glutamate is released from the activated cells and could activate mGluR5s. The emergence index even seems to be decreased by KCl. This might be due to a side effect that counteract the emergence of connections. Despite this effect, activation of group I mGluRs and triggering of cell activity simultaneously by the synchronized puffing of DHPG and KCl significantly increased the emergence index although it did not reach the values obtained with glutamate stimulation. This can be due to the negative effect from KCl but also from the expected weaker effect of DHPG compared to glutamate as the concentration of DHPG was not corresponding to the one that should have been used to mimic glutamate (see Materials and Methods).

The increase in synaptic efficacy due glutamate stimulation was not observed with the simultaneous stimulation by KCl and DHPG. This may be due to the lack of activation of AMPA and NMDA receptors that have been shown to affect the synaptic efficacy increase. It could be argued that the AP discharges of the cells following the KCl induced excitation should generate enough glutamate release for these receptors to be activated. It is likely however that glutamate application activates more receptors than would the AP discharges alone. For instance, silent synapses, that have only NMDA receptors in their post-synaptic density, might be more activated by artificial glutamate application than by AP dependent glutamate release.

The perfusion of L-SOP did not result in an increase in emergence index. This result is in agreement with the absence of emergence index variation after group III mGluRs inactivation by CPPG. The figure 4 of the paper presented in section 3.5 shows a tendency of

the group III mGluRs to act against the synaptic efficacy increase. The larger increase in A observed after the perfusion of CPPG while the cluster was stimulated by glutamate puffs was however not significant (compared to the increase in A with glutamate puffs only). This effect of decreased synaptic transmission due to group III mGluRs was already reported by other studies (see section 3.1). In the line of these results L-SOP perfusion significantly decreased the synaptic efficacy both with and without glutamate stimulation. The strength of these receptors is remarkable as they are already activated by glutamate and the additional activation due to their specific agonist is sufficient to alter the plasticity and bring it down to spontaneous variation.

In conclusion, the spontaneous emergence of connections might depend on a different mechanism than the glutamate evoked emergences. Both AP discharge and mGluR5 activation are required for the emergence of connections but might not be sufficient to mimic the glutamate action. Additionally, activation of group III mGluRs result in synaptic depression but does not influence the emergence of connections.

Preliminary results with intra-cellular pharmacology. Some preliminary test experiments have also been performed to probe the intracellular factors involved in the emergence of new connections in 12 hours.

The mGluR5 activation triggers on the one side the PLC cascade that finally results in the release of Ca^{2+} from the internal stores and on the other side the c-Jun pathway that leads to gene expression (see Nakanishi 1994; Conn and Pin 1997). SP600125 is a specific inhibitor of the c-Jun N-terminal kinase (JNK). When mGluR5 is activated, a rapid phosphorylation of JNK occurs that activates c-Jun (Yang *et al.* 2006).

In order to test for the implication of one or the other pathway in microcircuit plasticity, some of the cells in the cluster were filled either with SP600125 or BAPTA. None of the protocols resulted in a significant difference in emergence index. It tend however to be reduced by SP600125 on the post-synaptic side and by BAPTA on the pre-synaptic side. Although the cells were patched with a regular intra-cellular solution for the second recording, and the time in the cells during the first recording was not sufficient to block synaptic transmission, it is not inconceivable that BAPTA directly affected synaptic transmission and not the creation of new connections. It may also be that the concentration of BAPTA used has no effect at all and therefore the observed tendency is only a variation from chance. Even in the case of a clear influence of BAPTA, additional experiments would be required to allow any conclusion to be drawn as fast calcium buffering might affect synaptic and cellular function, especially over these experiments' long period of time. The localisation of mGluR5 on the cell membrane has been reported to be both on dendrites and on axon terminals (Romano *et al.* 1995) which is then not in contradiction with the preliminary results presented here.

The localization of the mGluR5s responsible for emergence of new connections as well as the mechanism underlying bouton and synapse activation require further investigation. Additional experiments with BAPTA in the patch pipette should maybe require additional protocols to ensure that Ca^{2+} chelating is not masking existing connections and to identify more precisely the Ca^{2+} dependent mechanisms that would underlie emergence of connections.

Microcircuit plasticity in the valproic acid rat model of autism. Autism is a wide-spectrum disorder striking as much as 1 person in 137 (see Fombonne 2006). Symptoms of autism are very diverse and classification into sub-classes is still controversial. To date, 5 subtypes of autism have been defined (see AmericanPsychiatricAssociation 1994). For a person to be classified as autistic, a number of impairments must be observed in social

interaction, communication and some characteristic behavioural patterns.

The observation that autism affects mainly high-level functions (social interaction impairments, hypersensitivity) suggests that neocortical abnormalities underlie some of the symptoms observed in autism. As the cortical column is the building unit of the neocortex, some of the autistic symptoms might originate from abnormal microcircuit function. Research at the microcircuit level is very difficult to be performed on humans and as for many other diseases, an animal model must be used. VPA injected in pregnant women at the time of neural tube closure greatly enhances the probability for the child to be autistic (E20-24) (Christianson *et al.* 1994; Koch *et al.* 1996; Williams and Hersh 1997; Moore *et al.* 2000; Williams *et al.* 2001; Mawer *et al.* 2002; Rasalam *et al.* 2005 and see Ardinger *et al.* 1988; Genton *et al.* 2006; Ornoy 2006). Injection of VPA to pregnant rats at the corresponding time of gestation (E11.5) induces behavioural impairments in the offspring (Chapman and Cutler 1989; Schneider and Przewlocki 2005; Wagner *et al.* 2006) and microcircuit alteration in somato-sensory, prefrontal cortices and well as in amygdala (Markram *et al.* 2007; Rinaldi *et al.* 2007a; Rinaldi *et al.* 2007b). One of the main characteristics of VPA treated rats is an increased connectivity (hyper-connectivity) of neocortical PCs (Rinaldi *et al.* 2007b). We wanted to determine whether a deficiency in the microcircuit plasticity underlies the observed microcircuit alterations and may therefore be the cause of some autism symptoms.

Previous work on the VPA rat model of autism showed that closely neighbouring (50µm apart) PCs in neocortical layer V were hyper-connected, while more distal neighbours were not hyper-connected, and for larger distances even hypo-connected (Rinaldi *et al.* 2007b). Our results show only a tendency in the line of the previous results. This absence of significance is however very likely due to a too small number of neuron pairs investigated.

Another difference observed between normal and VPA treated rats PCs connections was a higher degree of long term potentiation in treated animals (Rinaldi *et al.* 2007a). Here our results show a significant difference in the variation of synaptic efficacy with a greater increase in A for the treated animals. Although the experiments reported in (Rinaldi *et al.* 2007a) show an increase in the utilization parameter, the LTP is also significant. It might be that the two phenomenon show two faces of synaptic potentiation that are both strengthened in VPA treated animals.

The specificity of our study is in the emergence index variations from control to VPA treated rats. As in the case of connection rate, the small number of pairs investigated might be the cause of the absence of significance. There is however a clear tendency for the hyper-connected part of the circuit (with cell somata within 50 µm) to have a reduced emergence index. This result could be explained as a compensatory effect of the hyper-connectivity in the neighbouring PCs, aiming to get back to a viable equilibrium.

The emergence of new connections triggered by mGluR5 activation and AP discharge might be at the origin of the VPA treated rats local hyper-connectivity. Additionally, the lack of connection disappearance further supports microcircuit plasticity impairments in these animals. These malfunctions could affect the ability to learn adequately and therefore might be at the origin of some autism symptoms.

Future directions. The results presented in this chapter show a novel form of plasticity in the neocortical microcircuit, resulting in the emergence of new connections and the removal of weak connections. Additionally the glutamate receptors and ionic channels required for this phenomenon to occur have been identified. This is only a very first step in the understanding of the mechanism underlying functional rewiring of the neocortical columns. Further work would be required to determine the pre- or post-synaptic location of the various factors contributing to this mechanism. Metabotropic glutamate receptors have been shown to be located both pre-synaptically and post-synaptically depending on the cell type and the brain

area (see Cartmell and Schoepp 2000). For the cortical PCs, mGluR5s are likely to be pre-synaptically located (Tebano *et al.* 2005) although a post-synaptic localization was also reported (see Cartmell and Schoepp 2000). The activation of mGluR5 is known to trigger the IP3 pathway (see Nakanishi *et al.* 1998) and is then linked to a rise in the intracellular Ca^{2+} concentration (Rae and Irving 2004). As calcium underlies various molecular mechanisms, mGluR5 activation is likely to participate in the setting of the synaptic machinery via a Ca^{2+} triggered mechanism. The results presented here suggest an action of JNK on the post-synaptic side with gene expression activation and a pre-synaptic action of Ca^{2+}. The pathway linking the synapse creation and mGluR5 activation is yet to be investigated.

On another hand, AP activity also induces an increase in the intracellular Ca^{2+} as well as dendritic release of vesicles (see Zilberter *et al.* 2005). The investigation of axo-dendritic activity in close apposition regions for functionally unconnected neurons would shed more light on the physiological mechanism for creation of new synapses at these contacts.

The twelve hours period has shown to be sufficient for glutamate to induce the formation of 16% new connections. A detailed investigation of the time course of this formation of connections would be informative regarding the functional significance of this phenomenon in living brain. This could then be further related to the various memory types described (working memory, long term memory, etc). The time points presented in this chapter and the differential dependence on spiking activity for spontaneous and evoked emergences suggest that on the one side the synaptic strength variation varies differentially from the emergence of new synapses and on the other side that the emergence of connections are dependent on various mechanisms depending on the stage of maturation of the synapse. These questions could be addressed in the future by detailed experiments on the close axo-dendritic apposition with the help of fluorescence imaging and local stimulations.

3.5 The publication

Spontaneous and evoked synaptic rewiring in the neonatal neocortex

Jean-Vincent Le Bé and Henry Markram*

Brain Mind Institute, Ecole Polytechnique Fédérale de Lausanne, CH-1015 Lausanne, Switzerland

Communicated by Michael M. Merzenich, University of California, San Francisco, CA, July 3, 2006 (received for review March 21, 2006)

The local microcircuitry of the neocortex is structurally a tabula rasa, with the axon of each pyramidal neuron having numerous submicrometer appositions with the dendrites of all neighboring pyramidal neurons, but is functionally highly selective, with synapses formed onto only a small proportion of these targets. This design leaves a vast potential for the microcircuit to rewire without extensive axonal or dendritic growth. To examine whether rewiring does take place, we used multineuron patch-clamp recordings on 12- to 14-day-old rat neocortical slices and studied long-term changes in synaptic connectivity within clusters of neurons. We found pyramidal neurons spontaneously connecting and disconnecting from each other and that exciting the slice with glutamate greatly increases the number of new connections established. Evoked emergence of new synaptic connections requires action potential activity and activation of metabotropic glutamate receptor 5, but not NMDA receptor or group II or group III metabotropic glutamate receptor activation. We also found that it is the weaker connections that are selectively eliminated. These results provide direct evidence for spontaneous and evoked rewiring of the neocortical microcircuitry involving entire functional multisynaptic connections. We speculate that this form of microcircuit plasticity enables an evolution of the microcircuit connectivity by natural selection as a function of experience.

plasticity | pyramidal neurons | synaptic connections

Synapses are formed and pruned during development (1–3), but how is a neuron selected for or against becoming or remaining an output target of a presynaptic cell? Recent studies made an important step toward understanding target selection by showing that the axon of a pyramidal neuron approaches, at a submicrometer distance, the dendrites of every neighboring pyramidal neuron multiple times without any structural bias toward those with which synaptic connections are formed (4–6). This finding raised the possibility that the microcircuit could be in an all-to-all "readiness" to switch rapidly on and off connections between neurons in a form of rewiring plasticity without the axon or the dendrite growing toward a new target. Rapid proliferation of spines in slices (within the first 2 h after slicing) has been shown in young and adult rat hippocampus (7), but whether new functional connections are being formed and eliminated is not known. To determine whether the microcircuit can rewire we used the multineuron patch-clamp approach to study spontaneous and evoked changes in connectivity within small clusters of six to seven layer-5 thick tufted pyramidal neurons (TPCs) (see *Materials and Methods*). We began the experiments after a 2-h stabilization period after slicing.

Synaptic connections are easily revealed by presynaptic trains of action potentials, and averaged postsynaptic traces can detect very small events (≈10 μV) below the smallest synaptic responses typically recorded between neurons (≈50 μV) (8). Synaptic connections between TPCs are stable for many hours of recording, and no emergences or disappearances of connections have ever been observed in experiments lasting >8 h (H.M., unpublished data). This stability may be because plasticity is restricted to the scaling of existing synapses, because rewiring does not occur on such time scales, or because rewiring was prevented by the washout of the internal milieu by the patch pipette. We therefore prepared neocortical slices of the rat somatosensory cortex in the standard manner, but we patched and then repatched neurons after 12 h (see *Materials and Methods*). IR differential interference contrast microscopy allows selection of specific neurons (Fig. 1*A*) and repeated patching of the same neurons (Fig. 1*A Right*). We could further verify that the same neurons were repatched by staining the recorded cells (Fig. 1*B*; see *Materials and Methods*).

Brain slices display very little spontaneous activity under the standard conditions we use, and the slice was therefore activated with bath and local application of Na-glutamate. Periodic puffing of Na-glutamate from a patch pipette above the pyramidal cluster (50 mM, 2 s every 1 min, "Evoked 1" condition) caused similar discharges in all cells (Fig. 1*C*), which was reasonably stable for hours (Fig. 1*D*). Bath application of glutamate (100 μM, "Evoked 2" condition) brought cells rhythmically to spiking threshold (Fig. 1*E*).

Results

Spontaneous and Evoked Changes. A cluster of six to seven TPCs was typically recorded. The first recording in the experiment is referred to as "before" and the second recording, after 12 h in various conditions or 4 h with glutamate puffing, is referred to as "after." Two indices were used for quantifying the connectivity changes. The emergence index (*Ei*) is the proportion of new functionally connected pairs "after" among unconnected pairs "before," and the disappearance index (*Di*) is the proportion of existing connected pairs "before" that were not connected anymore "after." In control experiments we found that connections spontaneously emerged (*Ei* = 4 ± 1%, mean ± SD) (Fig. 2 *A* and *B*) and disappeared (*Di* = 13 ± 7%, mean ± SD) (Fig. 2 *A* and *C*), indicating that functional synaptic connections are formed and removed on the time scale of hours. Bath and periodic puff application of glutamate caused nearly a doubling of the total number of connected pairs and a >4-fold increase in the *Ei* (16 ± 3% and 14 ± 3% for Evoked 1 and Evoked 2, respectively) (Fig. 2*B*; see *Materials and Methods*), indicating that glutamate-mediated excitation strongly drives the formation of new connections. The application of glutamate did not increase the disappearance of connections. On the contrary, the trend was rather to prevent disappearances (Evoked 1: *Di* = 6 ± 4%), although this was not statistically significant (Fig. 2*C*). The patching procedure may also contribute some uncertainty to the significance of physiological disappearances of connections (but see *Selecting Against Weak Connections*).

Conflict of interest statement: No conflicts declared.

Abbreviations: *A*, absolute synaptic efficacy (strength); EPSP, excitatory postsynaptic potential; *Pr*, probability of release; TPC, layer-5 thick tufted pyramidal neurons; ACSF, artificial cerebrospinal fluid; TTX, tetrodotoxin; MPEP, 2-methyl-6-(phenylethynyl)pyridine; EGLU, (2*S*)-α-ethylglutamic acid; CPPG, (*RS*)-α-cyclopropyl-4-phosphonophenylglycine; *Ei*, emergence index; *Di*, disappearance index; CNQX, 6-cyano-7-nitroquinoxaline-2,3-dione; AP5, D-2-amino-5-phosphonopentanoic acid; AP3, DL-2-amino-3-phosphopropinionic acid; *CV*, coefficient of variation; mGluR, metabotropic glutamate receptor.

*To whom correspondence should be addressed. E-mail: henry.markram@epfl.ch.

www.pnas.org/cgi/doi/10.1073/pnas.0604691103

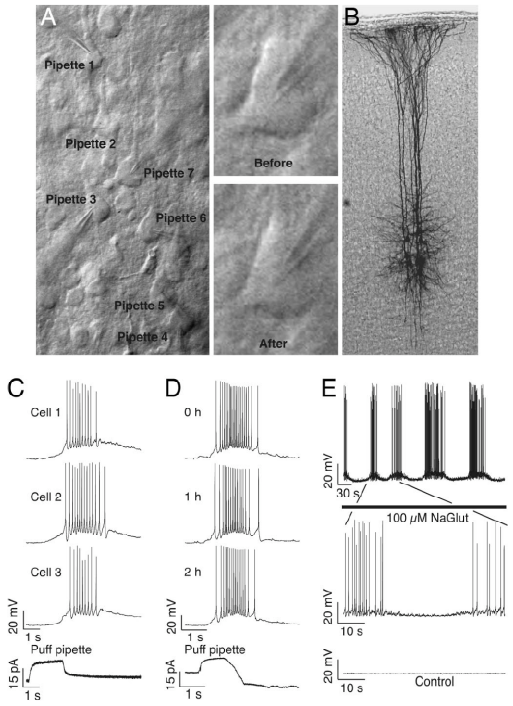

Fig. 1. Visualization and stimulation of TPC clusters. (*A*) IR differential interference contrast image of a seven-cell cluster patched. (*Right*) A neuron at first patch ("Before") and repatched after 12 h ("After"). (*B*) Biocytin-stained cluster shows that only seven cells were patched despite the two separated sessions. (*C*) Whole-cell recordings of three of the six cells recorded while glutamate was puffed from the seventh patch pipette located ≈100 μm above the cluster (bottom trace). (*D*) Stability of the response to glutamate puffing over time. (*E*) Response of a cell to bath application of glutamate. "Control" shows the same time and voltage scale trace of a cell in normal ACSF.

Selecting Few Targets with Many Synapses. We also examined how neurons select a very small fraction of neurons in a microcircuit and then place multiple synapses in a distributed manner across a relatively large volume of cortical space on the chosen target neurons (8–16). For these TPCs connectivity is known to be ≈10–15% (17), and multiple synapses are involved in each connection (8, 18). We therefore examined the strength [*A* − first excitatory postsynaptic potential (EPSP) amplitude/probability of release (*Pr*)] and *Pr* (see *Materials and Methods*) of the emerging and disappearing connections recorded at the cell soma to gain some insight into the types of synaptic connections that were being formed and removed. We found that the average strength (*A*) of new connections was smaller than those of existing connections (Fig. 2*D*) [1.5 ± 0.1 mV vs. 2.4 ± 0.1 mV, mean ± SEM ($P < 0.001$), $n = 122$ multisynaptic emerged connections overall and 322 existing connections "before"] as was the distribution of synaptic strengths with a higher number of weaker connections ($P < 0.001$, Kolmogorov–Smirnov test). The average *Pr* was also lower (Fig. 2*D*) [0.36 ± 0.01 vs. 0.45 ± 0.01, mean ± SEM ($P < 0.001$), $n = 122$ multisynaptic emerged connections overall and 322 existing connections "before"]. The coefficient of variation (*CV*) of responses was significantly but not proportionately higher [0.70 ± 0.07 vs. 0.43 ± 0.06, mean ± SEM ($P < 0.01$), $n = 14$ and 16, Evoked 1 emerged vs. existing "before"], requiring an assumption of a lower number of synapses per connection (*N*) to explain the magnitude of the increase in the *CV* (0.53, predicted for the same *N*; 0.70, *CV* actual; see *Materials and Methods*). Although binomial assumptions may not perfectly hold at these connections (8, 19, 20), a prediction of the number of functional release sites using binomial analysis does support new connections with fewer synapses at the time of the recording (binomial $N \approx 5$ for new connections, and $N \approx 8$ for existing ones; see *Materials and Methods*). Multisynapse connections are therefore being formed within hours, and synapses seem to have been progressively added over this time. Additions probably continue to achieve the same average number of synapses as for existing connections. The new connections also seem to begin with lower probabilities of release, which presumably increase to reach the same average as existing synapses.

Selecting Against Weak Connections. We also found that the synaptic connections that disappeared were preferentially the weaker ones [1.1 ± 0.3 mV vs. 2.4 ± 0.1 mV, $n = 24$ and 322 ($P < 0.001$)]. It could be that the patching procedure contributed to this finding, but it is more likely that such damage would affect connections randomly. These weak connections were also different from the newly emerging weak connections in that their probabilities of release were similar to those of remaining connections (0.44 ± 0.03 vs. 0.45 ± 0.01, $n = 24$ multisynaptic connections disappeared and 322 existing connections "before" which persisted) (Fig. 2*E*), whereas the *Pr* of new connections was lower. Thus, new weak connections do not seem to be subject to the same elimination process as existing weak connections. This could be a "grace" period for the new connections to be tested in the circuit, and only around the time that the average *Pr* of new connections reaches the average in the population do connections become subject to elimination. Such a process of delayed selection against the weakest connections may explain how the microcircuit ends up with a small and selected fraction of neurons wired with multisynapse connections.

The time course of emergence of new connections, "maturation" before elimination, and the elimination process will need to be exhaustively studied in the future, but we did some preliminary experiments after 4 h and found that the evoked emergences with 4 h already tended to exceed the spontaneous emergences after 12 h (6 ± 2%, $n = 140$ pairs in six clusters). Although this increase was not significant, a linear fit through 0, 4, and 12 h was 99.6% accurate, yielding an estimated rate of 1.2% newly connected pairs per hour after excitation (data not shown). One multisynapse connection had disappeared over all of the experiments performed in 4 h (>29 connected pairs "before" overall six clusters).

Plasticity of Connection Rate. The connection rate is characteristic for different microcircuits (17), and, although there are many forms of synaptic plasticity, it is not known whether the connection rate is plastic. We found that, even though connections are spontaneously added and removed, the connection hit rate remained the same over the 12-h period (13.2 ± 0.8%, mean ± SD, $n = 1{,}655$ pairs probed "before" vs. 14 ± 2% and 206 pairs probed "after" in spontaneous condition). Glutamate application however, caused a massive increase in the overall connection hit rate [29 ± 2% vs. 13.2 ± 0.8%, $n = 354$ pairs probed "after" in both evoked conditions pooled and 1,655 pairs probed "before" ($P < 0.001$)]. Blocking activity with tetrodotoxin (TTX) prevented the evoked change in the "after" connection hit rate (0.5 μM TTX, 13 ± 2%, $n = 228$ pairs probed "after").

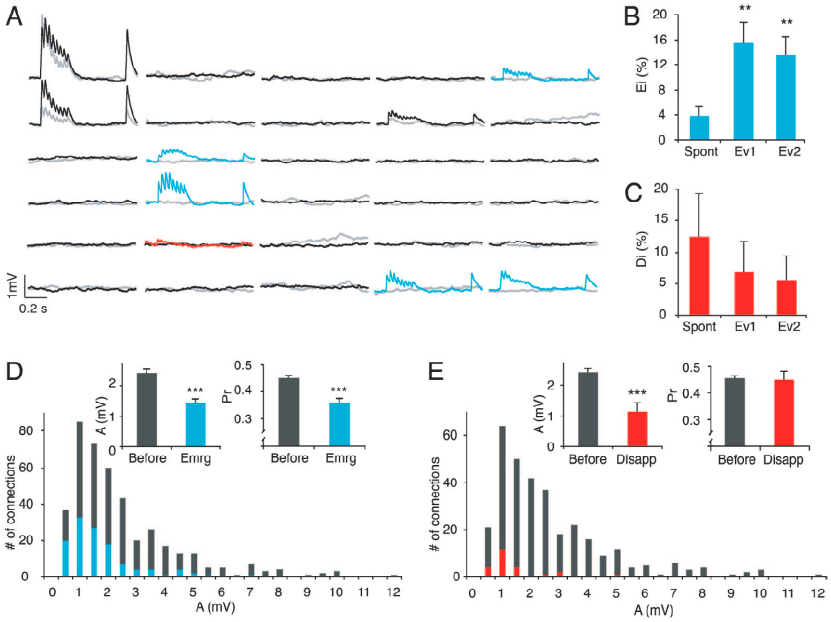

Fig. 2. Spontaneous and evoked emergences and disappearances of connections within 12 h. (*A*) A six cell cluster showing the EPSPs elicited in response to a train of eight action potentials at 30 Hz and a recovery action potential 500 ms later (average of 30 trials). Each line and column represents a cell. Gray and red traces were recorded at first patch ("before"), and black and blue traces were recorded 12 h later ("after") under Evoked 1 condition. The red trace indicates a disappearance, and blue traces indicate emergences. (*B*) *EI* (no. of pairs newly connected "after")/(no. of unconnected pairs "before") for spontaneous (n = 182), Evoked 1 (Ev1) (n = 135), and Evoked 2 (Ev2) (n = 154) conditions (**, $P < 0.001$). (*C*) *Di* (no. of pairs connected "before" that were not connected anymore "after")/(no. of connected pairs "before") for spontaneous (n = 24), Ev1 (n = 29), and Ev2 (n = 36) conditions. (*D*) Cumulative distributions of absolute synaptic efficacy (*A*) for recordings at first patch (gray) and emergences (blue) (n = 322 and 122, respectively; ***, $P < 0.001$). (*Insets*) Bar graphs of *A* and *Pr* for the same data. (*E*) Same as in *D* but for disappearances (red) (n = 322 and 24, respectively; ***, $P < 0.001$).

Obeying Nuclear Recurrence. Connections are also normally formed in a biased manner in that if a neuron receives a connection then the targeted neuron will reciprocate with an even higher connection hit rate (9). This biased connectivity is referred to as "nuclear recurrence," which can be defined as a higher probability of reciprocal connections than the unidirectional connection rate for the circuit. We confirm that, for these neurons, this conditional hit rate is three to four times higher than the unidirectional connection hit rate (37 ± 3%, n = 223 connected pairs "before"). Even though the mechanism for this reciprocity preference is not known, we did examine whether glutamate-evoked emergence of connections adheres to this biased connectivity rule. Although glutamate application nearly doubled the number of connections, the conditional hit rate for reciprocating connections remained remarkably similar (37 ± 5%, n = 104 connected pairs "after"), suggesting that the addition of new connections obeys the nuclear recurrence rule by adding proportionally more reciprocal connections than unidirectional ones.

Pharmacology of Microcircuit Plasticity. We next began to study the mechanisms that enable microcircuit plasticity. Blocking action potential activity with TTX caused a significant reduction in evoked emergences [Ei = 6 ± 2%, n = 209 unconnected pairs in six clusters, compared with Evoked 1, Ei = 16 ± 3%, n = 135 unconnected pairs in five clusters ($P < 0.05$)] (Fig. 3*B*) toward spontaneous levels (Ei = 4 ± 1%, n = 182 unconnected pairs in six clusters). Glutamate-evoked emergences therefore depend on action potential activity, but a component still does not. Such activity-independent emergences may account for the spontaneous ones in the quiescent slice and may be due to a tendency for synapse formation in development (21) and in slices (7). Although a strong trend was observed, antagonizing the AMPA receptors [20 μM 6-cyano-7-nitroquinoxaline-2,3-dione (CNQX), Ei = 9 ± 2%, n = 166 pairs in six clusters] or blocking the NMDA receptors [20 μM D-2-amino-5-phosphonopentanoic acid (AP5), Ei = 13 ± 3%, n = 159 pairs in six clusters] did not significantly block the evoked emergences (Fig. 3*B*). Blocking the group 3 [20 μM (*RS*)-α-cyclopropyl-4-phosphonophenylglycine (CPPG), Ei = 12 ± 3%, n = 126 pairs in four clusters] and group 2 [100 μM (2*S*)-α-ethylglutamic acid (EGLU), Ei = 14 ± 4%, n = 88 pairs in three clusters] metabotropic receptors also did not block evoked emergences of new connections (Fig. 3*B*). However, antagonizing the group I metabotropic glutamate receptors (mGluRs) [100 μM DL-2-amino-3-phosphopropinionic acid (AP3), Ei = 10 ± 5%, n = 42 pairs in three clusters], showed a strong tendency to block the emergences, and the specific mGluR5 antagonist [4 μM 2-methyl-6-(phenylethynyl)pyridine (MPEP), Ei = 7 ± 2%, n = 162 pairs in six clusters] caused a significant reduction in evoked emergences toward spontaneous levels [compared with Evoked 1, Ei = 16 ± 3% ($P < 0.05$)] (Fig. 3*B*). Detailed measures for the Evoked 1, TTX, and MPEP conditions are given in Table 1. These results indicate that glutamate excitation can drive the formation of new connections in a spiking and mGluR5-dependent manner.

We present the pharmacological experiments also for disappearances, but statistical analysis is not valid because the data set would need to be ≈10 times larger (based on statistical extrap-

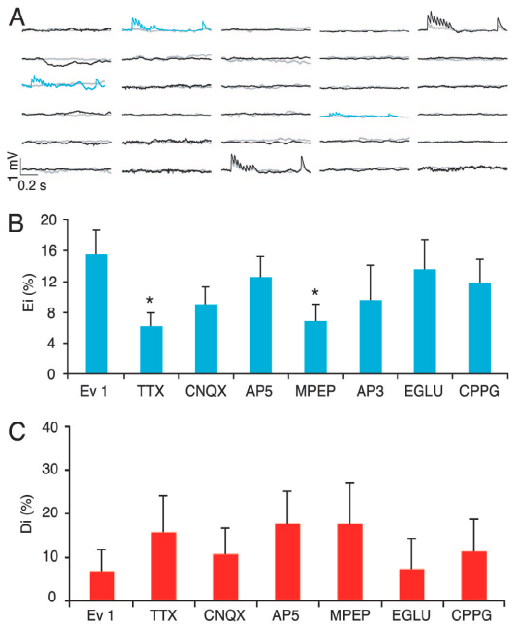

Fig. 3. Emergences depend on mGluR5 and cell action potential activity. (*A*) Six cells cluster EPSPs during continuous MPEP perfusion. (*B*) Bar graphs of the antagonist effects on *EI* (*, $P < 0.05$). TTX, $n = 209$; CNQX, $n = 166$; AP5, $n = 159$; MPEP, $n = 162$; AP3, $n = 42$; EGLU, $n = 88$; CPPG, $n = 126$. (*C*) Bar graph of the antagonist effects on *DI*. TTX, $n = 19$; CNQX, $n = 28$; AP5, $n = 28$; MPEP, $n = 14$; AP3, $n = 10$; EGLU, $n = 14$; CPPG, $n = 18$.

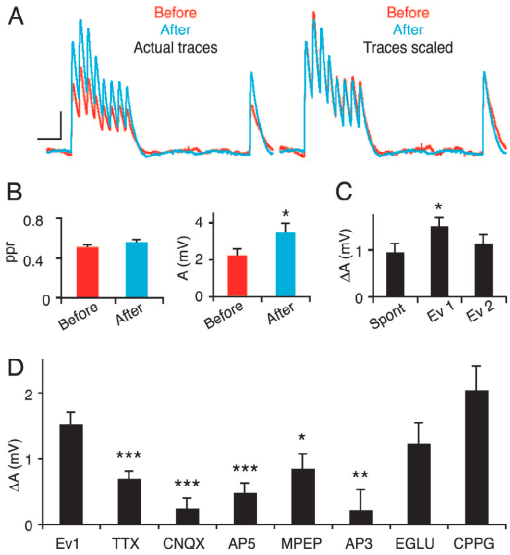

Fig. 4. Spontaneous and induced changes in existing synapses. (*A*) Same EPSP response as in Fig. 2*A*. (*Left*) Comparison of the raw traces at first recording (red) and 12 h later (blue). (*Right*) The same traces but with the first EPSP of the train scaled. The change is only in strength and not in dynamics. (Calibration: 10 ms and 0.5 mV.) (*B*) Bar graphs of the paired-pulse ratio (ppr) (*Left*) and *A* (*Right*) showing that the dynamics is constant and the strength varies over 12 h ($n = 34$ and 40 respectively; *, $P < 0.05$). (*C*) Variation of *A* in 12 h. Spontaneous, $n = 41$; Evoked 1 (Ev1), $n = 63$; Evoked 2 (Ev2), $n = 47$. (*D*) Antagonist effects on *A* variation when glutamate is puffed. TTX, $n = 19$; CNQX, $n = 39$; AP5, $n = 44$; MPEP, $n = 19$; AP3, $n = 14$; EGLU, $n = 21$; CPPG, $n = 37$.

olation from our data). TTX tends to bring disappearances back to spontaneous levels, but the effect was not statistically significant (Fig. 3*C*). Blocking group I mGluRs, but not mGluR5, tends to accelerate evoked disappearances, but the effect was also not statistically significant (Fig. 3*C*). We were unable to track the activity in each neuron for the entire period, so we do not yet know the precise activity patterns driving the switching on and off of connections.

Slow LTP at Existing Connections. We were surprised that NMDA receptors were not required for the rewiring of the circuit and we therefore also examined the changes that occurred at existing connections over this period (between the "before" recording and "after"). Whereas individual connections displayed slower, faster, or no changes in the rates of synaptic depression (*D*), the average changes in dynamics were unaffected, as could be seen by normalizing the responses to the first EPSP (Fig. 4*A*). There was also no average change in the paired-pulse ratio [0.51 ± 0.02 vs. 0.56 ± 0.03, mean $\pm$ SEM ($P = 0.14$), $n = 34$ connections in control experiment] (Fig. 4*B Left*). The change that did occur spontaneously over the 12-h period was that synapses became $\approx$55% stronger [*A* (the absolute efficacy calculated with the Tsodyks–Markram model; see *Materials and Methods*) = 2.3 ± 0.3 mV vs. 3.5 ± 0.5 mV, $n = 40$ connections in control experiment] (Fig. 4*B Right*), as indicated by the uniform change in all responses during the train (Fig. 4 *A* and *B*). This potentiation could be due to the up-scaling of synaptic strength by addition of postsynaptic receptors, when synaptic input is reduced (22). We additionally found that the evoked protocol produced a large and significant additional increase compared with spontaneous changes [$\Delta A = 1 \pm 0.2$ mV (Spontaneous) and 1.5 ± 0.2 mV (Evoked 1), $n = 41$ and 63 connections, respectively, which persisted from "before" to "after"] (Fig. 4*C*), and

Table 1. Detailed measures for the emergences in Evoked 1, TTX, and MPEP conditions

Condition	No. of clusters	No. of patched cells per cluster	No. of connected pairs per cluster		No. of new connections per cluster
			"Before"	"After"	
Evoked 1	5	5, 6, 7, 7, 6	4, 3, 8, 2, 12	5, 7, 13, 9, 14	1, 4, 6, 8, 2
TTX	6	6, 7, 6, 7, 7, 7	1, 2, 5, 6, 2, 3	4, 3, 6, 7, 4, 5	3, 1, 2, 2, 3, 2
MPEP	6	4, 6, 7, 6, 7, 5	2, 4, 3, 0, 3, 2	2, 5, 7, 3, 3, 2	1, 1, 4, 3, 1, 1

The lists give the values for each cluster.

that blocking action potential discharging with TTX and AMPA receptor antagonists prevented this induced change ($\Delta A = 0.7 \pm 0.1$ and 0.2 ± 0.2 mV, $n = 19$ and 39, respectively) (Fig. 4*D*). This slow form of long-term potentiation (sLTP) also depended on NMDA receptor activation ($\Delta A = 0.5 \pm 0.1$ mV, $n = 44$) (Fig. 4*D*) and on the activation of mGluR5 receptors ($\Delta A = 0.8 \pm 0.2$, $n = 19$) (Fig. 4*D*), but not on group II mGluRs ($\Delta A = 1.2 \pm 0.3$, $n = 21$). There was a tendency for greater sLTP when group III mGluRs were blocked ($\Delta A = 2.0 \pm 0.4$, $n = 37$) (Fig. 4*D*). The involvement of spiking activity as well as mGluR5 receptor activation in both the formation and strengthening of connections could imply some overlap in the mechanisms of these two phenomena.

Discussion

We provide direct evidence for a novel form of rewiring plasticity where entire synaptic connections, made up of multiple contacts, are switched on and off over a time scale of hours. Although a component of these changes may be due to ongoing developmental changes and deafferentation caused by the slicing of the tissue, by far the greatest effect is the induced formation of new connections by glutamate excitation in a manner that depends on spiking and mGluR5 activation. We also demonstrate for the first time that the connection rate between neurons is plastic, revealing a novel mechanism to dynamically alter network behavior. We additionally found evidence to suggest that weak connections are preferentially removed, which could explain the presence of strong multisynaptic connections between a small fraction of neurons in the microcircuit. This rewiring of the neocortical microcircuit could occur by conversion of the existing axodendritic close appositions into synapses and vice versa.

The extracellular glutamate concentration *in vivo* is ≈10 μM, whereas it can reach 1–10 mM in the cells (23–25) and 1.1 mM in the synaptic cleft (26). The artificial cerebrospinal fluid (ACSF) used in our experiments does not contain any glutamate. Although this is clearly an artificial excitation of the microcircuit, the amount of glutamate, added either by continuous perfusion or by puffing from a distance above the slice, was calibrated to produce moderate discharge responses by the neurons (as indicated in Fig. 1) and is therefore likely to be within physiological ranges. The manner in which activity, mGluRs, and the precise signaling cascade work to set up the signals to connect, not to connect, to remain connected, or to disconnect now requires further study. These changes may be particularly marked at this age of the neocortex because this is the period during which the first decisions are being made by neurons to choose their synaptic partners. We did attempt to carry out these experiments in adult slices, but these slices do not survive such long-lasting experiments in our experimental conditions. However, it is worth pointing out that, at this age, the axonal and dendritic arborizations have already elaborated to such an extent that all axons are able to be in close apposition with all dendrites multiple times (4, 5), which is most likely the essential substrate for microcircuit plasticity. In other words, a major component of microcircuit plasticity requires that the microcircuit has reached a minimal level of axonal and dendritic arborization.

This study shows that, after activity is evoked with glutamate application, the connection rate can increase >3-fold. It is unlikely that experience would continuously drive the rate up during the life of the animal. Indeed, these neurons in the adult somatosensory cortex have basically the same hit rate as in the 2-week-old rat [10–15% (15) in 3-month-old rats; T. Berger, G. Silberberg, and H.M., unpublished observations]. It is therefore more likely that the burst of new connections induced by a new stimulus is a transient process due to an imbalance between the formation of new and the removal of existing connections. Indeed, there was a trend to prevent removal of connections after the evoked activity. If the connection rate is to return to control levels after such activity, the rate of removal of connections would need to rise with a significant delay after the increase in the emergence of new connections.

We therefore speculate that a sequence of events is triggered by new experiences (a burst of many new connections in the network with more synapses added per connection over time, a window of grace for the new low-probability connections to be tested for their improved value in processing the new environment, an elimination process), which removes the weakest connections and reestablishes the connection rate characteristic for the microcircuit. Such a process could be analogous to a burst of mutations in a species caused by major environmental change followed by natural selection of the most adapted variants. We therefore speculate that microcircuit plasticity may allow neural networks to continue the evolutionary process in a Darwinian manner as a function of experience (see also ref. 27).

Materials and Methods

Electrophysiological Recordings. Young (postnatal day 12–14) Wistar rats were rapidly decapitated, and their brains were removed and sliced in an ACSF containing 125 mM NaCl, 2.5 mM KCl, 25 mM D-glucose, 25 mM $NaHCO_3$, 1.25 mM NaH_2PO_4, 2 mM $CaCl_2$, and 1 mM $MgCl_2$. The sagittal somatosensory cortex brain slices were then perfused with 35°C ACSF for the whole experiment. Somatic multiple whole-cell recordings were made, and signals were amplified by using Axoclamp-200B amplifiers (Axon Instruments, Union City, CA) and digitized by means of an ITC-18 interface (Instrutech, Great Neck, NY) to an Apple computer running Igor Pro (Wavemetrics, Portland, OR). Voltages were recorded with pipettes containing 100 mM potassium gluconate, 10 mM KCl, 4 mM ATP-Mg, 10 mM phosphocreatine, 0.3 mM GTP, 10 mM Hepes, and 5 $mg \cdot ml^{-1}$ biocytin (pH 7.3, 310 $mosmol \cdot liter^{-1}$, adjusted with sucrose). The pipettes were pulled with Flaming/Brown micropipette puller P-97 (Sutter Instruments, Novato, CA). All animal experiments were done under the authorization no. 1550 of the Service Vétérinaire de l'Etat de Vaud.

Clusters of six to seven TPCs were patched a first time ("before"), and their connectivity was recorded by using, successively, for each cell, a train of eight action potentials at 30 Hz followed by a recovery test spike 500 ms later. The stimulation was repeated 30 times, and the averaged trace was used for analysis. Recordings were obtained ≈2 h after slicing in an attempt to avoid the initial increase in synapses reported because of slicing (7). Within 20 min the pipettes were withdrawn, and the slice was left in the recording chamber with various conditions. For the spontaneous condition, we continued perfusing only ACSF. Evoked 1 was ACSF in the presence of puffs of 50 mM sodium glutamate 100 μm above the cell cluster (Fig. 1 *C* and *D*). Evoked 2 was ACSF perfused with 100 μM sodium glutamate (Sigma-Aldrich, St. Louis, MO) (Fig. 1*E*). The various antagonist conditions correspond to the slice perfused with ACSF containing the antagonist concentrations described below and glutamate puffing on the cluster.

The monitor display from the Axioskop (Zeiss, Jena, Germany) and charge-coupled device camera (Hamamatsu, Hamamatsu City, Japan) were used to capture IR differential interference contrast images, define landmarks, and find the same cell cluster 12–14 h later (Fig. 1*A*). The microscope focus on the cells was also maintained throughout the experiment. The cells were then repatched, and the same stimulation protocol was executed to monitor the connectivity in the new state ("after"). After recording, the slices were fixed and ABC-stained, and, because biocytin was used in the first and second patchings, we could double-check that the same cluster was patched for each experiment (Fig. 1*B*). In one case, when the IR differential interference contrast localization of the cluster was not convinc-

ing, two clusters were clearly seen corresponding to the "before" and "after" patching sessions. This finding shows that the biocytin is preserved in the cell even after >12 h in the recording chamber.

The electrophysiological responses were analyzed off-line (Igor), and the Tsodyks–Markram model was used on the averaged traces to determine synaptic properties. The model yields the absolute synaptic efficacy (A) that is the total amount of resources the unperturbed presynaptic neuron has over all of its synapses (expressed in millivolts measurable in the postsynaptic neuron). It then also yields the utilization of synaptic efficacy (ranged between 0 and 1), which is the fraction of the resources used by one action potential. The EPSP size is the product of A with the utilization of synaptic efficacy. Because A is the total amount of resources and the depression in TPCs is mostly presynaptically mediated (28, 29), A is equivalent to the number of release sites multiplied by the quantum size. The EPSP size is then A multiplied by the Pr. Consequently, the utilization of synaptic efficacy is equivalent to the Pr, which is then derived directly from the fitting of the model on the averaged traces.

The condition of slices at 12 h was excellent (Fig. 1*A*), with high visibility, no change in patchability (reflection of slice health), normal break-in resting potentials, normal discharge behavior, and no change in input resistances.

Histological Procedure. After the recording, the 300-μm slices were fixed for at least 24 h in a cold 0.1 M phosphate buffer (100 mM, pH 7.4) containing 2% paraformaldehyde and 1% glutaraldehyde. Thereafter, the slices were rinsed and then transferred into a phosphate-buffered 3% H_2O_2 to block endogenous peroxidases. After rinsing in the phosphate buffer, slices were incubated overnight at 4°C in an avidin–biotinylated horseradish peroxidase (ABC-Elite; Vector Laboratories; 2% A, 2% B, and 1% Triton X-100). Subsequently, sections were rinsed again in the phosphate buffer and developed with diaminobenzidine under visual control by using a bright-field microscope (Axioskop) until processes of the cells were clearly visible. Finally, the reaction was stopped by transferring the sections into the phosphate buffer. After rinsing in the phosphate buffer, slices were mounted in an aqueous mounting medium.

Pharmacology. The following pharmacological agents were used: 0.5 μM TTX, a sodium channel blocker (Alomone Labs, Jerusalem, Israel); 20 μM CNQX, an α-amino-3-hydroxy-5-methyl-4-isoxazolepropionic acid receptor antagonist (Sigma-Aldrich); 20 μM AP5, an *N*-methyl-D-aspartic acid receptor antagonist (Tocris, Ellisville, MO); 4 μM MPEP, an mGluR5 antagonist (Tocris); 100 μM AP3, a group I mGluR antagonist (Tocris); 100 μM EGLU, a group II mGluR antagonist (Tocris); and 20 μM CPPG, a group III mGluR antagonist (Tocris).

Statistical Tests. Student *t* tests were used on the Gaussian-like distributions such as the distribution of the Pr, the paired-pulse ratio distributions, the changes in A, and the natural logarithm of A"before" vs. A"after." The comparison of A"before" and A"after" was made with a Kolmogorov–Smirnov test. The proportion of emergences and disappearances and the proportion of reciprocal emergences were tested by using the χ^2 test. Because the connection hit rates and the proportions of emergences and disappearances were estimated as being the proportion of connections observed in the respective conditions (as opposed to the number of connections not observed, i.e., not present, not emerged, or not disappeared), the standard deviations were calculated on the base of a binomial distribution: $SD = \sqrt{(p(1-p)/n)}$.

Indices and Formulations. The Ei was calculated as follows: Ei = (no. of connections that emerged)/(no. of remaining possible connections) where (no. of remaining possible connections) = (no. of pairs) − (no. of connections at first recording).

The Di was calculated as follows: Di = (no. of connections that disappeared)/(no. of connections at first recording).

The CV of a connection was calculated by measuring the amplitude of the first EPSP of the 30-Hz train for each of the 30 trials. The standard deviation of these 30 amplitudes was calculated. CV is the standard deviation divided by the mean of the 30 amplitudes.

For a given number of synapses N in a connection, the expected CV can be calculated by using the binomial assumption $N = (1 - Pr)/(Pr\,CV^2)$ and knowing the Pr. Knowing the Pr for connection 1 (Pr_1) and both the Pr and the CV for connection 2 (Pr_2 and CV_2), the CV for the connection 1 can be derived (CV_1) assuming the same number of synapses for both connections: $CV_1 = CV_2\ \sqrt{[(1 - Pr_1)Pr_2]/[(1 - Pr_2)Pr_1]}$. The comparison between the predicted value of CV_1 and the actual value measured gives an indication of the relative number of synapses in both connections. If the actual CV is greater than the predicted, it can be concluded that connection 1 has fewer synapses than connection 2.

The connection hit rate is the number of connections divided by the number of neuron pairs considered, and the conditional reciprocal connection hit rate is the number of neuron pairs reciprocally connected divided by the total number of connected pairs.

1. Wolff, J. R. & Missler, M. (1993) *APMIS Suppl.* **40,** 9–23.
2. Montgomery, J. M. & Madison, D. V. (2004) *Trends Neurosci.* **27,** 744–750.
3. Hensch, T. K. (2005) *Nat. Rev. Neurosci.* **6,** 877–888.
4. Kalisman, N., Silberberg, G. & Markram, H. (2005) *Proc. Natl. Acad. Sci. USA* **102,** 880–885.
5. Chklovskii, D. B., Mel, B. W. & Svoboda, K. (2004) *Nature* **431,** 782–788.
6. Morishima, M. & Kawaguchi, Y. (2006) *J. Neurosci.* **26,** 4394–4405.
7. Kirov, S. A., Sorra, K. E. & Harris, K. M. (1999) *J. Neurosci.* **19,** 2876–2886.
8. Markram, H., Lubke, J., Frotscher, M., Roth, A. & Sakmann, B. (1997) *J. Physiol. (London)* **500,** 409–440.
9. Markram, H. (1997) *Cereb. Cortex* **7,** 523–533.
10. Bienenstock, E. (1996) *J. Physiol. (Paris)* **90,** 251–256.
11. Thomson, A. M. & Bannister, A. P. (2003) *Cereb. Cortex* **13,** 5–14.
12. Sjostrom, P. J., Turrigiano, G. G. & Nelson, S. B. (2001) *Neuron* **32,** 1149–1164.
13. Markram, H. & Tsodyks, M. (1996) *Nature* **382,** 807–810.
14. Markram, H., Lubke, J., Frotscher, M. & Sakmann, B. (1997) *Science* **275,** 213–215.
15. Thomson, A. M., West, D. C., Wang, Y. & Bannister, A. P. (2002) *Cereb. Cortex* **12,** 936–953.
16. Holmgren, C., Harkany, T., Svennenfors, B. & Zilberter, Y. (2003) *J. Physiol. (London)* **551,** 139–153.
17. Watts, J. & Thomson, A. M. (2005) *J. Physiol. (London)* **562,** 89–97.
18. Feldmeyer, D. & Sakmann, B. (2000) *J. Physiol. (London)* **525,** 31–39.
19. Redman, S. (1990) *Physiol. Rev.* **70,** 165–198.
20. Thomson, A. M. (1998) *C. R. Acad. Sci. III* **321,** 131–133.
21. Lendvai, B., Stern, E. A., Chen, B. & Svoboda, K. (2000) *Nature* **404,** 876–881.
22. Turrigiano, G. G. & Nelson, S. B. (2000) *Curr. Opin. Neurobiol.* **10,** 358–364.
23. Danbolt, N. C. (2001) *Prog. Neurobiol.* **65,** 1–105.
24. Erecinska, M. & Silver, I. A. (1990) *Prog. Neurobiol.* **35,** 245–296.
25. Chen, Y. & Swanson, R. A. (2003) *J. Cereb. Blood Flow Metab.* **23,** 137–149.
26. Clements, J. D., Lester, R. A., Tong, G., Jahr, C. E. & Westbrook, G. L. (1992) *Science* **258,** 1498–1501.
27. Edelman, G. M. (1993) *Neuron* **10,** 115–125.
28. Tsodyks, M., Pawelzik, K. & Markram, H. (1998) *Neural Comput.* **10,** 821–835.
29. Thomson, A. M., Deuchars, J. & West, D. C. (1993) *J. Neurophysiol.* **70,** 2354–2369.

4 Indirect inhibition between pyramidal cells

4.1 Introduction

PCs represent 80% of the neurons that compose the neocortex. The question of their classification according to various targets and the differences in PCs subpopulations were addressed in chapter 2. This excitatory network is regulated to avoid over-excitation partly by the action of inhibitory interneurons. GABAergic interneurons have been classified according to various criteria such as firing pattern, molecular content, morphology or the post-synaptic domain they target (see section 1.1). The interesting feature for this part is the post-synaptic domain targeted.

The inhibitory synapses can be located at the soma, the axon initial segment, the proximal dendrite and the distal dendrite. The Martinotti cells (MCs) are located in layers II-VI of the cortical column. They have irregular somata but mainly ovoid with a vertical orientation. Their dendritic arborisation is either bitufted or multipolar and is one of the most elaborate amongst interneurons. Their axonal arbour is characterized by its vertical ascending trunk and dense collateral spanning innervating layer I and layer IV (when the soma is located in layers V or VI). MCs are particularly interesting with their soma located in the same layer as the TTCs and their axons that cross all layers and can distally innervate the TTCs apical and tuft dendrites.

Excitation-inhibition balance is dynamically kept during cortical activity (Shu *et al.* 2003) but little is known about specific pathways underlying this equilibrium. Some of the synaptic connections between TTCs and GABAergic interneurons are facilitating (Markram *et al.* 1998; Reyes *et al.* 1998). In particular, connections between TTCs and layer V MCs are often facilitating enough so that a train of action potentials in a TTC is sufficient to elicit discharge in the post-synaptic MC (Markram *et al.* 1998; Silberberg and Markram 2007, see Figure 3 on page 15). It is then possible to elicit an inhibitory post-synaptic potential (IPSP) in a TTC by stimulation of a neighbouring TTC (Silberberg and Markram 2007). This discovery has been done by Gilad Silberberg (Silberberg and Markram 2007) and my participation in the results obtained is presented in this chapter.

4.2 Materials and Methods

Slicing. P12-P14 Wistar rats were rapidly decapitated and sagittal slices (300 μm thick) of the right hemisphere were cut in ACSF on a slicer HR2 (Sigmann Elektronik, Heidelberg). The hemisphere was glued at the surface of the sagittal plane onto a block, which was mounted at an angle of 10° such that the blade cut from the upper part of the cortex towards the caudal border and down towards the midline. Slices were incubated for 15 to 30 min at 35°C and then left at room temperature (20-22°C). The ACSF contained (in mM): 125 NaCl, 2.5 KCl, 25 D-glucose, 25 $NaHCO_3$, 1.25 NaH_2PO_4, 2 $CaCl_2$ and 1 $MgCl_2$.

IR-DIC microscopy. Neurons in somatosensory cortex were identified using IR-DIC microscopy, with an upright microscope (BX 51WI, Olympus, fitted with a 60x LUMPlan FI, Japan objective). The recorded neurons were selected up to 50 μm below the slice surface.

Electrophysiological recordings. Somatic whole-cell recordings were performed at 35°C and signals were amplified using Axoclamp-2B amplifiers (Axon Instruments, USA). Voltages were recorded with pipettes containing (in mM): 110 potassium gluconate, 10 KCl, 4 ATP-Mg, 10 phosphocreatine, 0.3 GTP, 10 Hepes (pH 7.3, 310 mOsm adjusted with sucrose) and 0.5% biocytin. The pipettes were pulled with a Flamming/Brown micropipette puller P-97 (Stutter Instruments CO, USA). The scaled output of the amplifier was connected to an ITC device (ITC-18, Instrutech Co, Port Washington, New York, USA) connected to an Apple computer running Igor Pro (Wavemetrics). The junction potential between the ACSF and the solution in the pipettes was around -10mV. The recordings were made without correction for it.

4.3 Results

The biphasic response. The first indication of the existence of these indirect connections between TTCs came with the unusual aspect of some direct connections (compare Figure 13*A* and Figure 13*B*). The stimulation in the pre-synaptic TTC was a train of 8 APs at 30 Hz followed by a recovery test AP 500 ms later. In the normal case (Figure 13*A*) the first excitatory post-synaptic potential (EPSP) is depolarizing and the subsequent ones are of less amplitude (depression) but also depolarising. The membrane potential does not reach values below the resting potential recorded at the beginning of the stimulation except from a small refractoriness. In some cases however, the membrane is hyperpolarized at the end of the 8 APs train (Figure 13*B*). The stimulation chosen as a reference for further investigation of these indirect connections was 15 APs at 70 Hz (Figure 14).

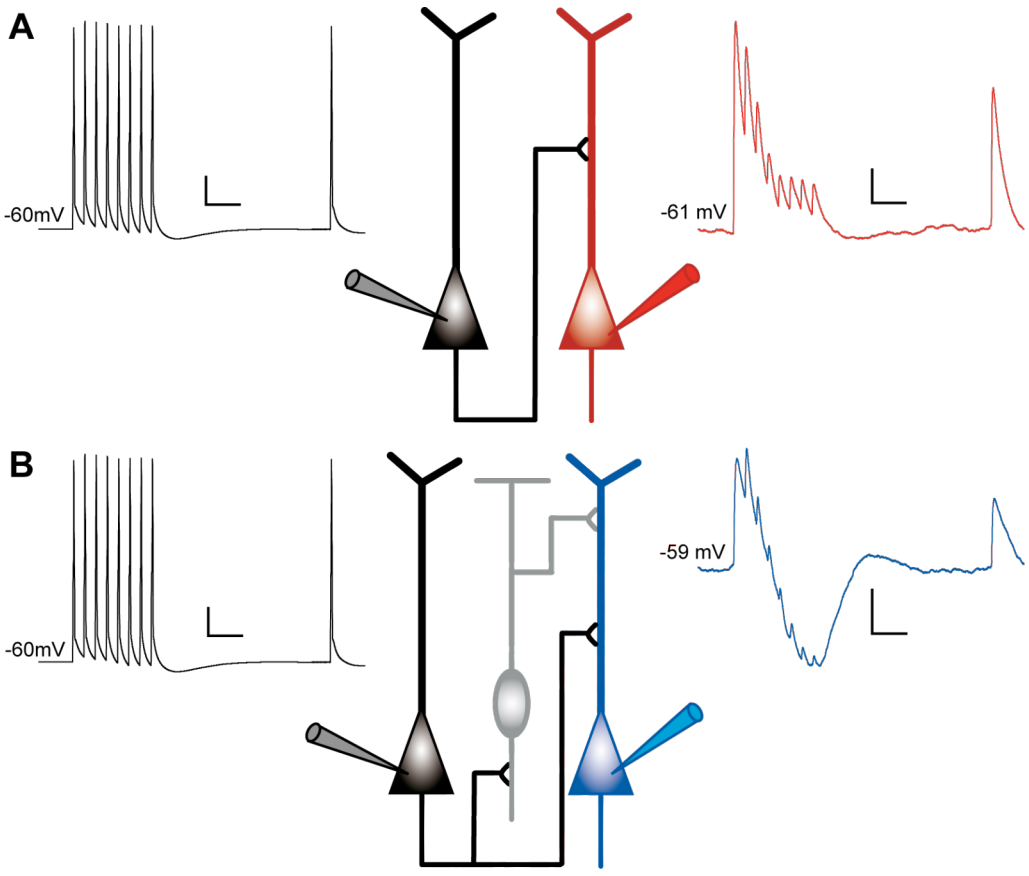

Figure 13 The direct and indirect connections between TTCs. A – Direct connection between the stimulated TTC (black) and the post-synaptic TTC (red). Horizontal scale bars : 0.1s, vertical scale bars : 20 mV and 0.5 mV for the stimulation and the post-synaptic recording respectively. B – Direct and indirect connection between the stimulated TTC (black) and the post-synaptic TTC (blue). Same scale bars as in A.

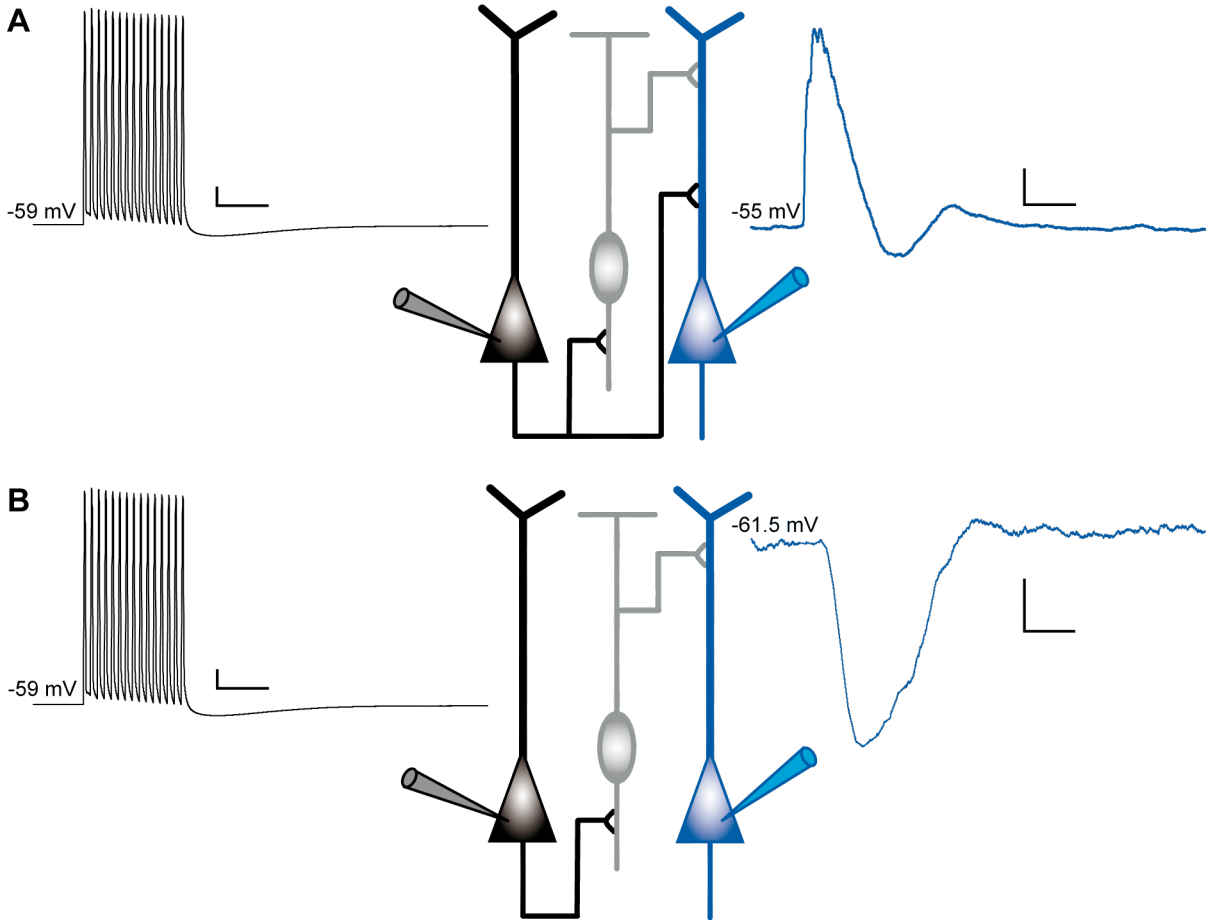

Figure 14 The stimulation at 70 Hz with 15 APs. A – Direct connection together with an indirect connection between two TTCs (pre-synaptic cell in black, post-synaptic cell in blue). Horizontal scale bars : 0.1s, vertical scale bars : 20 mV and 0.5 mV for the stimulation and the post-synaptic recording respectively. B – Indirect connection without a direct connection between two TTCs. Same colour code and scale bars as in A.

An unusual reversal potential. With this stimulation, indirect connections were found to be present in pairs of TTCs that were not directly connected (Figure 14*B*). The mediation of this inhibitory indirect connection by a GABAergic interneuron was proved by the application of biccuculine, Gabazine and picrotoxin (Silberberg and Markram 2007) as illustrated on Figure 15. Under our experimental conditions (see Materials and Methods) the reversal potential for chloride calculated by the Nernst equation is -69.2 mV. This corresponds to a measured potential of -59.2 mV after junction potential correction. We should then expect the IPSP amplitude to be zero with a post-synaptic cell holding potential around -59 mV. As it can be seen on Figure 14*B* and Figure 15, the IPSP is still far from reversing polarity when the post-synaptic cell is hold around -60 mV. The IPSP amplitude vs holding potential curve is illustrated on Figure 16*A* and shows in this case a reversal potential of -76 mV. Seventeen connections have been recorded and their reversal potentials extrapolated. These potentials are presented on Figure 16*B* giving an average reversal potential of -75 ± 8 mV.

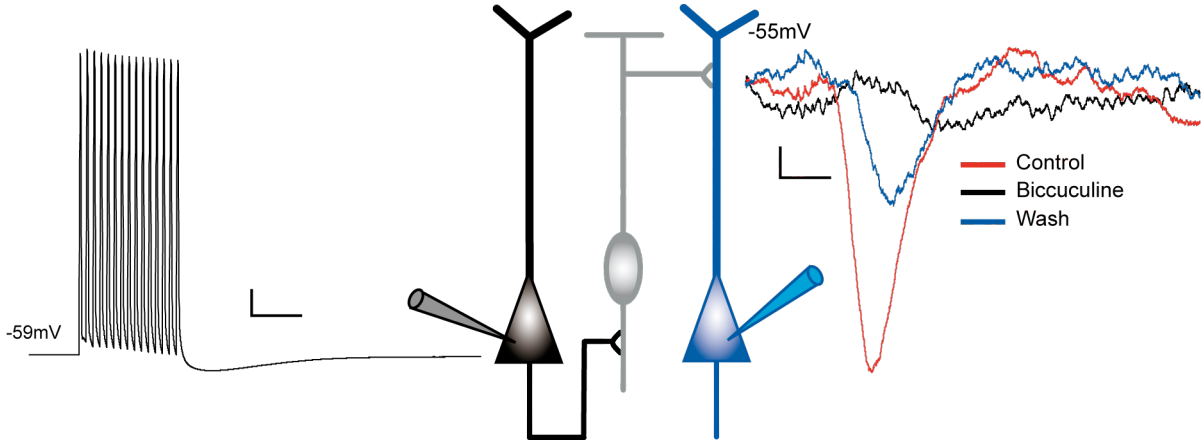

Figure 15 The indirect connections mediated by a GABAergic interneuron. Pre-synaptic TTC (black) generating IPSPs in a post-synaptic TTC (blue) via a GABAergic interneuron (grey) as shown by the disappearance of the IPSP when biccuculine is perfused in the bath. Horizontal scale bars : 0.1s, vertical scale bars : 20 mV and 0.1 mV for the stimulation and the post-synaptic recording respectively.

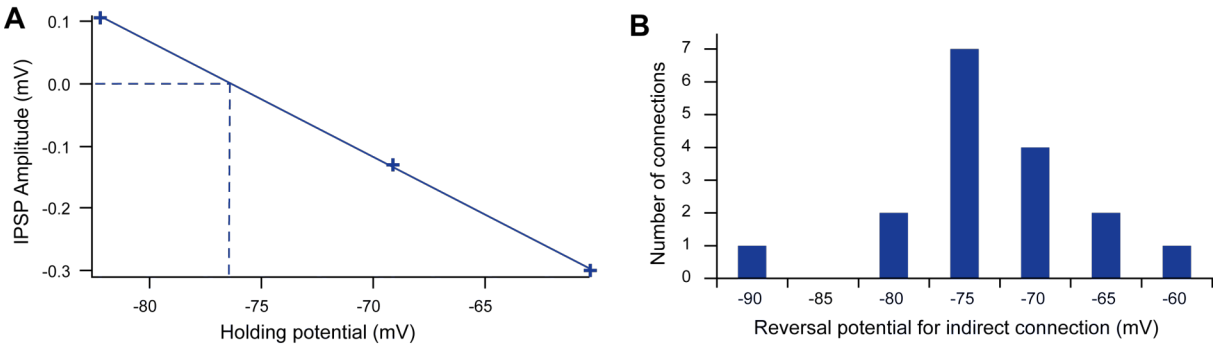

Figure 16 Reversal potentials of the indirect connections between TTCs. A - IPSPs amplitude measured at various holding potentials. Three measures were taken and the fitting linear curve is shown on the graph. The dashed lines illustrate the calculation of the reversal potential. B – Distribution of the reversal potentials; V_{rev} = -75±8 mV (mean±SD, n=17).

4.4 Discussion

TTCs can indirectly inhibit neighbouring TTCs via a GABAergic interneuron. The measured reversal potential is however much more hyperpolarized than what would be expected theoretically.

This difference between the expected and the actual reversal potential for chloride as measured at the soma suggests that the inhibitory synapses are located on distal dendrites. Morphological reconstructions of the complete pathway indeed showed a distal innervation of the post-synaptic TTC (Silberberg and Markram 2007).

This inhibitory input to the distal part of the TTC dendrite results in a hyperpolarizing response propagating electrotonically down to the soma, even in the case of somatic moderate hyperpolarization. Conversely, proximal dendritic innervations would be subject to the somatic hyperpolarization and then would be depolarizing. As a consequence, this indirect inhibitory pathway always shapes the TTCs dendritic integration in the same manner. This inhibition is activity dependent and can on the one side shape the TTCs transmission in a more phasic manner and also prevent over-excitation.

We saw in chapter 2 the difference in synaptic dynamics between CCPs and TTCs. CCPs have a more linear transmission and were then interpreted to be more transmitting than integrating. The even more phasic transmission between TTCs on an activity dependent manner suggests that the circuit integrates the incoming information differentially depending on the frequency rate of the input signal.

Interestingly, no indirect connection was found between CCPs (see Figure 7 in section 2.5). This further supports the differential role of the two populations of neurons with an integrating TTC sub-population and a transmitting CCP sub-population.

In further experiments probing the connectivity and connections dynamics between TTCs and CCPs as well as between other PCs sub-populations, the stimulation at higher frequency (15 spikes at 70Hz) should be systematically used to probe the indirect connections. There are other aspects of connectivity that can be probe with pairs of cells using specific stimulation protocols as for instance the variation in the dynamics with frequency (Thomson and West 2003; West *et al.* 2006). A complete description of synaptic transmission in the various sub-populations would require the use of all these protocols and analysis as well as retrograde labelling to identify with certainty the sub-populations. This implies long protocols with cells containing fluorescence and a particular care should be taken to ensure the survival of the cell as well as understanding the potential influence of fluorescence on the results.

5 Conclusion

Specificity and precision. Some fundamental rules pertaining to the neocortical microcircuit are supported by the results presented in this thesis. The low connection rates reported for both the TTCs and the CCPs populations are an indication of the *specificity* with which PCs target their post-synaptic partners. A cortical neuron receives on average ten thousand synapses and there is an all-to-all morphological connectivity observed in the TTCs population. This morphological connectivity is very likely to be also present in the CCPs population and across populations. If there was no specificity for the functional connections, the cortex would be fully interconnected, and likely resulting in over excitation.

Along with the specific targeting of neurons, there is a *precision* in the way synapses are formed on the post-synaptic partner. Interneurons are classified according to the region they target on the post-synaptic neuron (axon, soma and dendrites) and in our studies we show that synapses formed between CCPs target different areas of the post-synaptic cell than in the case of connections between TTCs. These differences are less striking than in the case of interneurons, but the non-linear and local integration of the information processed by the dendrites can rapidly amplify small differences in dendritic target. This structural specificity is likely to be set in place during neocortical development when neurons are embedded in the microcircuit. It would be interesting in future research to alter the axonal arborisation in order to study the effect of changing the post-synaptic target on the emerging cortical dynamics. An integration of the various pre-synaptic signals in a given domain might be more important than initially thought and recordings of the integration of various cells connections at the level of a given synaptic domain would be of great interest. These experiments would require accurate dendritic patching as well as identification of pre-synaptic neurons. These two requirements are not easily achieved, but are possible with a combination of techniques such as dendritic patching, photo-stimulation and various imaging techniques.

On a functional point of view, these concepts of *specificity* and *precision* can also be highlighted. We saw that the dynamics differ from one sub-population of PCs to another. Additionally, a change in the connection dynamics has implications on the computation performed by any given population of neurons. We showed that the newly formed connections were of a more linear dynamics than the connections already present in the circuit at first recording. This change in network dynamics also needs to be investigated more precisely with experiments designed with various stimulation durations. We reported here only 3 time points and these results suggest that the new connections have a more linear dynamics as soon as they appear and that this dynamics is kept for the next 8 hours at least. A longer lasting investigation, maybe with *in vivo* experiments, would be required to determine for how long these altered dynamics would last.

Reciprocity. Another main concept in the cortical column connectivity structure is *reciprocity*. This principle extents far beyond neuronal networks and can be applied to any dynamical network. In this work, reciprocity in the cortical column is supported by the indirect connections between PCs. It was observed here at the sub-population level within the cortical column, however it was shown that PCs that indirectly inhibit neighbouring PCs via the Martinotti loop also induce dendritic inhibition upon themselves (Silberberg and Markram 2007). The TTCs sub-population projects onto interneurons that in turn project back to TTCs. This allows on one hand a control of the global excitation of this circuit although over-excitation might already be partly prevented by the depressing dynamics of the synapses. On another hand, the inhibitory reciprocal connections change the resulting dynamics in TTCs to

TTCs connections. With the inhibitory interneuron, these connections are more phasic and hence the input signal is differentially computed when it is strong enough to trigger interneuron firing.

Reciprocity is also observed within the various pyramidal populations. We saw that the TTCs sub-population has higher reciprocity than the CCPs sub-population. The way a signal is computed within a sub-population will again be highly related to the degree of reciprocity in the connections for that microcircuit. The higher the degree of reciprocity, the higher the computation is. Indeed, the more linear dynamics and low interconnectivity suggest a more transmitting than integrating role for the CCPs. In contrast, TTCs have a higher interconnectivity, are reciprocally connected with interneurons that rends the connections between TTCs more phasic (their connections being already more phasic than the CCPs). These results overall suggest a high integrative role for the TTCs or at least a more integrative role than in the case of the CCPs.

MCs, which have been shown to participate in the indirect connection between TTCs (Silberberg and Markram 2007), innervate largely the distal dendrites of their target cell. This distal synapses seem to be weakly influenced by somatic depolarization. Consequently, the bi-phasic shaping of TTCs integration due to the indirect connections is then dependent on the level of activity of the pre-synaptic TTC (which should be high enough to trigger MC firing) but not on the level of depolarization at the post-synaptic cell soma.

Equilibrium. The last phenomenon considered here is *equilibrium*. It is worth pointing out that equilibrium does not necessarily mean equal levels of a given element at all points in time and space. Some differences exist and then give rise to a dynamical equilibrium in the sense that the forces acting on the system equilibrate each other and allow the system to be stable and long lasting. In the case of membrane properties, chemical forces are equilibrated with electrical forces. At the microcircuit level dynamics equilibrium is also achieved by the various dynamical parameters constraining the system.

Deviation from equilibrium is however necessary for life. In fact, it might be as important as equilibrium itself. All neuronal activity is based on small variations, or short lasting variations (like APs), from rest membrane potential. At the microcircuit level, deviations from equilibrium allow memory formation by both increasing or decreasing synaptic transmission. Indeed, in order to ensure only small deviations from equilibrium limiting synaptic transmission is unavoidable. We showed in this thesis that microcircuit plasticity mainly increased excitatory connectivity. The artificial stimulation given might however be specific to a pattern that results in an increase in connectivity and connection strength. Despite this tendency, some connections disappeared and some weakened (although not in a proportion large enough to compensate the overall increase). Some mechanisms for LTD and synaptic disappearance are therefore activated, although only one metabotropic glutamate receptor group causing LTD has been identified here. It might be that the regulation of connectivity decrease requires the action of certain neuromodulators and different activity patterns in the microcircuit. These might be activated in a different state than during the increase of connections like for instance during some sleep cycles.

Another reason why the removal of connections was not massively observed in the experiments presented here can be the lack of time for synapses to reach maturation. It is worth noticing that the dynamics was the same for new connections that appeared after 4 and 12 hours of stimulation. The massive removal could then be greatly delayed after the first appearances. This would suggest that the stimulus required for the network to acquire a new computing pattern would indeed increase the connections rate and strengths and later, after synapse maturation and in a different state, redundant connections would be removed for the circuit to go back to equilibrium, but a “new” equilibrium.

It is important to notice that the artificial stimulation by glutamate can also affect the dynamical parameters. The stimulation pattern induced in the experiments presented here is very different from *in vivo* activity in the sense that the slice is in a quiescent state and only a small group of neurons is stimulated. When stimulation was performed by glutamate puffing onto a neuron cluster, activity was very limited in space while the rest of the slice was virtually "in coma". When stimulation was performed by perfusion, the entire slice was excited at firing rates in the physiological range, yet specific inputs to the microcircuit were lacking.

We differentiate between two mechanisms for network plasticity. The first is the modification of existing synaptic connections (LTP and LTD) and the second, appearance or disappearance of connections. The two mechanisms seem to follow different dynamics in that strengthening of synapses was more transient while the appearance of new connections increased linearly with stimulation time. Our results suggest that these plasticity mechanisms are regulated by different processes and may not necessarily be interdependent.

Perspectives. In conclusion, the contribution of this work to our understanding of neocortical structure and function is twofold. Firstly, a characterization of well-defined PC sub-populations was performed for the first time at the synaptic level. The cortico-callosally projecting PCs have a specific functional role in the neocortical microcircuit and this is the first report of their synaptic connectivity and dynamics. Secondly, new experimental methods have been developed in this study, leading to the discovery of a novel form of network plasticity. The discovery of network dynamic rewiring will undoubtedly stimulate further work in the field of cortical plasticity.

The neocortical microcircuit still holds many unanswered questions regarding its structural and functional connectivity, in particular regarding connectivity within and between the different sub-populations of PCs. Retrograde labelling is a very precise method for identification of the various sub-populations of PCs, and it is likely to continue being a major technical component in the investigation of the neocortical microcircuit.

The microcircuit rewiring study raised numerous questions regarding the intracellular mechanisms that govern the formation and deletion of synaptic connections. Understanding these mechanisms and processes is crucial and is likely to have a major impact on research related to memory and memory disorders such as Alzheimer's disease. Recent findings show that certain types of Autism might be associated with hyper-connectivity and hyper-plasticity in the neocortex and amygdala. Although this observed hyper-connectivity might be of different origin, the microcircuit rewiring reported in this work could eventually be used to restore the connectivity rate back to normal values.

The dynamics of this microcircuit plasticity as well as the conditions for the microcircuit to return to the baseline connectivity level should be further studied. Indeed, equilibrium in the microcircuit is essential for its normal function. It is important to investigate the borders of synaptic connectivity, what are its saturation levels, under what conditions does synaptic elimination dominate. Eventually, microcircuit reorganization would have to be observed and controlled *in vivo* in order to further understand the mechanisms underlying memory and learning in the intact brain under natural conditions.

Abbreviations

A: Absolute synaptic efficacy
ACSF: Artificial cerebro-spinal fluid
AMPA : α-amino-3-hydroxy-5-methyl-4-isoxazole-propionic acid
AMPAR: AMPA receptor
AP: Action potential
AP5: 2-amino-5-phosphonopentanoic acid
ASE: Absolute synaptic efficacy
ATC: Axon Targeting Cell
BC: Basket cell
BTC: Bi-tufted cell
CCP: Cortico-callosally projecting cell, Cortico-callosal cells
ChC: Chandelier cell
CNQX: 6-cyano-7-nitroquinoxaline-2,3-dione
CNS: Central Nervous System
CPPG: (RS)-α-Cyclopropyl-4-phosphonophenyl-glycine
CRC: Cajal-Retzius cell
DBC: Double-bouquet cell
DHPG: Dihydroxyphenylglycine
DTC: Dendrite Targeting Cell
DTTC: Dendrite and Tuft Targeting Cell
EEG: Electro-encephalogram
EPSP: Excitatory post-synaptic potential
GABA: γ-amino-butyric acid
IB: Intrinsically bursting
IPSP: Inhibitory Post-Synaptic Potential
IR-DIC: Infra-Red Differential Interference Contrast
L-SOP: O-Phospho-L-serine
LTP: Long-term potentiation
LTD: Long-term depression
MC: Martinotti cell
MCPG: (RS)-α-methyl-4-carboxyphenylglycine
mGluR: metabotropic Glutamate receptor
MPEP: 2-methyl-6(phenylethynyl)pyrine
NMDA: N-methyl-D-aspartic acid
PC: Pyramidal cell
Pr: Probability of release
REM: Rapid-Eye Movement sleep (also known as paradoxical sleep)
PKC: protein kinase C
PKMζ: protein kinase Mzeta
S1: Primary sensory cortex
SDTC: Soma and Dendrite Targeting Cell
SSC: Spiny-stellate cell
SWS: Slow-Wave Sleep
τ_D: Time constant of recovery from depression
τ_F: Time constant of recovery from facilitation
TTC: Thick-tufted pyramidal cell
TTX: tetrodotoxin

U: Utilization of synaptic efficacy (equivalent to Pr in a depressing synapse)
VPA: Valproic Acid

Acknowledgements

I thank Prof. Henry Markram for having given me the opportunity to work and learn in his Laboratory of Neural Microcircuitry for this PhD. I would like to thank him for his enthusiasm and his constant new ideas production and for the trust he had in me throughout my time in his lab. Despite my physicist background, he allowed me to join a neuroscientist team and gave me the time to update my knowledge to be efficient in this field I knew very few about before coming in his lab.

I thank my PhD thesis jury members who were Prof. Ralf Schenggenburger, president of the jury and head of the Laboratory of Synaptic Mechanisms at EPFL, Prof. Carl Petersen, head of the Laboratory of Sensory Processing at EPFL, Prof. Alex Thomson, head of the Department of Pharmacology at the School of Pharmacy, University of London and Prof. Andreas Lüthi, head of the Cellular Mechanisms of Learning and Memory group at the Friedrich Miescher Institute for Biomedical Research in Basel for their time and attention on my thesis.

My special thanks to Gilad Silberberg who taught me the mysteries of patch clamping and electrophysiology while he was doing his post-doc at the LNMC. I also thank him for his availability to help me, discuss issues and comment my thesis manuscript even when he was far away to the north.

I thank all the collaborators of the Brain Mind Institute and specially Sandrine Lefort, Tania Rinaldi, Deborah La Mendola, Sonia Garcia, Katia Antoniello, Thomas Berger, Rodrigo Perin and Luca Gambazzi for all the personal and scientific discussions and support they gave me. I also would like to thank Sandrine Lefort, Tania Rinaldi, Michele Giugliano, Luc Gentet, Sean Hill and James Poulet for their comments on the manuscript of this thesis.

I also thank all my friends and family for their support and interest in my activity and for the moments we spent together having fun or sweating on stages, moments without which it would have been much more difficult to complete this PhD.

I greatly thank my parents, Philippe and Marie-Pascale, for the ideal atmosphere they gave me for all my studies and the constant love and care they had for me.

Last but not least, I deeply thank Jaïa for her constant love, support and understanding.

More about the PNAS paper

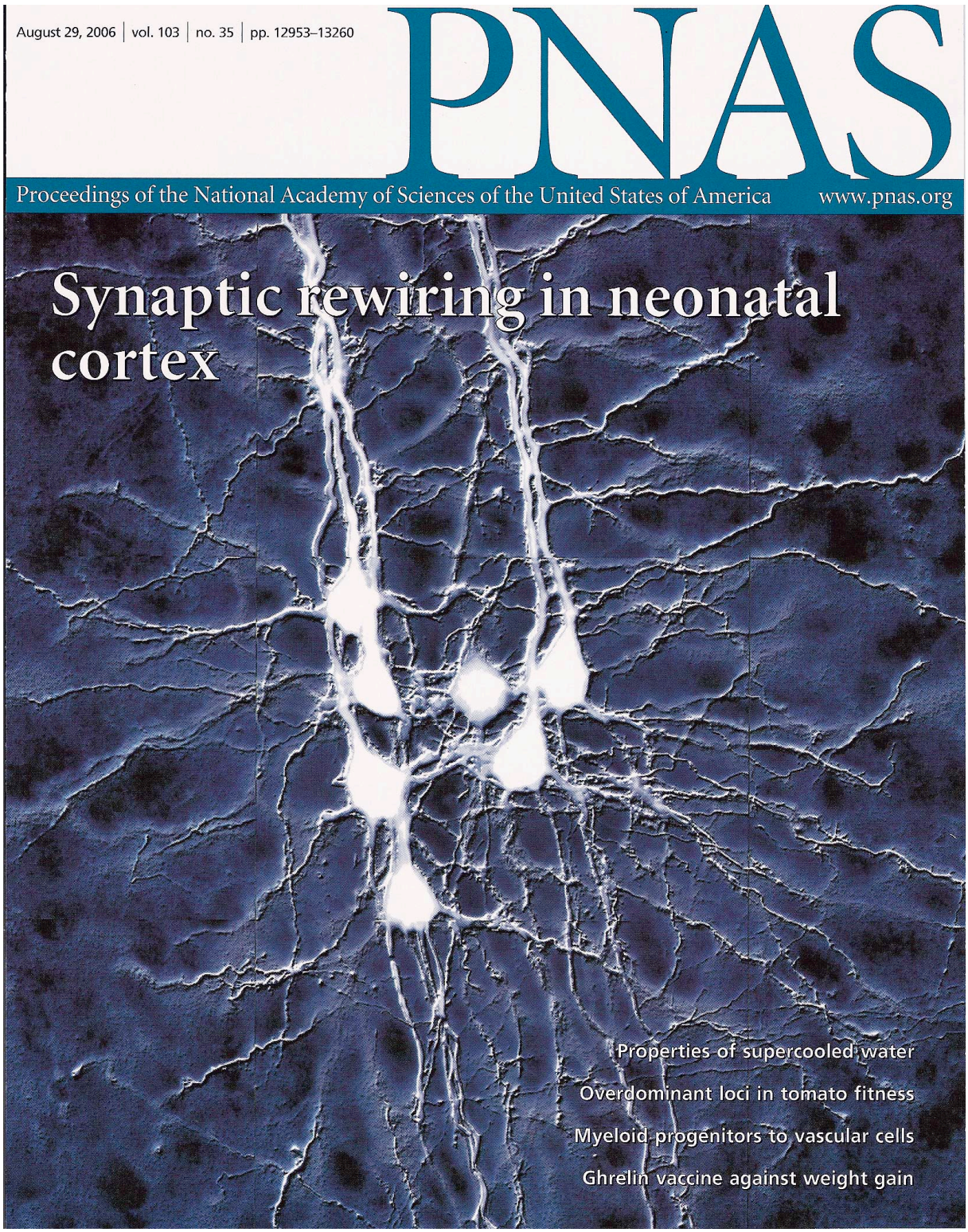

August 29, 2006 | vol. 103 | no. 35 | 12953–13260

PNAS

Proceedings of the National Academy of Sciences of the United States of America www.pnas.org

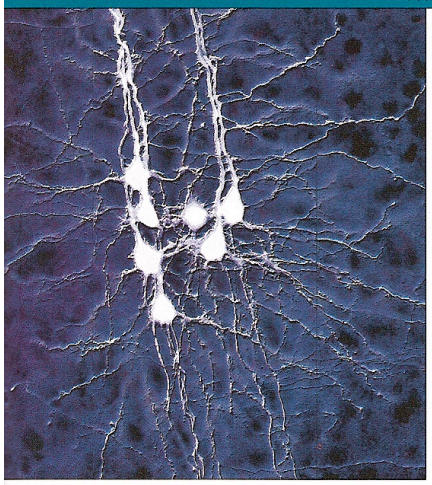

Cover image: Micrograph of seven neurons in the rat neonatal neocortex, recorded and stained with a dye. These neurons connect and disconnect from each other spontaneously. When a stimulus is presented, each neuron tends to connect to many more neurons and then prunes weaker connections to settle down to a new circuit configuration. See the article by Le Bé and Markram on pages 13214–13219. Image courtesy of Jean-Vincent Le Bé and Henry Markram.

From the Cover

Contents

Freely available online through the PNAS open access option.

August 29, 2006 | vol. 103 | no. 35 | 12953–13260

PNAS

Proceedings of the National Academy of Sciences of the United States of America www.pnas.org

In This Issue

APPLIED PHYSICAL SCIENCES

Unusual property of supercooled water

Despite the ubiquity of water, many of its physical properties are still not fully understood. Sow-Hsin Chen *et al.* have found that supercooled water, kept in a liquid state despite being well below its freezing point, violates the Stokes–Einstein relation and undergoes a glass-like, fragile-to-strong transition around the temperature of 225 K. The Stokes–Einstein relation ties together diffusion, viscosity, and temperature and is typically accurate for normal- and high-temperature liquids. Chen *et al.* confined water samples in a nanosized pore to prevent it from freezing at very cold temperatures, providing experimental access to liquid water at temperatures at which it is normally solid cubic ice. The authors found a well defined decoupling of transport properties of water, which implies a breakdown of the Stokes–Einstein relation. They also used the measurements to study water's fragile-to-strong transition temperature, which they found to be ≈225 K. At this temperature, water's hydrogen-bonding structure changes, marking a phase change from low-density liquid to high-density liquid. The Stokes–Einstein relation broke down in different ways on each side of the transition temperature. The authors say their results support the hypothesis that normal water exists as a mixture of these two liquid phases. — P.D.

"The violation of the Stokes–Einstein relation in supercooled water" by Sow-Hsin Chen, Francesco Mallamace, Chung-Yuan Mou, Matteo Broccio, Carmelo Corsaro, Antonio Faraone, and Li Liu (see pages 12974–12978)

ECOLOGY

Bacterial biodiversity predicted by ocean conditions

Environmental factors such as temperature, nutrient availability, and interspecies competition play a major role in animal and plant biodiversity. Although bacteria contribute to a wide variety of ecosystem processes, the effects of these factors on bacterial biodiversity have not been well understood. By studying the ocean waters off the southern coast of California, Jed Fuhrman *et al.* show that marine bacterioplankton exhibit strong patterns in distribution and abundance associated with oceanic environmental factors. Over 4.5 years, the authors took monthly water samples, filtered them free of eukaryotes, categorized the remaining bacteria into taxonomic units by DNA fingerprinting, and tested the samples for a suite of oceanographic environmental variables including temperature, salinity, dissolved oxygen, chlorophyll, bacterial heterotrophic production, and nutrients. Fuhrman *et al.* found that these factors had predictive values; the environmental conditions could predict the distribution and abundance of sets of bacterial taxonomic units, and, conversely, the diversity of the taxonomic units predicted not only the month the sample was collected but also the likely environmental conditions at the time of collection. These results demonstrate that bacterial communities operate much like animal and plant communities, in which the biodiversity of an ecosystem relies on environmental cues. — F.A.

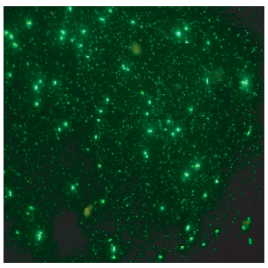

Ocean environment and bacterial diversity.

"Annually reoccurring bacterial communities are predictable from ocean conditions" by Jed A. Fuhrman, Ian Hewson, Michael S. Schwalbach, Joshua A. Steele, Mark V. Brown, and Shahid Naeem (see pages 13104–13109)

MEDICAL SCIENCES

Bone marrow progenitor cells contribute to blood vessels

Endothelial progenitor cells play an important role in vascular development and repair and have potential uses in targeted therapies. Alexis Bailey *et al.* have isolated common myeloid (CMP) and granulocyte/macrophage (GMP) progenitors that can give rise to vascular endothelial cells. To discern endothelial progenitor activity in distinct bone marrow populations, Bailey *et al.* fractionated genetically tagged myeloid progenitors according to cell surface marker expression. After transplanting

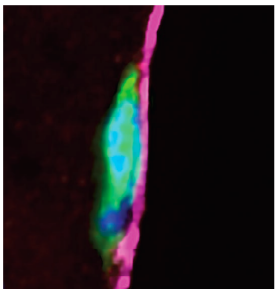

Endothelial cell derived from stem cell progeny.

the cells into irradiated mice, myeloid progenitor cells, the differentiated progeny of hematopoietic stem cells, were found to produce endothelial cells. This differentiation occurred independent of cell fusion between the transplanted myeloid cells and host endothelial cells. The liver portal veins of recipient animals contained up to 1.3% donor-derived endothelial cells when transplanted with CMPs or GMPs. In addition, nonirradiated mice that were surgically joined (from shoulder to thigh) for 12 weeks, separated, and then analyzed 4–6 months later displayed nearly 4% donor-derived endothelial cells. Because myeloid progenitor cells can infiltrate both healthy and diseased tissues, these findings may aid in the treatment of vascular diseases by providing clues to vessel regeneration. — F.A.

"Myeloid lineage progenitors give rise to vascular endothelium" by Alexis S. Bailey, Holger Willenbring, Shuguang Jiang, Daniel A. Anderson, David A. Schroeder, Melissa H. Wong, Markus Grompe, and William H. Fleming (see pages 13156–13161)

NEUROSCIENCE

Examining spontaneous and evoked neuron rewiring

During development, neurons must make connections with other cells to properly relay signals and wire a functioning brain. Jean-Vincent Le Bé and Henry Markram investigated how neurons choose their targets and found a high degree of plasticity, or ability to rewire connections. Neuronal axons extend to all neighboring dendrites numerously and with equal affinity, suggesting that neurons may not preferentially grow toward a specific receiver, but instead they stand ready for a connection to any dendrite at any time. To test this idea, Le Bé and Markram measured neuronal connections in the brains of rats and found that, within hours, new connections were spontaneously formed and old ones were discontinued many times, at all points along a specific neuron. To specifically evoke neuronal rewiring, glutamate was used, and its application increased the rate of new connections, suggesting that this connection rate is subject to modulation. After some time, weaker connections disappeared, and the connection rate returned to baseline levels. The authors hypothesize that new experiences trigger an increase in network connections that are then pruned as they are tested with repeated experience, shaping pathways in a Darwinian fashion. — T.D.

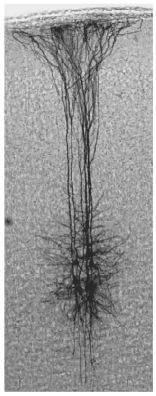

Assessing neuronal connections.

"Spontaneous and evoked synaptic rewiring in the neonatal neocortex" by Jean-Vincent Le Bé and Henry Markram (see pages 13214–13219)

PHARMACOLOGY

Galantamine protects against organophosphorus poisoning

Organophosphorus compounds (OPs) include the deadly nerve agents soman and sarin, which have been used in insecticides and biochemical warfare. These toxicants irreversibly inhibit the acetylcholinesterase enzyme, leading to loss of muscle control and adverse CNS effects, followed by coma and death. Galantamine, which is approved for use in treating Alzheimer's disease, reversibly inhibits acetylcholinesterase in the brain and the periphery and prevents seizures and neurodegeneration. Edson Albuquerque *et al.* studied the ability of galantamine to counteract OP toxicity in guinea pigs. The authors found that the guinea pigs survived acute exposure to lethal doses of OPs when given moderate doses of galantamine plus atropine before or after the exposure. Galantamine appeared more effective than pyridostigmine, the currently approved regimen for soldiers, and less toxic than huperzine. Albuquerque *et al.* say the galantamine/atropine combination may be a safe and effective countermeasure against OP intoxication. — P.D.

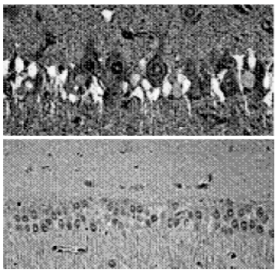

Galantamine-treated cells protected against degeneration.

"Effective countermeasure against poisoning by organophosphorus insecticides and nerve agents" by Edson X. Albuquerque, Edna F. R. Pereira, Yasco Aracava, William P. Fawcett, Maristela Oliveira, William R. Randall, Tracey A. Hamilton, Robert K. Kan, James A. Romano, Jr., and Michael Adler (see pages 13220–13225)

Bibliography

Abbott, L. F. and Nelson, S. B. (2000). "Synaptic plasticity: taming the beast." Nat Neurosci 3 Suppl: 1178-83.

Adolphs, R., Tranel, D., Damasio, H. and Damasio, A. (1994). "Impaired recognition of emotion in facial expressions following bilateral damage to the human amygdala." Nature 372(6507): 669-672.

Aggleton, J. P. (1992). The Amygdala. Neurobiological Aspects of Emotion, Memory and Mental Dysfunction. New York, Wiley.

Ahmed, B., Anderson, J. C., Douglas, R. J., Martin, K. A. and Nelson, J. C. (1994). "Polyneuronal innervation of spiny stellate neurons in cat visual cortex." J Comp Neurol 341(1): 39-49.

Ali, A. B., Bannister, A. P. and Thomson, A. M. (2007). "Robust correlations between action potential duration and the properties of synaptic connections in layer 4 interneurones in neocortical slices from juvenile rats and adult rat and cat." J Physiol 580(Pt 1): 149-69.

Ali, A. B., Deuchars, J., Pawelzik, H. and Thomson, A. M. (1998). "CA1 pyramidal to basket and bistratified cell EPSPs: dual intracellular recordings in rat hippocampal slices." J Physiol 507 (Pt 1): 201-17.

AmericanPsychiatricAssociation (1994). Diagnostic and Statistical Manual of Mental Disorders. Washington, American Psychiatric Press.

Ardinger, H. H., Atkin, J. F., Blackston, R. D., Elsas, L. J., Clarren, S. K., Livingstone, S., Flannery, D. B., Pellock, J. M., Harrod, M. J., Lammer, E. J. and et al. (1988). "Verification of the fetal valproate syndrome phenotype." Am J Med Genet 29(1): 171-85.

Ascher, P. and Nowak, L. (1988). "The role of divalent cations in the N-methyl-D-aspartate responses of mouse central neurones in culture." J Physiol 399: 247-66.

Ashby, M. C., De La Rue, S. A., Ralph, G. S., Uney, J., Collingridge, G. L. and Henley, J. M. (2004). "Removal of AMPA receptors (AMPARs) from synapses is preceded by transient endocytosis of extrasynaptic AMPARs." J Neurosci 24(22): 5172-6.

Bannister, A. P. (2005). "Inter- and intra-laminar connections of pyramidal cells in the neocortex." Neuroscience Research 53(2): 95-103.

Barria, A., Muller, D., Derkach, V., Griffith, L. C. and Soderling, T. R. (1997). "Regulatory Phosphorylation of AMPA-Type Glutamate Receptors by CaM-KII During Long-Term Potentiation." Science 276(5321): 2042-2045.

Bell, C. C., Han, V. Z., Sugawara, Y. and Grant, K. (1997). "Synaptic plasticity in a cerebellum-like structure depends on temporal order." Nature 387(6630): 278-281.

Berger, T. W. (1984). "Long-term potentiation of hippocampal synaptic transmission affects rate of behavioral learning." Science 224(4649): 627-630.

Bezzi, P., Carmignoto, G., Pasti, L., Vesce, S., Rossi, D., Rizzini, B. L., Pozzan, T. and Volterra, A. (1998). "Prostaglandins stimulate calcium-dependent glutamate release in astrocytes." Nature 391(6664): 281-5.

Bi, G.-q. and Poo, M.-m. (1998). "Synaptic Modifications in Cultured Hippocampal Neurons: Dependence on Spike Timing, Synaptic Strength, and Postsynaptic Cell Type." J. Neurosci. 18(24): 10464-10472.

Bi, G.-q. and Poo, M.-m. (2001). "Synaptic Modification by Correlated Activity: Hebb's Postulate Revisited." Annual Review of Neuroscience 24(1): 139-166.

Bliss, T. V. and Lomo, T. (1973). "Long-lasting potentiation of synaptic transmission in the dentate area of the anaesthetized rabbit following stimulation of the perforant path." J

Physiol 232(2): 331-56.
Bliss, T. V. P. and Collingridge, G. L. (1993). "A synaptic model of memory: long-term potentiation in the hippocampus." Nature 361(6407): 31-39.
Bortolotto, Z. A., Bashir, Z. I., Davies, C. H. and Collingridge, G. L. (1994). "A molecular switch activated by metabotropic glutamate receptors regulates induction of long-term potentiation." Nature 368(6473): 740-743.
Bortolotto, Z. A. and Collingridge, G. L. (1993). "Characterisation of LTP induced by the activation of glutamate metabotropic receptors in area CA1 of the hippocampus." Neuropharmacology 32(1): 1-9.
Bortolotto, Z. A. and Collingridge, G. L. (1995). "On the mechanism of long-term potentiation induced by (1S,3R)-1-aminocyclopentane-1,3-dicarboxylic acid (ACPD) in rat hippocampal slices." Neuropharmacology 34(8): 1003-1014.
Bourassa, J., Pinault, D. and Deschenes, M. (1995). "Corticothalamic projections from the cortical barrel field to the somatosensory thalamus in rats: a single-fibre study using biocytin as an anterograde tracer." Eur J Neurosci 7(1): 19-30.
Brown, T. H., Chapman, P. F., Kairiss, E. W. and Keenan, C. L. (1988). "Long-term synaptic potentiation." Science 242(4879): 724-728.
Buldakova, S. L., Vorobjev, V. S., Sharonova, I. N., Samoilova, M. V. and Magazanik, L. G. (1999). "Characterization of AMPA receptor populations in rat brain cells by the use of subunit-specific open channel blocking drug, IEM-1460." Brain Research 846(1): 52-58.
Buonomano, D. V. and Merzenich, M. M. (1998). "Cortical Plasticity: From Synapses to Maps." Annual Review of Neuroscience 21(1): 149-186.
Cantero, J. L., Atienza, M. and Salas, R. M. (2002). "Human alpha oscillations in wakefulness, drowsiness period, and REM sleep: different electroencephalographic phenomena within the alpha band." Neurophysiol Clin 32(1): 54-71.
Cartmell, J. and Schoepp, D. D. (2000). "Regulation of neurotransmitter release by metabotropic glutamate receptors." J Neurochem 75(3): 889-907.
Catsman-Berrevoets, C. E., Lemon, R. N., Verburgh, C. A., Bentivoglio, M. and Kuypers, H. G. (1980). "Absence of callosal collaterals derived from rat corticospinal neurons. A study using fluorescent retrograde tracing and electrophysiological techniques." Exp Brain Res 39(4): 433-40.
Chagnac-Amitai, Y. and Connors, B. W. (1989). "Synchronized excitation and inhibition driven by intrinsically bursting neurons in neocortex." J Neurophysiol 62(5): 1149-62.
Chagnac-Amitai, Y., Luhmann, H. J. and Prince, D. A. (1990). "Burst generating and regular spiking layer 5 pyramidal neurons of rat neocortex have different morphological features." J Comp Neurol 296(4): 598-613.
Chapman, J. B. and Cutler, M. G. (1989). "Effects of sodium valproate on development and social behaviour in the Mongolian gerbil." Neurotoxicol Teratol 11(2): 193-8.
Cho, R.-H., Segawa, S., Mizuno, A. and Kaneko, T. (2004). "Intracellularly labeled pyramidal neurons in the cortical areas projecting to the spinal cord: I. Electrophysiological properties of pyramidal neurons." Neuroscience Research 50(4): 381-394.
Christianson, A. L., Chesler, N. and Kromberg, J. G. (1994). "Fetal valproate syndrome: clinical and neuro-developmental features in two sibling pairs." Dev Med Child Neurol 36(4): 361-9.
Christophe, E., Doerflinger, N., Lavery, D. J., Molnar, Z., Charpak, S. and Audinat, E. (2005). "Two populations of layer v pyramidal cells of the mouse neocortex: development and sensitivity to anesthetics." J Neurophysiol 94(5): 3357-67.
Chung, H. J., Xia, J., Scannevin, R. H., Zhang, X. and Huganir, R. L. (2000). "Phosphorylation of the AMPA receptor subunit GluR2 differentially regulates its

interaction with PDZ domain-containing proteins." The Journal Of Neuroscience: The Official Journal Of The Society For Neuroscience 20(19): 7258-7267.

Clark, B. A., Farrant, M. and Cull-Candy, S. G. (1997). "A Direct Comparison of the Single-Channel Properties of Synaptic and Extrasynaptic NMDA Receptors." J. Neurosci. 17(1): 107-116.

Conn, P. J. and Pin, J. P. (1997). "Pharmacology and functions of metabotropic glutamate receptors." Annu Rev Pharmacol Toxicol 37: 205-37.

Cozzi, A., Attucci, S., Peruginelli, F., Marinozzi, M., Luneia, R., Pellicciari, R. and Moroni, F. (1997). "Type 2 metabotropic glutamate (mGlu) receptors tonically inhibit transmitter release in rat caudate nucleus: in vivo studies with (2S,1'S,2'S,3'R)-2-(2'-carboxy-3'-phenylcyclopropyl)glycine, a new potent and selective antagonist." Eur J Neurosci 9(7): 1350-5.

Damasio, A. (2001). "Fundamental feelings." Nature 413(6858): 781-781.

Davis, M. (1992). "The Role of the Amygdala in Fear and Anxiety." Annual Review of Neuroscience 15(1): 353-375.

Debanne, D., Gahwiler, B. H. and Thompson, S. M. (1998). "Long-term synaptic plasticity between pairs of individual CA3 pyramidal cells in rat hippocampal slice cultures." J Physiol (Lond) 507(1): 237-247.

DeFelipe, J. (1993). "Neocortical Neuronal Diversity: Chemical Heterogeneity Revealed by Colocalization Studies of Classic Neurotransmitters, Neuropeptides, Calcium-binding Proteins, and Cell Surface Molecules." Cereb. Cortex 3(4): 273-289.

DeFelipe, J., Alonso-Nanclares, L. and Arellano, J. I. (2002). "Microstructure of the neocortex: comparative aspects." J Neurocytol 31(3-5): 299-316.

DeFelipe, J., Hendry, S. H. and Jones, E. G. (1986). "A correlative electron microscopic study of basket cells and large GABAergic neurons in the monkey sensory-motor cortex." Neuroscience 17(4): 991-1009.

Del Castillo, J. and Katz, B. (1954). "Quantal components of the end-plate potential." J Physiol 124(3): 560-73.

Deuchars, J., West, D. C. and Thomson, A. M. (1994). "Relationships between morphology and physiology of pyramid-pyramid single axon connections in rat neocortex in vitro." J Physiol 478 Pt 3: 423-35.

Di Iorio, P., Battaglia, G., Ciccarelli, R., Ballerini, P., Giuliani, P., Poli, A., Nicoletti, F. and Caciagli, F. (1996). "Interaction between A1 adenosine and class II metabotropic glutamate receptors in the regulation of purine and glutamate release from rat hippocampal slices." J Neurochem 67(1): 302-9.

East, S. J., Hill, M. P. and Brotchie, J. M. (1995). "Metabotropic glutamate receptor agonists inhibit endogenous glutamate release from rat striatal synaptosomes." Eur J Pharmacol 277(1): 117-21.

Edwards, F. A., Konnerth, A. and Sakmann, B. (1990). "Quantal analysis of inhibitory synaptic transmission in the dentate gyrus of rat hippocampal slices: a patch-clamp study." J Physiol 430: 213-49.

Egger, V., Feldmeyer, D. and Sakmann, B. (1999). "Coincidence detection and changes of synaptic efficacy in spiny stellate neurons in rat barrel cortex." Nat Neurosci 2(12): 1098-1105.

Eliassen, J. C., Baynes, K. and Gazzaniga, M. S. (2000). "Anterior and posterior callosal contributions to simultaneous bimanual movements of the hands and fingers." Brain 123 Pt 12: 2501-11.

Faber, D. S. and Korn, H. (1991). "Applicability of the coefficient of variation method for analyzing synaptic plasticity." Biophys J 60(5): 1288-94.

Faber, D. S., Young, W. S., Legendre, P. and Korn, H. (1992). "Intrinsic quantal variability

due to stochastic properties of receptor-transmitter interactions." Science 258(5087): 1494-8.

Fairen, A. and Valverde, F. (1980). "A specialized type of neuron in the visual cortex of cat: a Golgi and electron microscope study of chandelier cells." J Comp Neurol 194(4): 761-79.

Farinas, I. and DeFelipe, J. (1991). "Patterns of synaptic input on corticocortical and corticothalamic cells in the cat visual cortex. I. The cell body." J Comp Neurol 304(1): 53-69.

Fatt, P. and Katz, B. (1952). "Spontaneous subthreshold activity at motor nerve endings." J Physiol 117(1): 109-28.

Feldman, D. E. (2000). "Timing-Based LTP and LTD at Vertical Inputs to Layer II/III Pyramidal Cells in Rat Barrel Cortex." Neuron 27(1): 45-56.

Feldmeyer, D., Lubke, J., Silver, R. A. and Sakmann, B. (2002). "Synaptic connections between layer 4 spiny neurone-layer 2/3 pyramidal cell pairs in juvenile rat barrel cortex: physiology and anatomy of interlaminar signalling within a cortical column." J Physiol 538(Pt 3): 803-22.

Feldmeyer, D. and Sakmann, B. (2000). "Synaptic efficacy and reliability of excitatory connections between the principal neurones of the input (layer 4) and output layer (layer 5) of the neocortex." J Physiol 525(Pt 1): 31-9.

Ferri, R., Cosentino, F. I. I., Elia, M., Musumeci, S. A., Marinig, R. and Bergonzi, P. (2001). "Relationship between Delta, Sigma, Beta, and Gamma EEG bands at REM sleep onset and REM sleep end." Clinical Neurophysiology 112(11): 2046-2052.

Fitzjohn, S. M., Irving, A. J., Palmer, M. J., Harvey, J., Lodge, D. and Collingridge, G. L. (1996). "Activation of group I mGluRs potentiates NMDA responses in rat hippocampal slices." Neurosci Lett 203(3): 211-3.

Flanders, M. (2005). "Functional somatotopy in sensorimotor cortex." Neuroreport 16(4): 313-6.

Fombonne, E. (2006). Past and Future Perspectives on Autism Epidemiology. Understanding Autism: From basic science to treatment. S. O. Moldin and J. L. Rubenstein. Boca Raton, CRC Press.

Freund, T. F., Martin, K. A., Smith, A. D. and Somogyi, P. (1983). "Glutamate decarboxylase-immunoreactive terminals of Golgi-impregnated axoaxonic cells and of presumed basket cells in synaptic contact with pyramidal neurons of the cat's visual cortex." J Comp Neurol 221(3): 263-78.

Froemke, R. C., Poo, M. M. and Dan, Y. (2005). "Spike-timing-dependent synaptic plasticity depends on dendritic location." Nature 434(7030): 221-5.

Fuhrmann, G., Cowan, A., Segev, I., Tsodyks, M. and Stricker, C. (2004). "Multiple mechanisms govern the dynamics of depression at neocortical synapses of young rats." J Physiol 557(Pt 2): 415-38.

Games, K. D. and Winer, J. A. (1988). "Layer V in rat auditory cortex: projections to the inferior colliculus and contralateral cortex." Hear Res 34(1): 1-25.

Gazzaniga, M. S., Kutas, M., Van Petten, C. and Fendrich, R. (1989). "Human callosal function: MRI-verified neuropsychological functions." Neurology 39(7): 942-946.

Genton, P., Semah, F. and Trinka, E. (2006). "Valproic acid in epilepsy : pregnancy-related issues." Drug Saf 29(1): 1-21.

Gott, P. S. and Saul, R. E. (1978). "Agenesis of the corpus callosum: limits of functional compensation." Neurology 28(12): 1272-1279.

Grady, C. L., McIntosh, A. R., Horwitz, B., Maisog, J. M., Ungerleider, L. G., Mentis, M. J., Pietrini, P., Schapiro, M. B. and Haxby, J. V. (1995). "Age-related reductions in human recognition memory due to impaired encoding." Science 269(5221): 218-21.

Grassi, S., Frondaroli, A. and Pettorossi, V. E. (2002). "Different metabotropic glutamate receptors play opposite roles in synaptic plasticity of the rat medial vestibular nuclei." J Physiol 543(Pt 3): 795-806.

Groc, L., Heine, M., Cognet, L., Brickley, K., Stephenson, F. A., Lounis, B. and Choquet, D. (2004). "Differential activity-dependent regulation of the lateral mobilities of AMPA and NMDA receptors." Nat Neurosci 7(7): 695-6.

Guillery, R. W. and Harting, J. K. (2003). "Structure and connections of the thalamic reticular nucleus: Advancing views over half a century." The Journal of Comparative Neurology 463(4): 360-371.

Gupta, A., Toledo-Rodriguez, M., Silberberg, G. and Markram, H. (2004). Interneuron Heterogeneity in the Neocortex. Escitatory - Inhibitory balance. Synapses, Circuits, Systems. T. K. Hensch and M. Fagiolini. New York, Plenum press: 149-172.

Gupta, A., Wang, Y. and Markram, H. (2000). "Organizing Principles for a Diversity of GABAergic Interneurons and Synapses in the Neocortex." Science 287(5451): 273-278.

Gustafsson, B. and Wigstrom, H. (1986). "Hippocampal long-lasting potentiation produced by pairing single volleys and brief conditioning tetani evoked in separate afferents." J. Neurosci. 6(6): 1575-1582.

Gustafsson, B., Wigstrom, H., Abraham, W. C. and Huang, Y. Y. (1987). "Long-term potentiation in the hippocampus using depolarizing current pulses as the conditioning stimulus to single volley synaptic potentials." J. Neurosci. 7(3): 774-780.

Halasy, K., Buhl, E. H., Lorinczi, Z., Tamas, G. and Somogyi, P. (1996). "Synaptic target selectivity and input of GABAergic basket and bistratified interneurons in the CA1 area of the rat hippocampus." Hippocampus 6(3): 306-29.

Hallman, L. E., Schofield, B. R. and Lin, C. S. (1988). "Dendritic morphology and axon collaterals of corticotectal, corticopontine, and callosal neurons in layer V of primary visual cortex of the hooded rat." J Comp Neurol 272(1): 149-60.

Handelmann, G. E. and Olton, D. S. (1981). "Spatial memory following damage to hippocampal CA3 pyramidal cells with kainic acid: impairment and recovery with preoperative training." Brain Res 217(1): 41-58.

Hedberg, T. G. and Stanton, P. K. (1996). "Long-term plasticity in cingulate cortex requires both NMDA and metabotropic glutamate receptor activation." Eur J Pharmacol 310(1): 19-27.

Henderson, J., Henderson, R. and Greene, E. (1973). "Impairment of memory with administration of KCl to the hippocampus." Behav Biol 9(6): 655-70.

Hendry, S. H., Houser, C. R., Jones, E. G. and Vaughn, J. E. (1983). "Synaptic organization of immunocytochemically identified GABA neurons in the monkey sensory-motor cortex." J Neurocytol 12(4): 639-60.

Herrero, I., Castro, E., Miras-Portugal, M. T. and Sanchez-Prieto, J. (1996). "Two components of glutamate exocytosis differentially affected by presynaptic modulation." J Neurochem 67(6): 2346-54.

Herrero, I., Miras-Portugal, M. T. and Sanchez-Prieto, J. (1998). "Functional switch from facilitation to inhibition in the control of glutamate release by metabotropic glutamate receptors." J Biol Chem 273(4): 1951-8.

Holtmaat, A., Wilbrecht, L., Knott, G. W., Welker, E. and Svoboda, K. (2006). "Experience-dependent and cell-type-specific spine growth in the neocortex." Nature 441(7096): 979-983.

Holtmaat, A. J. G. D., Trachtenberg, J. T., Wilbrecht, L., Shepherd, G. M., Zhang, X., Knott, G. W. and Svoboda, K. (2005). "Transient and Persistent Dendritic Spines in the Neocortex In Vivo." Neuron 45(2): 279-291.

Horton, J. C. (2006). "Ocular integration in the human visual cortex." Can J Ophthalmol 41(5): 584-93.

Hosli, L., Andres, P. F. and Hosli, E. (1973). "Ionic mechanisms underlying the depolarization of L-glutamate on rat and human spinal neurones in tissue culture." Experientia 29(10): 1244-7.

Hubel, D. H. and Wiesel, T. N. (1962). "Receptive fields, binocular interaction and functional architecture in the cat's visual cortex." The Journal Of Physiology 160: 106-154.

Hubener, M. and Bolz, J. (1988). "Morphology of identified projection neurons in layer 5 of rat visual cortex." Neurosci Lett 94(1-2): 76-81.

Innocenti, G. M. (1986). General Organization of Callosal Connections in the Cerebral Cortex. Sensory-Motor Areas and Aspects of Cortical Connectivity. E. G. Jones and A. Peters. New York, Plenum Press. 5.

Izquierdo, I. (1994). "Pharmacological evidence for a role of long-term potentiation in memory." FASEB J. 8(14): 1139-1145.

Izquierdo, I. and Medina, J. H. (1995). "Correlation between the Pharmacology of Long-Term Potentiation and the Pharmacology of Memory." Neurobiology of Learning and Memory 63(1): 19-32.

Jack, J. J., Redman, S. J. and Wong, K. (1981). "The components of synaptic potentials evoked in cat spinal motoneurones by impulses in single group Ia afferents." J Physiol 321: 65-96.

Jarrard, L. E. (1975). "Role of interference in retention by rats with hippocampal lesions." J Comp Physiol Psychol 89(5): 400-8.

Jarrard, L. E. (1993). "On the role of the hippocampus in learning and memory in the rat." Behav Neural Biol 60(1): 9-26.

Johnston, D. and Wu, S. M.-S. (1997). Foundations of Cellular Neurophysiology. Cambridge, Massachusetts, MIT Press.

Jonas, P., Racca, C., Sakmann, B., Seeburg, P. H. and Monyer, H. (1994). "Differences in Ca2+ permeability of AMPA-type glutamate receptor channels in neocortical neurons caused by differential GluR-B subunit expression." Neuron 12(6): 1281-1289.

Kaiser, K. M., Lubke, J., Zilberter, Y. and Sakmann, B. (2004). "Postsynaptic calcium influx at single synaptic contacts between pyramidal neurons and bitufted interneurons in layer 2/3 of rat neocortex is enhanced by backpropagating action potentials." J Neurosci 24(6): 1319-29.

Kaldy, Z. and Sigala, N. (2004). "The neural mechanisms of object working memory: what is where in the infant brain?" Neuroscience & Biobehavioral Reviews 28(2): 113-121.

Kalisman, N., Silberberg, G. and Markram, H. (2005). "The neocortical microcircuit as a tabula rasa." PNAS 102(3): 880-5.

Kasper, E. M., Larkman, A. U., Lubke, J. and Blakemore, C. (1994a). "Pyramidal neurons in layer 5 of the rat visual cortex. I. Correlation among cell morphology, intrinsic electrophysiological properties, and axon targets." J Comp Neurol 339(4): 459-74.

Kasper, E. M., Larkman, A. U., Lubke, J. and Blakemore, C. (1994b). "Pyramidal neurons in layer 5 of the rat visual cortex. II. Development of electrophysiological properties." J Comp Neurol 339(4): 475-94.

Kasper, E. M., Lubke, J., Larkman, A. U. and Blakemore, C. (1994c). "Pyramidal neurons in layer 5 of the rat visual cortex. III. Differential maturation of axon targeting, dendritic morphology, and electrophysiological properties." J Comp Neurol 339(4): 495-518.

Katz, B. and Miledi, R. (1968). "The role of calcium in neuromuscular facilitation." J Physiol 195(2): 481-92.

Katz, L. C. (1987). "Local circuitry of identified projection neurons in cat visual cortex brain slices." J Neurosci 7(4): 1223-49.

Katz, L. C., Burkhalter, A. and Dreyer, W. J. (1984). "Fluorescent latex microspheres as a retrograde neuronal marker for in vivo and in vitro studies of visual cortex." Nature 310(5977): 498-500.

Katz, L. C. and Iarovici, D. M. (1990). "Green fluorescent latex microspheres: a new retrograde tracer." Neuroscience 34(2): 511-20.

Kawaguchi, Y. and Kubota, Y. (1998). "Neurochemical features and synaptic connections of large physiologically-identified GABAergic cells in the rat frontal cortex." Neuroscience 85(3): 677-701.

Keller, A. (1991). "Intrinsic synaptic organization of the motor cortex." Cereb Cortex 3(5): 430-441.

Kimura, F., Tsumoto, T., Nishigori, A. and Yoshimura, Y. (1990). "Long-term depression but not potentiation is induced in Ca(2+)-chelated visual cortex neurons." Neuroreport 1(1): 65-8.

Kirov, S. A., Sorra, K. E. and Harris, K. M. (1999). "Slices have more synapses than perfusion-fixed hippocampus from both young and mature rats." J Neurosci 19(8): 2876-86.

Koch, S., Jager-Roman, E., Losche, G., Nau, H., Rating, D. and Helge, H. (1996). "Antiepileptic drug treatment in pregnancy: drug side effects in the neonate and neurological outcome." Acta Paediatr 85(6): 739-46.

Korn, H. and Faber, D. S. (1991). "Quantal analysis and synaptic efficacy in the CNS." Trends Neurosci 14(10): 439-45.

Larkman, A. and Mason, A. (1990). "Correlations between morphology and electrophysiology of pyramidal neurons in slices of rat visual cortex. I. Establishment of cell classes." J Neurosci 10(5): 1407-14.

Larkum, M. E., Kaiser, K. M. and Sakmann, B. (1999). "Calcium electrogenesis in distal apical dendrites of layer 5 pyramidal cells at a critical frequency of back-propagating action potentials." Proc Natl Acad Sci U S A 96(25): 14600-4.

Lavond, D. G., Kim, J. J. and Thompson, R. F. (1993). "Mammalian Brain Substrates of Aversive Classical Conditioning." Annual Review of Psychology 44(1): 317-342.

Letzkus, J. J., Kampa, B. M. and Stuart, G. J. (2006). "Learning Rules for Spike Timing-Dependent Plasticity Depend on Dendritic Synapse Location." J. Neurosci. 26(41): 10420-10429.

LeVay, S. (1973). "Synaptic patterns in the visual cortex of the cat and monkey. Electron microscopy of Golgi Preparations." The Journal of Comparative Neurology 150(1): 53-85.

LeVay, S. and Sherk, H. (1981). "The visual claustrum of the cat. I. Structure and connections." J Neurosci 1(9): 956-80.

Levy, W. B. and Steward, O. (1983). "Temporal contiguity requirements for long-term associative potentiation/depression in the hippocampus." Neuroscience 8(4): 791-7.

Li, X. G., Somogyi, P., Tepper, J. M. and Buzsaki, G. (1992). "Axonal and dendritic arborization of an intracellularly labeled chandelier cell in the CA1 region of rat hippocampus." Exp Brain Res 90(3): 519-25.

Liao, D., Hessler, N. A. and Malinow, R. (1995). "Activation of postsynaptically silent synapses during pairing-induced LTP in CA1 region of hippocampal slice." Nature 375(6530): 400-4.

Linden, D. J. and Routtenberg, A. (1989). "The role of protein kinase C in long-term potentiation: a testable model." Brain Research Reviews 14(3): 279-296.

Lledo, P., Hjelmstad, G. O., Mukherji, S., Soderling, T. R., Malenka, R. C. and Nicoll, R. A. (1995). "Calcium/Calmodulin-Dependent Kinase II and Long-Term Potentiation Enhance Synaptic Transmission by the Same Mechanism." PNAS 92(24): 11175-

11179.
Lorente de Nó, R. (1938). Architectonics and structure of the cerebral cortex. Physiology of the Nervous System. J. F. Fulton. New York, Oxford University Press: 291-330.
Lu, W.-Y., Man, H.-Y., Ju, W., Trimble, W. S., MacDonald, J. F. and Wang, Y. T. (2001). "Activation of Synaptic NMDA Receptors Induces Membrane Insertion of New AMPA Receptors and LTP in Cultured Hippocampal Neurons." Neuron 29(1): 243-254.
Lu, Y. M., Jia, Z., Janus, C., Henderson, J. T., Gerlai, R., Wojtowicz, J. M. and Roder, J. C. (1997). "Mice lacking metabotropic glutamate receptor 5 show impaired learning and reduced CA1 long-term potentiation (LTP) but normal CA3 LTP." J Neurosci 17(13): 5196-205.
Lubke, J., Egger, V., Sakmann, B. and Feldmeyer, D. (2000). "Columnar Organization of Dendrites and Axons of Single and Synaptically Coupled Excitatory Spiny Neurons in Layer 4 of the Rat Barrel Cortex." J. Neurosci. 20(14): 5300-5311.
Lund, J. S. (1973). "Organization of neurons in the visual cortex, area 17, of the monkey Macaca mulatta." The Journal of Comparative Neurology 147(4): 455-495.
Lund, J. S. (1988). "Anatomical organization of macaque monkey striate visual cortex." Annu Rev Neurosci 11: 253-88.
Magee, J. C. and Johnston, D. (1997). "A Synaptically Controlled, Associative Signal for Hebbian Plasticity in Hippocampal Neurons." Science 275(5297): 209-213.
Malinow, R. and Malenka, R. C. (2002). "AMPA receptor trafficking and synaptic plasticity." Annu Rev Neurosci 25: 103-26.
Markram, H. (1997). "A network of tufted layer 5 pyramidal neurons." Cereb Cortex 7(6): 523-33.
Markram, H., Helm, P. J. and Sakmann, B. (1995). "Dendritic calcium transients evoked by single back-propagating action potentials in rat neocortical pyramidal neurons." J Physiol 485 (Pt 1): 1-20.
Markram, H., Lubke, J., Frotscher, M., Roth, A. and Sakmann, B. (1997a). "Physiology and anatomy of synaptic connections between thick tufted pyramidal neurones in the developing rat neocortex." J Physiol 500 (Pt 2): 409-40.
Markram, H., Lubke, J., Frotscher, M. and Sakmann, B. (1997b). "Regulation of Synaptic Efficacy by Coincidence of Postsynaptic APs and EPSPs." Science 275(5297): 213-215.
Markram, H., Toledo-Rodriguez, M., Wang, Y., Gupta, A., Silberberg, G. and Wu, C. (2004). "Interneurons of the Neocortical Inhibitory System." Nature Reviews Neuroscience 5(10): 793-807.
Markram, H. and Tsodyks, M. (1996a). "Redistribution of synaptic efficacy between neocortical pyramidal neurons." Nature 382(6594): 807-10.
Markram, H. and Tsodyks, M. (1996b). "Redistribution of synaptic efficacy: a mechanism to generate infinite synaptic input diversity from a homogeneous population of neurons without changing absolute synaptic efficacies." J Physiol Paris 90(3-4): 229-32.
Markram, H., Wang, Y. and Tsodyks, M. (1998). "Differential signaling via the same axon of neocortical pyramidal neurons." PNAS 95(9): 5323-5328.
Markram, K., Rinaldi, T., La Mendola, D., Sandi, C. and Markram, H. (2007). "Abnormal fear conditioning and amygdala processing in an animal model of autism." Submitted.
Martin, K. A., Somogyi, P. and Whitteridge, D. (1983). "Physiological and morphological properties of identified basket cells in the cat's visual cortex." Exp Brain Res 50(2-3): 193-200.
Martinez-Garcia, F., Gonzalez-Hernandez, T. and Martinez-Millan, L. (1994). "Pyramidal and nonpyramidal callosal cells in the striate cortex of the adult rat." J Comp Neurol

350(3): 439-51.
Mawer, G., Clayton-Smith, J., Coyle, H. and Kini, U. (2002). "Outcome of pregnancy in women attending an outpatient epilepsy clinic: adverse features associated with higher doses of sodium valproate." Seizure 11(8): 512-8.
Mayer, M. L., Westbrook, G. L. and Guthrie, P. B. (1984). "Voltage-dependent block by Mg2+ of NMDA responses in spinal cord neurones." Nature 309(5965): 261-3.
McCormick, D. A., Connors, B. W., Lighthall, J. W. and Prince, D. A. (1985). "Comparative electrophysiology of pyramidal and sparsely spiny stellate neurons of the neocortex." J Neurophysiol 54(4): 782-806.
McLin Iii, D. E., Miasnikov, A. A. and Weinberger, N. M. (2003). "CS-specific gamma, theta, and alpha EEG activity detected in stimulus generalization following induction of behavioral memory by stimulation of the nucleus basalis." Neurobiology of Learning and Memory 79(2): 152-176.
McNaughton, N. C., Bleakman, D. and Randall, A. D. (1998). "Electrophysiological characterisation of the human N-type Ca2+ channel II: activation and inactivation by physiological patterns of activity." Neuropharmacology 37(1): 67-81.
Mercer, A., West, D. C., Morris, O. T., Kirchhecker, S., Kerkhoff, J. E. and Thomson, A. M. (2005). "Excitatory connections made by presynaptic cortico-cortical pyramidal cells in layer 6 of the neocortex." Cereb Cortex 15(10): 1485-96.
Miledi, R. and Slater, C. R. (1966). "The action of calcium on neuronal synapses in the squid." J Physiol 184(2): 473-98.
Miserendino, M. J. D., Sananes, C. B., Melia, K. R. and Davis, M. (1990). "Blocking of acquisition but not expression of conditioned fear-potentiated startle by NMDA antagonists in the amygdala." Nature 345(6277): 716-718.
Miyashita, Y. (2004). "Cognitive Memory: Cellular and Network Machineries and Their Top-Down Control." Science 306(5695): 435-440.
Moore, S. J., Turnpenny, P., Quinn, A., Glover, S., Lloyd, D. J., Montgomery, T. and Dean, J. C. (2000). "A clinical study of 57 children with fetal anticonvulsant syndromes." J Med Genet 37(7): 489-97.
Morgan, J. I. and Curran, T. (1988). "Calcium as a modulator of the immediate-early gene cascade in neurons." Cell Calcium 9(5-6): 303-11.
Moroni, F., Cozzi, A., Lombardi, G., Sourtcheva, S., Leonardi, P., Carfi, M. and Pellicciari, R. (1998). "Presynaptic mGlu1 type receptors potentiate transmitter output in the rat cortex." Eur J Pharmacol 347(2-3): 189-95.
Morris, J. S., Frith, C. D., Perrett, D. I., Rowland, D., Young, A. W., Calder, A. J. and Dolan, R. J. (1996). "A differential neural response in the human amygdala to fearful and happy facial expressions." Nature 383(6603): 812-815.
Morris, R. G. M. (2003). "Long-term potentiation and memory." Philosophical Transactions of the Royal Society B: Biological Sciences 358(1432): 643-647.
Mountcastle, V. B. (1957). "Modality and topographic properties of single neurons of cat's somatic sensory cortex." J Neurophysiol 20(4): 408-34.
Mountcastle, V. B. (1997). "The columnar organization of the neocortex." Brain 120 (Pt 4): 701-22.
Mulkey, R. M., Herron, C. E. and Malenka, R. C. (1993). "An essential role for protein phosphatases in hippocampal long-term depression." Science 261(5124): 1051-1055.
Nakanishi, S. (1994). "Metabotropic glutamate receptors: synaptic transmission, modulation, and plasticity." Neuron 13(5): 1031-7.
Nakanishi, S., Nakajima, Y., Masu, M., Ueda, Y., Nakahara, K., Watanabe, D., Yamaguchi, S., Kawabata, S. and Okada, M. (1998). "Glutamate receptors: brain function and signal transduction." Brain Res Brain Res Rev 26(2-3): 230-5.

Neuper, C. and Pfurtscheller, G. (2001). "Event-related dynamics of cortical rhythms: frequency-specific features and functional correlates." Int J Psychophysiol 43(1): 41-58.

Nevian, T., Larkum, M. E., Polsky, A. and Schiller, J. (2007). "Properties of basal dendrites of layer 5 pyramidal neurons: a direct patch-clamp recording study." Nat Neurosci 10(2): 206-14.

Nevian, T. and Sakmann, B. (2006). "Spine Ca2+ Signaling in Spike-Timing-Dependent Plasticity." J. Neurosci. 26(43): 11001-11013.

Nowak, L., Bregestovski, P., Ascher, P., Herbet, A. and Prochiantz, A. (1984). "Magnesium gates glutamate-activated channels in mouse central neurones." Nature 307(5950): 462-5.

O'Connor, J. J., Rowan, M. J. and Anwyl, R. (1995). "Tetanically induced LTP involves a similar increase in the AMPA and NMDA receptor components of the excitatory postsynaptic current: investigations of the involvement of mGlu receptors." J. Neurosci. 15(3, Part 1): 2013-2020.

O'Mara, S. M., Rowan, M. J. and Anwyl, R. (1995). "Metabotropic glutamate receptor-induced homosynaptic long-term depression and depotentiation in the dentate gyrus of the rat hippocampus in vitro." Neuropharmacology 34(8): 983-989.

Ohki, K., Chung, S., Ch'ng, Y. H., Kara, P. and Reid, R. C. (2005). "Functional imaging with cellular resolution reveals precise micro-architecture in visual cortex." Nature 433(7026): 597-603.

Oliet, S. H. R., Malenka, R. C. and Nicoll, R. A. (1997). "Two Distinct Forms of Long-Term Depression Coexist in CA1 Hippocampal Pyramidal Cells." Neuron 18(6): 969-982.

Olton, D. S. and Feustle, W. A. (1981). "Hippocampal function required for nonspatial working memory." Exp Brain Res 41(3-4): 380-9.

Ornoy, A. (2006). "Neuroteratogens in man: an overview with special emphasis on the teratogenicity of antiepileptic drugs in pregnancy." Reprod Toxicol 22(2): 214-26.

Pastalkova, E., Serrano, P., Pinkhasova, D., Wallace, E., Fenton, A. A. and Sacktor, T. C. (2006). "Storage of Spatial Information by the Maintenance Mechanism of LTP." Science 313(5790): 1141-1144.

Perez-Garci, E., Gassmann, M., Bettler, B. and Larkum, M. E. (2006). "The GABAB1b isoform mediates long-lasting inhibition of dendritic Ca2+ spikes in layer 5 somatosensory pyramidal neurons." Neuron 50(4): 603-16.

Pin, J. P. and Acher, F. (2002). "The metabotropic glutamate receptors: structure, activation mechanism and pharmacology." Curr Drug Targets CNS Neurol Disord 1(3): 297-317.

Polsky, A., Mel, B. W. and Schiller, J. (2004). "Computational subunits in thin dendrites of pyramidal cells." Nat Neurosci 7(6): 621-7.

Pons, T. P., Garraghty, P. E., Cusick, C. G. and Kaas, J. H. (1985). "The somatotopic organization of area 2 in macaque monkeys." J Comp Neurol 241(4): 445-66.

Pouille, F. and Scanziani, M. (2004). "Routing of spike series by dynamic circuits in the hippocampus." Nature 429(6993): 717-23.

Press, G. A., Amaral, D. G. and Squire, L. R. (1989). "Hippocampal abnormalities in amnesic patients revealed by high-resolution magnetic resonance imaging." Nature 341(6237): 54-7.

Rae, M. G. and Irving, A. J. (2004). "Both mGluR1 and mGluR5 mediate Ca2+ release and inward currents in hippocampal CA1 pyramidal neurons." Neuropharmacology 46(8): 1057-69.

Rahamimoff, R. (1968). "A dual effect of calcium ions on neuromuscular facilitation." J Physiol 195(2): 471-80.

Rasalam, A. D., Hailey, H., Williams, J. H., Moore, S. J., Turnpenny, P. D., Lloyd, D. J. and

Dean, J. C. (2005). "Characteristics of fetal anticonvulsant syndrome associated autistic disorder." Dev Med Child Neurol 47(8): 551-5.

Reyes, A., Lujan, R., Rozov, A., Burnashev, N., Somogyi, P. and Sakmann, B. (1998). "Target-cell-specific facilitation and depression in neocortical circuits." Nat Neurosci 1(4): 279-85.

Reymann, K. G., Matthies, H. K., Schulzeck, K. and Matthies, H. (1989). "N-methyl-D-aspartate receptor activation is required for the induction of both early and late phases of long-term potentiation in rat hippocampal slices." Neurosci Lett 96(1): 96-101.

Ribak, C. E. (1978). "Aspinous and sparsely-spinous stellate neurons in the visual cortex of rats contain glutamic acid decarboxylase." J Neurocytol 7(4): 461-78.

Rinaldi, T., Kulangara, K., Antoniello, K. and Markram, H. (2007a). "Elevated NMDA receptor levels and enhanced postsynaptic long term potentiation induced by prenatal exposure to valproic acid." Submitted.

Rinaldi, T., Silberberg, G. and Markram, H. (2007b). "Hyperconnectivity of local neocortical microcircuitry induced by prenatal exposure to valproic acid." Submitted.

Romano, C., Sesma, M. A., McDonald, C. T., O'Malley, K., Van den Pol, A. N. and Olney, J. W. (1995). "Distribution of metabotropic glutamate receptor mGluR5 immunoreactivity in rat brain." J Comp Neurol 355(3): 455-69.

Rossi, P., D'Angelo, E. and Taglietti, V. (1996). "Differential long-lasting potentiation of the NMDA and non-NMDA synaptic currents induced by metabotropic and NMDA receptor coactivation in cerebellar granule cells." The European Journal Of Neuroscience 8(6): 1182-1189.

Salt, T. E. and Eaton, S. A. (1996). "Functions of ionotropic and metabotropic glutamate receptors in sensory transmission in the mammalian thalamus." Prog Neurobiol 48(1): 55-72.

Schlosser, R., Roschke, J., Rossbach, W. and Benkert, O. (1998). "Conventional and spectral power analysis of all-night sleep EEG after subchronic treatment with paroxetine in healthy male volunteers." European Neuropsychopharmacology 8(4): 273-278.

Schneider, T. and Przewlocki, R. (2005). "Behavioral alterations in rats prenatally exposed to valproic acid: animal model of autism." Neuropsychopharmacology 30(1): 80-9.

Schofield, B. R., Hallman, L. E. and Lin, C. S. (1987). "Morphology of corticotectal cells in the primary visual cortex of hooded rats." J Comp Neurol 261(1): 85-97.

Schwindt, P. and Crill, W. (1999). "Mechanisms underlying burst and regular spiking evoked by dendritic depolarization in layer 5 cortical pyramidal neurons." J Neurophysiol 81(3): 1341-54.

Sharp, P. E., McNaughton, B. L. and Barnes, C. A. (1985). "Enhancement of hippocampal field potentials in rats exposed to a novel, complex environment." Brain Res 339(2): 361-5.

Shu, Y., Hasenstaub, A. and McCormick, D. A. (2003). "Turning on and off recurrent balanced cortical activity." Nature 423(6937): 288-93.

Silberberg, G., Gupta, A. and Markram, H. (2002). "Stereotypy in neocortical microcircuits." Trends Neurosci 25(5): 227-30.

Silberberg, G. and Markram, H. (2007). "Disynaptic Inhibition between Neocortical Pyramidal Cells Mediated by Martinotti Cells." Neuron 53(5): 735-746.

Silver, R. A., Lubke, J., Sakmann, B. and Feldmeyer, D. (2003). "High-probability uniquantal transmission at excitatory synapses in barrel cortex." Science 302(5652): 1981-4.

Sjostrom, P. J. and Hausser, M. (2006). "A cooperative switch determines the sign of synaptic plasticity in distal dendrites of neocortical pyramidal neurons." Neuron 51(2): 227-38.

Skelton, R. W., Miller, J. J. and Phillips, A. G. (1985). "Long-term potentiation facilitates behavioral responding to single-pulse stimulation of the perforant path." Behav

Neurosci 99(4): 603-20.
Somogyi, J., Baude, A., Omori, Y., Shimizu, H., El Mestikawy, S., Fukaya, M., Shigemoto, R., Watanabe, M. and Somogyi, P. (2004). "GABAergic basket cells expressing cholecystokinin contain vesicular glutamate transporter type 3 (VGLUT3) in their synaptic terminals in hippocampus and isocortex of the rat." Eur J Neurosci 19(3): 552-69.
Somogyi, P., Kisvarday, Z. F., Martin, K. A. and Whitteridge, D. (1983). "Synaptic connections of morphologically identified and physiologically characterized large basket cells in the striate cortex of cat." Neuroscience 10(2): 261-94.
Somogyi, P., Tamas, G., Lujan, R. and Buhl, E. H. (1998). "Salient features of synaptic organisation in the cerebral cortex." Brain Res Brain Res Rev 26(2-3): 113-35.
Spiegel, A., Tonner, P. H. and Renna, M. (2006). "Altered states of consciousness: processed EEG in mental disease." Best Pract Res Clin Anaesthesiol 20(1): 57-67.
Spruston, N., Schiller, Y., Stuart, G. and Sakmann, B. (1995). "Activity-dependent action potential invasion and calcium influx into hippocampal CA1 dendrites." Science 268(5208): 297-300.
Staiger, J. F., Kotter, R., Zilles, K. and Luhmann, H. J. (2000). "Laminar characteristics of functional connectivity in rat barrel cortex revealed by stimulation with caged-glutamate." Neurosci Res 37(1): 49-58.
Steriade, M., Timofeev, I. and Grenier, F. (2001). "Natural Waking and Sleep States: A View From Inside Neocortical Neurons." J Neurophysiol 85(5): 1969-1985.
Stuart, G., Schiller, J. and Sakmann, B. (1997). "Action potential initiation and propagation in rat neocortical pyramidal neurons." J Physiol (Lond) 505(3): 617-632.
Tamas, G., Somogyi, P. and Buhl, E. H. (1998). "Differentially interconnected networks of GABAergic interneurons in the visual cortex of the cat." J Neurosci 18(11): 4255-70.
Tardin, C., Cognet, L., Bats, C., Lounis, B. and Choquet, D. (2003). "Direct imaging of lateral movements of AMPA receptors inside synapses." Embo J 22(18): 4656-65.
Tebano, M. T., Martire, A., Rebola, N., Pepponi, R., Domenici, M. R., Gro, M. C., Schwarzschild, M. A., Chen, J. F., Cunha, R. A. and Popoli, P. (2005). "Adenosine A2A receptors and metabotropic glutamate 5 receptors are co-localized and functionally interact in the hippocampus: a possible key mechanism in the modulation of N-methyl-d-aspartate effects." Journal of Neurochemistry 95(4): 1188-1200.
Thomson, A. M. (2003). "Presynaptic frequency- and pattern-dependent filtering." J Comput Neurosci 15(2): 159-202.
Thomson, A. M. and Bannister, A. P. (1999). "Release-independent depression at pyramidal inputs onto specific cell targets: dual recordings in slices of rat cortex." J Physiol (Lond) 519(1): 57-70.
Thomson, A. M. and Bannister, A. P. (2003). "Interlaminar connections in the neocortex." Cereb Cortex 13(1): 5-14.
Thomson, A. M., Deuchars, J. and West, D. C. (1993a). "Large, deep layer pyramid-pyramid single axon EPSPs in slices of rat motor cortex display paired pulse and frequency-dependent depression, mediated presynaptically and self-facilitation, mediated postsynaptically." J Neurophysiol 70(6): 2354-69.
Thomson, A. M., Deuchars, J. and West, D. C. (1993b). "Single axon excitatory postsynaptic potentials in neocortical interneurons exhibit pronounced paired pulse facilitation." Neuroscience 54(2): 347-60.
Thomson, A. M. and West, D. C. (2003). "Presynaptic frequency filtering in the gamma frequency band; dual intracellular recordings in slices of adult rat and cat neocortex." Cereb Cortex 13(2): 136-43.
Thomson, A. M., West, D. C. and Lodge, D. (1985). "An N-methylaspartate receptor-

mediated synapse in rat cerebral cortex: a site of action of ketamine?" Nature 313(6002): 479-81.

Thomson, A. M., West, D. C., Wang, Y. and Bannister, A. P. (2002). "Synaptic connections and small circuits involving excitatory and inhibitory neurons in layers 2-5 of adult rat and cat neocortex: triple intracellular recordings and biocytin labelling in vitro." Cereb Cortex 12(9): 936-53.

Toledo-Rodriguez, M., Gupta, A., Wang, Y., Wu, C. Z. and Markram, H. (2002). Neocortex: basic neuron types. The handbook of brain theory and neural network. M. A. Arbib. Cambridge, The MIT Press: 719-725.

Trachtenberg, J. T., Chen, B. E., Knott, G. W., Feng, G., Sanes, J. R., Welker, E. and Svoboda, K. (2002). "Long-term in vivo imaging of experience-dependent synaptic plasticity in adult cortex." Nature 420(6917): 788-794.

Tsodyks, M., Pawelzik, K. and Markram, H. (1998). "Neural networks with dynamic synapses." Neural Comput 10(4): 821-35.

Tsodyks, M. V. and Markram, H. (1997). "The neural code between neocortical pyramidal neurons depends on neurotransmitter release probability." Proc Natl Acad Sci U S A 94(2): 719-23.

Vazquez, E., Herrero, I., Miras-Portugal, M. T. and Sanchez-Prieto, J. (1995). "Developmental change from inhibition to facilitation in the presynaptic control of glutamate exocytosis by metabotropic glutamate receptors." Neuroscience 68(1): 117-24.

Vercelli, A., Assal, F. and Innocenti, G. M. (1992). "Emergence of callosally projecting neurons with stellate morphology in the visual cortex of the kitten." Exp Brain Res 90(2): 346-58.

Voronin, L. L. (1993). "On the quantal analysis of hippocampal long-term potentiation and related phenomena of synaptic plasticity." Neuroscience 56(2): 275-304.

Wagner, G. C., Reuhl, K. R., Cheh, M., McRae, P. and Halladay, A. K. (2006). "A new neurobehavioral model of autism in mice: pre- and postnatal exposure to sodium valproate." J Autism Dev Disord 36(6): 779-93.

Wang, Y., Gupta, A., Toledo-Rodriguez, M., Wu, C. Z. and Markram, H. (2002). "Anatomical, physiological, molecular and circuit properties of nest basket cells in the developing somatosensory cortex." Cereb Cortex 12(4): 395-410.

Wang, Y., Toledo-Rodriguez, M., Gupta, A., Wu, C., Silberberg, G., Luo, J. and Markram, H. (2004). "Anatomical, physiological and molecular properties of Martinotti cells in the somatosensory cortex of the juvenile rat." J Physiol 561(Pt 1): 65-90.

West, D. C., Mercer, A., Kirchhecker, S., Morris, O. T. and Thomson, A. M. (2006). "Layer 6 cortico-thalamic pyramidal cells preferentially innervate interneurons and generate facilitating EPSPs." Cereb Cortex 16(2): 200-11.

White, E. L. (1989). Cortical Circuits. Synaptic Organization of the Cerebral Cortex. Boston, Birkhauser.

Whitlock, J. R., Heynen, A. J., Shuler, M. G. and Bear, M. F. (2006). "Learning Induces Long-Term Potentiation in the Hippocampus." Science 313(5790): 1093-1097.

Williams, G., King, J., Cunningham, M., Stephan, M., Kerr, B. and Hersh, J. H. (2001). "Fetal valproate syndrome and autism: additional evidence of an association." Dev Med Child Neurol 43(3): 202-6.

Williams, P. G. and Hersh, J. H. (1997). "A male with fetal valproate syndrome and autism." Dev Med Child Neurol 39(9): 632-4.

Williams, S. R. and Stuart, G. J. (2000). "Site independence of EPSP time course is mediated by dendritic I(h) in neocortical pyramidal neurons." J Neurophysiol 83(5): 3177-82.

Woodin, M. A., Ganguly, K. and Poo, M.-m. (2003). "Coincident Pre- and Postsynaptic

Activity Modifies GABAergic Synapses by Postsynaptic Changes in Cl- Transporter Activity." Neuron 39(5): 807-820.

Wyllie, D. J. and Nicoll, R. A. (1994). "A role for protein kinases and phosphatases in the Ca(2+)-induced enhancement of hippocampal AMPA receptor-mediated synaptic responses." Neuron 13(3): 635-43.

Xu-Friedman, M. A., Harris, K. M. and Regehr, W. G. (2001). "Three-dimensional comparison of ultrastructural characteristics at depressing and facilitating synapses onto cerebellar Purkinje cells." J Neurosci 21(17): 6666-72.

Yang, L., Mao, L., Chen, H., Catavsan, M., Kozinn, J., Arora, A., Liu, X. and Wang, J. Q. (2006). "A signaling mechanism from G alpha q-protein-coupled metabotropic glutamate receptors to gene expression: role of the c-Jun N-terminal kinase pathway." J Neurosci 26(3): 971-80.

Zalutsky, R. A. and Nicoll, R. A. (1990). "Comparison of two forms of long-term potentiation in single hippocampal neurons." Science 248(4963): 1619-1624.

Zhang, L. I., Tao, H. W., Holt, C. E., Harris, W. A. and Poo, M.-m. (1998). "A critical window for cooperation and competition among developing retinotectal synapses." Nature 395(6697): 37-44.

Zho, W. M., You, J. L., Huang, C. C. and Hsu, K. S. (2002). "The group I metabotropic glutamate receptor agonist (S)-3,5-dihydroxyphenylglycine induces a novel form of depotentiation in the CA1 region of the hippocampus." J Neurosci 22(20): 8838-49.

Zilberter, Y., Harkany, T. and Holmgren, C. D. (2005). "Dendritic release of retrograde messengers controls synaptic transmission in local neocortical networks." Neuroscientist 11(4): 334-44.

CV

Le Bé Jean-Vincent

Route de Vaulion 2 , CH – 1323 Romainmôtier
Phone : + 41.24.453.10.69., Mobile : +41.76.330.95.12.
e-mail : jean-vincent.lebe@myself.com

Citizenship : French, C permit Birth date : 08.09.1980

Diplomas :

Diploma of **Physical Engineer from the Swiss Federal Institute of Technology, Lausanne** (**Prize of Youth** rewarding the youngest graduated of the school).	2002
French baccalaureate, S series (Physical sciences, speciality physics-chemistry) **distinction good**.	1997

Working Experiences:

PhD student at the Laboratory of Neural Microcircuitry of the Swiss Federal institute of Technology, Lausanne. Research on the connectivity between pyramidal cells in wistar rat neocortex. Use of the patch clamp technique and electrophysiological recordings, calcium imaging, stereotaxic injections.	Since Sept. 2003
Navy Officer in the French navy (watch officer on a mine hunter).	2002-2003
Development of a scientific vulgarization web site on the physics of sailing ships at the vice presidency for the formation of the Swiss Federal Institute of Technology, Lausanne.	Apr-Jun 2002
Crew member by “Etoile Marine” (rental of old sailing ships with crew).	March 2002
Assistant for the first year students at the Swiss Federal Institute of Technology, Lausanne	2001-2002
Placement at the R&D department of Bühler AG, Uzwil (SG), Switzerland (development of printing ink mills).	Aug-Oct. 2000
Miscellaneous temporary jobs (building restoration, inventories, private lessons,…).	1996-2002

Studies :

PhD student at the Swiss Federal Institute of Technology, Neuroscience doctoral school program. Research at the Laboratory of Neural Microcircuitry under the supervision of Prof. Henry Markram.	Since Sept. 2003
Studies at the Swiss Federal Institute of Technology, Lausanne. Physics department. Diploma in theoretical high energy physics.	1997-2002
Third year of studies at the Physics and Astronomy department of the University of Nottingham. Practical work on hybrid Hall sensors.	1999-2000
French high school last year at the "Centre National d'Enseignement à Distance".	1996-1997
Studies at the "Gymnase du Bugnon" in sport-studies program.	1995-1997

Languages :

- French (mother tongue).
- English (fluent, working language since 2003).
- German (intermediate, working language for a placement in 2000).

Computer skills:

- Operating systems: macOS, Windows, Unix (notions).
- Software: Igor, MS Office, Matlab, Labview, TillVision, Photoshop, Illustrator, LaTex.

Publications :

- Massimo Giovannini, Jean-Vincent Le Bé and Stéphane Riederer, "Zero modes of six-dimensional Abelian vortices" (2002), *Class. Quantum Grav. 19 3357–3385*.

- Jean-Vincent Le Bé and Henry Markram, "Spontaneous and evoked synaptic rewiring in the neonatal neocortex" (2006), *PNAS*, 103(35) 13214-13219.

- Jean-Vincent Le Bé, Gilad Silberberg, Yun Wang and Henry Markram, "Morphological, Electrophysiological and Synaptic Properties of Corticocallosal Pyramidal Cells in the Neonatal Rat Neocortex" (2006), Cerebral Cortex, bhl127.

- Jean-Vincent Le Bé and Henry Markram, "A new mechanism for memory: neuronal networks rewiring in the young rat neocortex", Médecine/Sciences décembre 2006, 22(12), 1031-1033.

Posters and presentations :

- "Neuronal and Synaptic Properties of Neocortical Pyramidal Neurons Projecting to Different Targets", **Poster and Talk** at the Lemanic Neuroscience meeting, Les Diablerets, Switzerland, September 27th and 28th 2004.

- "Neuronal and Synaptic Properties of Neocortical Pyramidal Neurons Projecting to Different Targets", **Poster** at the School of Dendrites, Jerusalem, Israel, April 9th-15th 2005.

- "Long-Term Microcircuit Plasticity: A Novel Form of Spontaneous and Evoked Rewiring of Pyramidal Networks", **Poster and Talk** at the Lemanic Neuroscience meeting, Les Diablerets, Switzerland, September 30th and October 1st 2005.

- "Long-Term Microcircuit Plasticity: A Novel Form of Spontaneous and Evoked Rewiring of Pyramidal Networks", **Talk** at the Columbia University in Rafael Yuste's laboratory, New York, USA, November 11th 2005.

- "Long-Term Microcircuit Plasticity: A Novel Form of Spontaneous and Evoked Rewiring of Pyramidal Networks", **Poster** at Society for Neuroscience annual meeting, Washington DC, USA, November 12th-16th 2005.

- "Morphological, Electrophysiological and Synaptic Properties of Connections Between Callosal Layer V Pyramidal Cells", **Poster** at Society for Neuroscience annual meeting, Washington DC, USA, November 12th-16th 2005.

- "The Cortico-Callosal Layer V Pyramidal Cells Network; Morphological, Electrophysiological and Synaptic Properties", **Poster** at the "Channels, Receptors and Synapses" meeting at the Cold Spring Harbor Laboratory, April 18th-22nd 2006.

- "Microcircuit Plasticity, A Novel Form of Spontaneous and Evoked Rewiring of Pyramidal Neurons", **Talk** at the BMI retreat, Le Brassus, Switzerland, June 1st 2006.

- "Spontaneous and Evoked Rewiring of Layer 5 Pyramidal in the Neocortical Microcircuit", **Poster** at the Lemanic Neuroscience meeting, Les Diablerets, Switzerland, September 8th and 9th 2006.

Other activities:

- Ancient fencing – courses since 1997, treasurer (2003-2004) then president (2004-2006) of the "Ecole Lémanique d'Armes Anciennes". Since 2004 semi-professional stunt man in the group Flamenor.

- Webmaster for sports and theatre associations.

- Windsurf and sailing (1996-2002, regular crewmen on a sailing ship - regatta).

- Summers 2001 and 2002, responsible of groups of young people in camps.